

Dimitra Alkisti Pliatsika

**Aeolian sediment transport potentials and dune evolution  
in Ancão Peninsula (Ria Formosa), Portugal**

**Master in Marine and Coastal Sciences**

Work performed under the supervision of  
Dr. Susana Costas, PhD and Prof. Dr. Óscar Ferreira



**UNIVERSIDADE DO ALGARVE**  
**FACULDADE DE CIÊNCIAS E TECNOLOGIA**  
**2018**

Copyright ©

Declaro ser a autora deste trabalho, que é original e inédito. Autores e trabalhos consultados estão devidamente citados no texto e constam da listagem de referências incluída.

I declare to be the author of this work, which is original and unpublished. Authors and works consulted are duly cited in the text and are included in the list of references.

A Universidade do Algarve reserva para si o direito, em conformidade com o disposto no Código do Direito de Autor e dos Direitos Conexos, de arquivar, reproduzir e publicar a obra, independentemente do meio utilizado, bem como de a divulgar através de repositórios científicos e de admitir a sua cópia e distribuição para fins meramente educacionais ou de investigação e não comerciais, conquanto seja dado o devido crédito ao autor e editor respetivos.

The University of Algarve reserves the right, in accordance with the provisions of the Code of the Copyright Law and related rights, to file, reproduce and publish the work, regardless of the used mean, as well as to disseminate it through scientific repositories and to allow its copy and distribution for purely educational or research purposes and non-commercial purposes, although be given due credit to the respective author and publisher.



---

Dimitra Alkisti Pliatsika

## Table of Contents

1. Introduction.....	1
2. Objectives.....	3
3. State of the Art.....	5
3.1. Dune morphology.....	5
3.1.1. Incipient/ Embryo Dunes .....	6
3.1.2. Foredunes.....	7
3.1.3. Hind dunes.....	8
3.2. Beach-dune interaction .....	8
3.4. Shear velocity and threshold of sand movement.....	14
3.5. Sediment Transport.....	16
3.5.1. Aeolian transport modes.....	16
3.5.2. Sediment transport factors.....	16
4. Study Area.....	18
4.1. Geographical and geomorphological setting .....	18
4.2. Oceanographic setting.....	23
4.3. Ancão Inlet.....	23
4.4. Vegetational setting.....	24
5. Methodology.....	25
5.1. Evaluation of dune geomorphology and morphological changes.....	26
5.2. Dune geomorphology .....	28
5.3. Vegetation communities mapping.....	31
5.4. Textural analysis.....	35
5.5. Wind field regime.....	36
5.6. Aeolian sediment transport potentials and dune activity.....	37
5.7. Shoreline evolution.....	39
6. Results.....	42
6.1. Textural analysis.....	42
6.2. Wind field regime.....	45
6.3. Dune morphology.....	49
6.4. Shoreline evolution.....	55
6.5. Vegetation identification and mapping.....	62
6.6. Aeolian sediment transport potentials estimation.....	65
6.7. Volumetric changes.....	66
7. Discussion.....	73
8. Conclusions.....	84
Bibliography .....	87
Annex 1.....	99
Annex 2.....	100

## List of Figures

<b>Figure 1.1:</b> Image of Ria Formosa showing the peninsulas, inlets and barrier islands (Ceia et al., 2010).	3
<b>Figure 3.1:</b> Exchange of sand within the sand-sharing system, the arrows represent the sediment exchange derived from wave (black arrows) and from wind processes (blue arrows) (modified from Psuty, 2004).	6
<b>Figure 3.2:</b> Illustration of the three geomorphological zones of the backshore. (adapted from <a href="http://www.mrstevennewman.com/geo/Stockton/Biophysical_Interactions/geomorphological_processes">http://www.mrstevennewman.com/geo/Stockton/Biophysical_Interactions/geomorphological_processes</a> ).	7
<b>Figure 3.3:</b> In a stable dune ecosystem the landform consists of an incipient dune, followed by the foredune and landward by a hind dune.	8
<b>Figure 3.4:</b> Sallenger's (2000) regimes and predictions of beach changes applied for barrier islands. (a) Swash regime: wave run-up confined to beach, temporary erosion, offshore sediment transport followed by non-storm return and no net change to the system. (b) Collision regime: wave run-up exceeds the elevation of the base of the dune, run-up collision causes erosion and occasionally net or (semi-) permanent dune retreat, depending on the sediment availability. (c) Overwash regime: wave run-up exceeds the dune elevation or beach berm, overtopping transports the sand landward to produce net profile change and eventually landward barrier migration. (d) Inundation regime: combined wave run-up and storm surge exceeds the elevation of low seaward dunes to inundate the entire beach; if the barrier is also narrow, the entire island may be inundated, which can result in net change and landward barrier migration landward. $R_{high}$ is the maximum Runup elevation and $R_{low}$ is the effective still-water level during a storm, $D_{high}$ is the elevation of the dune crest and $D_{low}$ is the elevation of the dune toe. (Credit: (USGS) United States Geological Survey, in: Hansom et al., 2015).	9
<b>Figure 3.5:</b> Schematic diagram showing the progressive effect of storm waves on a foredune/beach system. During the initial stages of wave attack, the average level of the foreshore is lowered and the berm is removed as sand is moved offshore (after CERC, 1977 in Pye & Tsoar, 2009).	11
<b>Figure 3.6:</b> Scheme of sand transport by aeolian mechanisms over foredunes, for bare and vegetated foredunes, with different combinations of wind speed (high-low). + : potential deposition, - : erosion; $\emptyset$ : no transport (Arens, 1996).	13
<b>Figure 3.7:</b> Variation of the fluid threshold velocity and the impact threshold velocity with grain size. The distinctions between the saltation and suspension modes of transport, and between erosion, transportation and deposition are also shown. (Data partly from Bagnold (1941) and Chepil (1945b) in Pye & Tsoar, 2009).	15
<b>Figure 3.8:</b> Schematic diagram illustrating the drag force (FD), lift force (FL) and gravitational force (FG) exerted on a static grain by wind flow, as the arrows indicate. On the upper left are the wind profile and the streamlines ensuing from it. The grain starts to roll when the drag and lift force exceed the gravitational force.	17
<b>Figure 4.1:</b> Close up view (upper panel) of the study area of Ancão Peninsula, including the two parts of interest (sectors A: western and B: eastern) at the lower panels (map: <a href="http://www.bing.com/maps">www.bing.com/maps</a> ).	19
<b>Figure 4.2:</b> Perspective of the western side of the peninsula. The early vegetation zone is quite narrow and well defined and the ridge is distinct and continuous with some evidence of ancient dune scarping.	21

<b>Figure 4.3:</b> Dune setting in the east sector at a stable dune position. The subtle undulations are evident. Praia de Faro settlement (central sector) is visible at the top-wright corner of the picture.	22
<b>Figure 4.4:</b> Map of the Iberian Peninsula coastline divided in stretches of specified bioclimatic and biogeographic features. The study area lies within the ‘Iberian Atlantic Coast’ section that stretches between Ria de Aveiro, Portugal (6) and Punta de Tarifa, Spain (17). Adapted from Asensi & Diez-Garretas, 2017.	25
<b>Figure 5.1:</b> Overall illustrative map of the used dataset (Orthophoto of 2014).	28
<b>Figure 5.2:</b> Detailed map of vegetation sampling locations in eastern and western sector at seven selected sites.	32
<b>Figure 5.3:</b> Scheme of a typical coastal zonation representing EU habitats complementing Table 2. In Ancão Peninsula the given developed habitat types extend until the fixed dunes (code 2130) (adapted from Prisco et al., 2012).	34
<b>Figure 5.4:</b> The profiles in Ancão Peninsula, across which the sand samples were acquired (beachface, backshore and dune toe), with the positions being obtained by RTK-GPS (photo from 2011 Lidar dataset).	36
<b>Figure 6.1:</b> Mean Grain size ( $\mu\text{m}$ ) vs sorting per zone.	42
<b>Figure 6.2:</b> Grain size distribution per site and morphology of all samples in respect to their sampling date. The vertical dashed lines discriminate each profile. BF: beachface, BS: backshore, D: Dune toe/Dune	43
<b>Figure 6.3:</b> Mean grain size ( $\mu\text{m}$ ) versus sorting per profile for 29 beach samples of 2016-2017.	44
<b>Figure 6.4:</b> Skewness vs mean grain size per position plot for all sites.	44
<b>Figure 6.5:</b> Wind rose showing the speed and frequency of wind blowing for the study area.	45
<b>Figure 6.6:</b> a) Wind velocities distribution of favourable directions (1997-2016). The dark blue line represents the shoreline orientation. b) Wind velocities direction above the threshold ( $>8.9$ m/s).	46
<b>Figure 6.7:</b> Average monthly velocities for events above the threshold (8.9 m/s), in blue, and number of these events per month (in green) for the 1997-2016 period. The gaps in the graph line represent either absence of windy events in the corresponding month or as referred in the ‘Methodology’ section for November and December 2013 and for 2014 a deficiency of the direction data. On the graph, the months with more than 180 windy events are noted.	48
<b>Figure 6.8:</b> Location of the six extracted profiles in the study area (UAV dataset, 2016).	50
<b>Figure 6.9:</b> Cross-shore profiles at four selected sites in the eastern area of Ancão Peninsula extracted from Lidar datasets (2009 and 2011) and DTM (2016).	52
<b>Figure 6.10:</b> Cross-shore profiles at two selected sites in the western area of Ancão Peninsula extracted from Lidar datasets (2009 and 2011) and RTK-GPS surveyed cross-shore profiles (2016).	53
<b>Figure 6.11:</b> Dune ridge elevation at the eastern (upper panel) and western (lower panel) areas. The primary dune area is not depicted, rather the height of the dune ridge is emphasized. The studied profiles are depicted as well for each side respectively.	55
<b>Figure 6.12:</b> Net shoreline movement (NSM) between 1952 and 2014, using the dune vegetation line proxy (Orthophoto of 2014).	56
<b>Figure 6.13:</b> Linear regression rate variation (vegetation line approach) between 1952-2014 (Orthophoto of 2014).	57

<b>Figure 6.14:</b> Shoreline movement rates per year using the vegetation line proxy, for the analysed periods.....	58
<b>Figure 6.15:</b> Net shoreline movement (NSM) for 1952-2014 period using the tide mark line approach.....	60
<b>Figure 6.16:</b> Linear regression rate using the tide mark line approach for 1952-2014 period.....	61
<b>Figure 6.17:</b> Representation of the correlation coefficient ranges (no threshold application).....	61
<b>Figure 6.18:</b> Annual sediment transport potentials for 1997-2016 by use of one mena grain size (beachface environment) and the cosine of the angle of wind perpendicular to the shore. For the 11th and 12th month of 2013 and for 2014 the sediment transport potentials were not calculated and thus not presented, due to gap in the data. The plot is presented in kg/m and m <sup>3</sup> /m. ....	65
<b>Figure 6.19:</b> Annual sediment transport potentials using the percentages of weights presented for the western area.....	66
<b>Figure 6.20:</b> Polygon R5 of the western area. The elevation of the specified surface is displayed for 2009 and 2011 in the top panels. The vertical difference for this period is presented in the bottom left polygon. Lidar dataset of 2009 had a higher grid resolution compared to the 2011 dataset, hence the representation of raster polygon (top right) for 2011 is poorer. ....	67
<b>Figure 6.21:</b> R3 polygon for the eastern area is demonstrated for years 2009, 2011 and 2016. The vertical difference is presented in the bottom polygons for periods 2009-2011 (left) and 2011-2016 (right). ....	69
<b>Figure 6.22:</b> Surface vertical elevations for polygon R2 for the 2009-2011 (down left) and 2011-2016 period (bottom right).....	70

## List of Tables

<b>Table 1:</b> Unified applied dataset with all constituents used for the investigation of the dune system state, development and sediment transport potentials.....	26
<b>Table 2:</b> Habitat type classification (within the Natural Park of Ria Formosa) in dune systems of the surveyed areas according to EU Habitats Directive (92/43/EEC) (European Environmental Agency (EEA)). .....	36
<b>Table 3:</b> Supplementary table of existing species in Ancão Peninsula. ....	38
<b>Table 4:</b> Morphological zones of distinct dune habitats at the selected transects in the western area. The (-) sign signifies the absence of that morphological zone at the specific transect. The numbering of the morphologies starts from the shore. Transect 5 is the most eastern transect in the western area (near the bridge) and Transect 8 is the most westward.....	53
<b>Table 5:</b> Geomorphological zone classification with distinct dune habitats at the selected transects in the eastern area. The numbering of the morphologies starts from the shore. The (-) sign signifies the absence of that morphological zone at the specific transect. ....	54
<b>Table 6:</b> Average annual evolution rates for the western, middle and eastern area of Ancão Peninsula in four distinct periods of examination. ....	63
<b>Table 7:</b> Volumetric difference as resulted for the respective polygons and periods. ....	75
<b>Table 8:</b> Comparison table of results from formula estimations (two methods of calculation) and from the Lidar and UAV datasets for volumes and average annual transport rates. For the period 2009-2011 computations, the percentages-of-weights approach was applied using the grain size results of the western area, as R5 site (of western area) was included. Conversely, for the period 2011-2016, the results of the eastern grain size analysis were used. ....	75
<b>Table 9:</b> Comparison table of average annual velocity of windy events, sum of windy events (10-min) each year and annual estimation of potential sediment transport.....	80

## **Acknowledgments**

I am thankful to my supervisors, Susana Costas for all her guidance and assistance and Professor Óscar Ferreira for his constant help and detailed explanations. Appreciation is also owed to Katerina Kombiadou (CIMA, University of Algarve) for her instructions and support in GIS. A hearty thanks to my parents for always being present.



## Abstract

In the present study is attempted to examine aeolian sediment transport potential and to determine the constituents that promote/restrict the dune system development of Ancão Peninsula, where, apparent alongshore geomorphological differences, i.e. western and eastern sector, exist. In this study were investigated: wind potential for sediment transfer over the last 20 years (1997-2016) using recent granulometric data, dune morphology and elevation changes obtained from RTK-GPS beach profiles (2016), volumetric changes in three backshore polygons extracted from Lidar and UAV datasets (2009-2011 and 2011-2016) in both sectors. Presence of species communities of vegetation and shoreline evolution rates (1958-2014) as an indirect indicator for dune morphology were also used. Additional key parameters, namely littoral drift, updrift nourishment interventions and effect of Ancão Inlet were also considered.

A windy event was defined at velocity above 8.9 m/s for a mean beachface grain size of 466  $\mu\text{m}$ . Accounting for onshore winds and steering of the peninsula, only 1.7% of the winds was responsible for potential sediment transport. Moreover, the wind records, revealed that the windier years for potential transfer were 2002 (1.7  $\text{m}^3/\text{m}$ ), 2009 (2.1  $\text{m}^3/\text{m}$ ) and 2010 (1.8  $\text{m}^3/\text{m}$ ). Shoreline evolution showed negative values (retreat) for the western and central sector of the peninsula (-0.2 m/yr and -0.25 m/yr respectively) and accretional (+0.79 m/yr) for the eastern. The volume change rates for 2009-2011 show accumulation with very low positive values for the western sector that progressively increase towards the eastern (from eastern polygon: 0.85  $\text{m}^3/(\text{m}\cdot\text{yr})$  to western: 7.32  $\text{m}^3/(\text{m}\cdot\text{yr})$ ). The vegetational communities in the two sectors are compatible to the respective morphologies. In the western sector the absence of typical embryo dune vegetation (e.g. *Elymus farctus*, *Eryngium maritimum*) conforms with the absence of new foredune development. In the western part of the eastern sector, sparse embryo dune vegetation with low density is present, whereas in the most eastward part of the peninsula -in the inlet vicinity- two seaward developing foredunes are formed.

Assembling all elements, it is concluded that the mild wind regime in conjunction with the existing coarse grain size permits the development of relatively small dunes. In the western sector the vegetation suggests dune maturity, however the updrift nourishments have contributed to shoreline stabilization and subsequently to restriction of dune erosion. On the eastern sector nevertheless, the presence of Ancão inlet fostered creation of accommodation space through shoreline progradation, and hence incipient dune vegetation and new embryo dunes formation.

## Resumo

No presente estudo avaliou-se o potencial eólico de transporte sedimentar e determinaram-se os fatores responsáveis pela promoção/restricção do desenvolvimento do sistema dunar da Península do Ancão, onde se verificam diferenças geomorfológicas, por exemplo entre os sectores este e oeste. Este estudo analisou o potencial eólico na transferência de sedimentos nos últimos 20 anos (1997-2016), utilizando para tal dados granulométricos recentes, a morfologia dunar e variações de elevação obtidas a partir de perfis de praia efetuados com RTK-GPS (2016) e a determinação de mudanças volumétricas em três polígonos costeiros extraídos de conjuntos de dados de Lidar e UAV (2009-2011 e 2011-2016). Utilizou, ainda, a presença de comunidades de espécies de vegetação dunar e taxas de evolução da linha de costa (1958-2014) como indicadores indiretos para a evolução da morfologia das dunas. Parâmetros-chave adicionais, nomeadamente a deriva litoral, as intervenções de realimentação de praia e o efeito da Barra do Ancão foram também considerados na análise.

Foram definidos como eventos com capacidade de transporte eólica os registos em que a velocidade do vento foi superior a 8,9 m/s, para um tamanho médio de grão de praia de 466  $\mu\text{m}$ . Tendo em consideração os ventos dirigidos para terra e a direção da península, verifica-se que apenas 1,7 % dos ventos foram responsáveis por transporte potencial de sedimentos. Os registos de vento revelaram que os anos com maior potencial de transporte eólico foram 2002 (1,7  $\text{m}^3/\text{m}$ ), 2009 (2,1  $\text{m}^3/\text{m}$ ) e 2010 (1,8  $\text{m}^3/\text{m}$ ). A evolução da linha de costa mostrou valores negativos (reco) para os setores ocidental e central da península (-0,2 m/ano e -0,25 m/ano, respetivamente) e avanço da linha de costa (+0,79 m/ano) no sector este. As taxas de variação volumétrica, entre 2009 e 2011, mostram acumulação, com valores positivos muito baixos para o setor ocidental que aumentam progressivamente em direção a leste (R5: 0,85  $\text{m}^3/\text{m}$  ano, R3: 1,2  $\text{m}^3/\text{m}$  ano, R2: 7,32  $\text{m}^3/\text{m}$  ano). As comunidades vegetais dos dois setores são compatíveis com as respetivas morfologias. No sector ocidental, a ausência de vegetação típica das dunas embrionárias (por exemplo *Elymus farctus*, *Eryngium maritimum*) está em conformidade com a ausência de desenvolvimento de um novo cordão dunar frontal. Para oeste do setor oriental, verifica-se a existência de vegetação de dunas embrionárias, com baixa densidade, enquanto que na parte mais a leste da península - na vizinhança da barra de maré – se desenvolveram duas crista de dunas frontais, em direção ao mar.

Conclui-se que o regime de ventos moderado, em conjunção com o tamanho de grão grosseiro existente, limita a promoção do crescimento dunar. No setor ocidental, a vegetação sugere que as dunas apresentam um elevado estado de maturidade. As realimentações de praia efetuadas a barlamar contribuíram para a estabilização da evolução da linha de costa e, subsequentemente, para a redução da erosão das dunas. No sector oriental, a presença da Barra do Ancão fomentou a criação de espaço de acomodação, através da progradação da linha de costa e permitiu, consequentemente, a formação de vegetação dunar incipiente e a formação de novas dunas embrionárias.

This page is intentionally left blank.

## **1. Introduction**

A large proportion of the world population lives at, or near, the coastal zone, which results in high impact and degradation of coastal ecosystems, such as the coastal dunes. These ecosystems are particularly threatened by the impact of human activities, because of increasing demand of sun and beach tourism throughout the world, and also by residential, touristic or industrial purposes (e.g. Martínez et al., 2004; Martinez et al., 2013).

It has been also widely demonstrated that coastal dune systems represent beach sand reservoirs, especially during extreme episodes of wave storms, equinoctial spring tides or overwashes, including those generated by tsunamis (Navarro et al., 2015). Therefore, sand dunes play an essential role in sedimentary beach equilibrium protecting the littoral fringe from erosion (Navarro et al., 2015), especially on low-lying coasts. In many cases, opposed to sea dikes, dunes have the advantage of being built by naturally occurring processes and are in favour of recreational use. The disadvantage is that dune systems are dynamic and the safety level provided by dunes is variable in time. Therefore, significant management and frequent safety assessments are needed (de Vries et al., 2012). As an example, in many parts of the western Netherlands, where extensive areas of agricultural land and urban development lie at or below mean high water level (MHWL), and up to 5 m below storm surge level, the primary sea defence system depend on great extent on sandy beaches and dunes (see Pye & Tsoar, 2009). For instance, at the northern coastline of France, an 8-km preserved dune barrier is not only an appreciated recreational area and a ‘natural’ landscape, but mostly a protective natural barrier against marine intrusion (Ruz et al., 2005). Also, along large sections of the Atlantic East and Gulf Coasts (USA), barrier dune systems have been erected as stabilizing agents (Leatherman, 1979).

Under this perspective, a continuous belt of coastal dunes acts as a barrier to wave overwash and flooding of the inland area, performing a similar function as a seawall, but representing a nature-based solution. In many situations coastal dunes have a number of advantages over seawalls: (a) they are considerably less expensive to construct and maintain (Sutton-Grier et al., 2015); (b) dunes act as a sand store which can release sand to the beach during periods of storm wave attack, thereby helping to dissipate wave energy (Leatherman, 1979); (c) they are more flexible than seawalls and can adjust to changing conditions, such as a long-term fall in beach levels or a natural tendency for shoreline retreat; and (d) they have a less damaging visual impact on the coastline

(Pye & Tsoar, 2009). Additionally, although dunes reflect some wave energy during storms, the degree of wave reflection and consequent beach scouring is less severe than that induced by seawalls (Leatherman, 1979).

Another undeniable aspect is that coastal dunes and adjacent broad sandy beaches due to their attractiveness have provided settings for permanent residential development, holiday homes, caravan parks and camping sites. Such developments not only have a direct physical impact arising from the levelling of dunes and extraction of sand for construction, but also have a number of indirect effects which arise when large numbers of residents or visitors are attracted to the area (Nordstrom & McCluskey, 1985). Damaging effects associated with a large number of pedestrians include picking and trampling of vegetation, physical erosion by the passage of feet and initiation of wind funnelling along trackways, leading to the development of blowouts. Pressure is particularly severe around beach access points, and great care must be taken to ensure that public facilities are properly sited and cordoned off from adjoining sensitive areas (see Pye & Tsoar, 2009). Additionally, they may serve as groundwater recharge areas and storage against saltwater intrusion (Martínez et al., 2004).

In the present study, the aeolian activity that is responsible for dune formation and development, will be investigated for Ancão Peninsula of the Ria Formosa barrier island system (Figure 1.1) Principally, wind is the main contributor to dune formation or modification. Sand blown from the beach or foreshore is transferred to accumulate on the zone above high tide level, and developed as dunes, which may remain deposited or be swept further inland or along the coast by wind action. Dune growth and shaping is related to a source of, usually, dry sand that can be moved by wind, governed by wind flow characteristics, rates of aeolian transport, vegetation and patterns of erosion and deposition. Dune development takes place in the backshore and is aided by frequent strong onshore winds and by availability of a wide sandy beach as a source area (long fetch distance). It is also influenced by wave processes, especially when storm waves trim back the seaward dune margins. They are more often found behind wide gently sloping dissipative beaches than behind steeper, coarser and narrower reflective. Therefore, newly formed dunes are usually associated with prograding sandy coasts (Bird, 2008).

The multiple array of contributions that dune ecosystems provide are at risk, either if induced from erosional processes, related to climatic and hydrodynamic conditions, or caused from man constructions and interference. Yet, erosion is probably the most substantial factor of dune

shrinkage and retreat. Sediment erosion dominates over accretion on at least 70% of the world's sandy shorelines, which results in an inland displacement of the shoreline (Bird, 1985) and consequently coastal dune retreat is a major concern along coastlines. In addition, among the causes behind coastal erosion, sea level rise is one of the major global concerns that is likely to affect coastlines and barrier islands throughout the world in the upcoming years. Hence, no barrier island system is immune to erosional or sea level rise threats; however, some areas will be affected more than others and only the most robust systems will be able to withstand sea level rise without sustaining great damage (Greene, 2002). Such systems will be to a lesser or greater extent preserved by providing adequate sediment supply (Ceia et al., 2010).

The dune system of Ancão Peninsula of Ria Formosa barrier island system is therefore attempted for investigation to render explanations regarding its activity and whether dune development is governed by aeolian sand transfer or further components, as shoreline evolution and present geomorphological features, i.e. Ancão Inlet. Within this framework, understanding the processes that occur and affect a dune system in a low-lying peninsula, will give additional insights into vulnerabilities and impacts on coastal dunes.

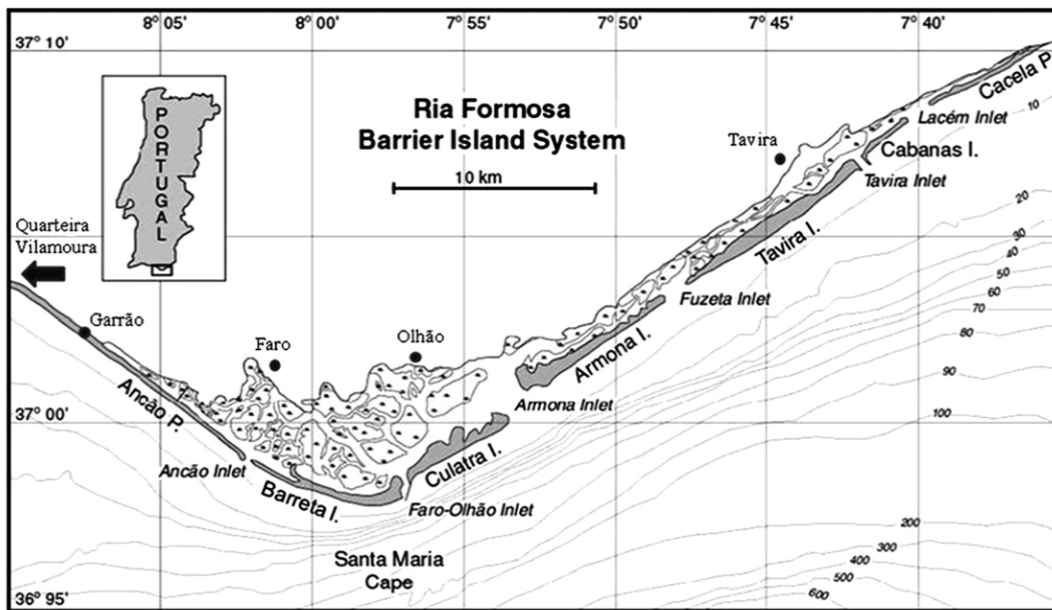


Figure 1.1: Image of Ria Formosa showing the peninsulas, inlets and barrier islands (Ceia et al., 2010).

## 2. Objectives

More specifically, the present study is aiming to:

- i. characterise the morphology of the sand dunes of the east and western part of Ancão Peninsula based on aerial photographs and Lidar data.
- ii. estimate the evolution of the dunes and their vertical variation within two pre-selected areas, using available Lidar datasets (2009 and 2011), UAV (Unmanned aerial vehicle, “UAV”) dataset (2016) and cross-shore profiles surveyed during 2016 and 2017.
- iii. determine recent (decadal) shoreline changes and compare the obtained trends with the observed dune morphologies.
- iv. characterize the wind field regime and determine the conditions under which aeolian sediment transport can occur, based on observations from the meteorological station located at Faro airport (1997-2016).
- v. evaluate aeolian sediment transport potentials based on windfield regimes, sediment texture and observed morphological changes.
- vi. classify the vegetation cover and correlate the different species with dune morphology and evaluate linkages with dune maturity.

Finally, all above results will be integrated to determine which factors may have a major impact on aeolian sediment transport and dune growth within the explored areas.



### 3. State of the Art

#### 3.1. *Dune morphology*

Aeolian sand dunes can be discriminated in continental and coastal, depending on the setting where they form and evolve, and depending on the major processes responsible for their shaping and growth. The present study will focus on coastal dunes.

Coastal sand dunes are aeolian land formations of accumulated sand sized sediments in coastal areas, where, provided the adequate sediment supply, energetic/strong enough onshore winds can move the sand (Pye, 1983; Kocurek & Lancaster, 1999; Martínez et al., 2004). The sediments for the development and evolution of most dunes are derived from material transported by fluvial or littoral processes (Lancaster, 2009). Their deposition occurs against obstacles such as driftwood or within vegetation or strand litter (Bird, 2008). Coastal dunes are broadly distributed ecosystems, notably along the Atlantic coasts of Europe, the Pacific coast of America, or the SE Australia and southern Africa coasts, and feature great diversity in terms of geomorphological dimensions and environmental heterogeneity (Martínez et al., 2004; Bird, 2008). They occur more extensively on the windward coasts behind sandy beaches and in a variety of dimensions from minor hummocks of 0.5 m to huge ridges measuring more than 100 m in elevation; from a single, shore-parallel, linear ridge with a width of a few tens of meters to a complex of dune forms that extend inland tens of kilometers (Psuty, 2004; Bird, 2008). Psuty (2004) proposed the conceptual setting of the dune morphological development; the geomorphology of the coastal dunes is shaped by the action of wind, waves and currents upon sediments to produce a set of landforms that are causally related. To particularize it, in coastal areas of adequate sediment supply, Psuty's coastal process-response conceptual model is applied on the beach profile: the accumulation of sand that extends from the offshore bar, through the dry beach, and into the adjacent coastal foredune. If the foredune is vegetated, its stabilisation is further enhanced and additionally it is actively affecting the foredune morphological shaping. This dune-beach profile is the basic sand-sharing system whose components respond to variations in energy level and to mobilization of sand from one portion to another. Each component episodically stores and releases sand in an exchange of sediment, i.e. in sediment budget terms, the beach is the source and the dunes represent the sink (Davidson-Arnott, 2010) (Figure 3.1).

Overall, there are three basic requirements that control backshore dune development: (a)

availability of sand; (b) sufficient wind energy to transport the sand or rework it *in situ* and (c) suitable topographic and climatic conditions maintained over a long period, which allow accumulation of sand (Pye & Tsoar, 2009). On the other hand, coastal dunes are reformed with wave processes, changing wind patterns, sediment supply, and human impact. Their presence or absence, vegetation cover, volume and elevation, and even their precise positional changes are important (Bush & Young, 2009) for nature conservation (Pye & Neal, 1994), socio-economic and ecological system services (Everard et al., 2010).

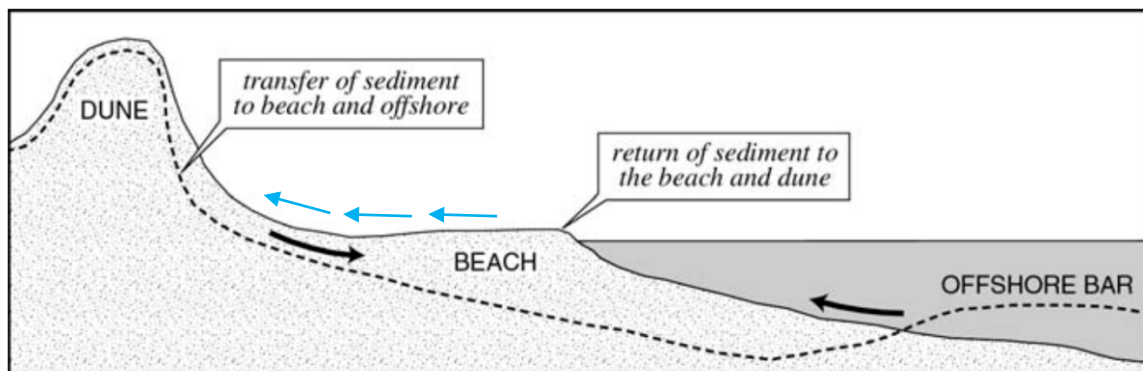


Figure 3. 1: Exchange of sand within the sand-sharing system, the arrows represent the sediment exchange derived from wave (black arrows) and from wind processes (blue arrows) (modified from Psuty, 2004).

### 3.1.1 Incipient/ Embryo Dunes

Incipient or embryo dunes (also referred as white dunes) are new or developing dunes forming within pioneer plant communities reaching 1 to 2 m height (Hesp, 2002; Maun, 2009). They form by sand deposition within discrete or relatively discrete clumps of vegetation, individual plants, driftwood, flotsam, etc. (Hesp, 1989), forming shadow dunes, or low unconnected mounds or hummocks of sand (Maun, 2009). Incipient dunes develop in the seaward most vegetated sand surface ranging from the immediate backshore to backbarrier sand flats (Carter et al., 1991; Hesp, 1989). There, the organic matter brought by the waves accumulates and decomposes, creating a substrate rich in sea salts and organic matter decomposition (Prisco et al., 2012). Their morphological development principally depends on a) plant species, b) density and architecture, c) distribution, d) height and cover, e) wind velocity and f) rates of sand transport. As an example, Hesp (2002) reviewed that most vegetation canopies can vary alongshore in intensity or distribution either because of variations in the vigour of a particular dominant species, or because the distribution of species varies spatially. As a result, the morphology of the foredune varies alongshore accordingly. The greater the variations in density or distribution or in sand supply, the

greater the morphological variation (see Hesp, 2002). Secondary factors such as the rate of occurrence of storm wave erosion, overwash incidence and wind direction can also be important in determining subsequent dune evolution (Pye & Tsoar, 2009; Maun, 2009).

### 3.1.2. *Foredunes*

Foredunes (usually mentioned yellow dunes) are actively growing dunes, developing from incipient dunes (Figure 3.2) and are characterized by the growth of intermediate, often woody plant species. They are commonly attributed by greater morphological complexity, height and width, in contrast to the incipient dunes (Short, 1999). Usually they are defined as shore-parallel dune ridges formed on the top of the backshore (above the dry sand beach) by aeolian sand deposition within vegetation (Hesp, 2002; Duran & Moore, 2013) or any other material and obstacle (Feagin, et al., 2015). They can form on any shore, as beaches, estuaries, lakes or lagoons and in almost any climate from tropical to arctic (Hesp, 2002). The morphological development and evolution of established foredunes depends on a number of factors including: a) sand supply, b) the degree of vegetation cover, c) present plant species, d) the rate of aeolian sand accretion and erosion, d) the frequency and magnitude of wave and wind forces, e) the occurrence and magnitude of storm erosion, dune scarping, and overwash processes, f) the medium to long-term beach or barrier state (stable, accreting or eroding), g) sea/lake/estuary water level and increasingly, h) the extend of human impact and use (Sherman & Bauer, 1993; Hesp, 2002) and j) the morphodynamic state of the beach (dissipative, intermediate or reflective) (Short & Hesp, 1982). In a simple profile, the foredune exists at the boundary between the marine processes to its seaward part and continental processes to its landward (Psuty, 2004). Foredunes constitute the most stable/conservative component of the coastal profile that undergo temporal and dimensional variations of far less magnitude compared to the beach (Psuty, 2004).

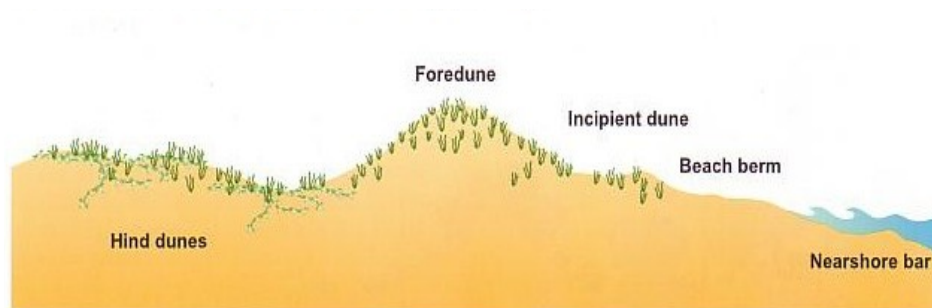


Figure 3.2: Illustration of the three geomorphological zones of the backshore. (adapted from [http://www.mrstevennewman.com/geo/Stockton/Biophysical\\_Interactions/geomorphological\\_processes](http://www.mrstevennewman.com/geo/Stockton/Biophysical_Interactions/geomorphological_processes)).

### 3.1.3 Hind dunes

The hind dunes are usually extended tertiary foredunes occupied by more complex and developed vegetation such as scrubs, also with trees and forests at several coastal dune ecosystems. They are protected from the strong winds and salt spray experienced closer to the beach enabling for less hardy and specialised trees to survive. The more complex species in this area result in more humus and organic matter produced, thus providing sufficient nutrients for diversity of species. Eventually plant communities are established in this zone that further contribute to nutrient enhancement of the area (Beachapedia, 2013).

In Figure 3.3 a setting of a typical coastal zone cross-profile is demonstrated, with the distinct vegetational zones: the incipient dune with primary zone species (grasses and creepers) colonize the lower parts of the beach and trap abrasive sand particles forming a “foundation”. The foredune constitutes an elevated “wall” that can be colonized by secondary zone species (mainly shrubs) to provide a wind deflecting “shutter” near the shoreline. Finally, on the hind dunes, tertiary species are established (usually taller shrubs and/or trees) forming a “roof” from their canopy. By this, wind is additionally lifted and increased shelter is provided to vegetation, ecosystem or settlement farther inland (NSW Department of Land and Water Conservation, 2001).

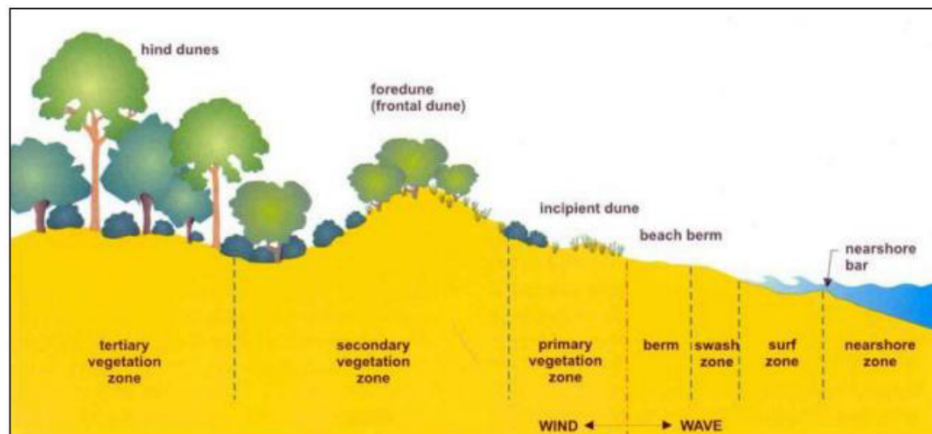


Figure 3.3: In a stable dune ecosystem the landform consists of an incipient dune, followed by the foredune and landward by a hind dune.

### 3.2. Beach-dune interaction

Erosion of coastal dunes can be induced by several natural factors, such as storm events, elevated water levels and high wave run-up (e.g. Hesp, 1988; Psuty, 1988; Sherman & Bauer, 1993; Aagard et al., 2007) causing wave scarping or overwash. Both cross-shore and longshore components cause coastal erosion and accretion. Dune and soft cliff erosion during extreme events mainly is a

cross-shore process bringing the sediments from the immobile dune front into the mobile littoral system (van Rijn, 2010). There are several studies that have demonstrated the importance of storm events and storm-related variables as agents in dunes shape (Davidson-Arnott et al., 2005; Hesp, et al., 2005; Bauer, et al., 2009; Mathew et al., 2010; Davidson-Arnott, et al., 2012). Incipient dunes and foredunes are directly affected by storms, since they occupy the immediate landward position relatively to the beach and thus are exposed to coastal winds as well as to storm surge and wave impacts (Brinks et al., 2013). Sallenger (2000) defined an impact scale that relates sea level and runup level to the dune morphology, whereas four impact regimes are defined: swash, collision, overwash and inundation (Figure 3.4). Nevertheless, beach erosion also is an alongshore process due to the presence of eroding longshore currents including tidal currents (van Rijn, 2010).

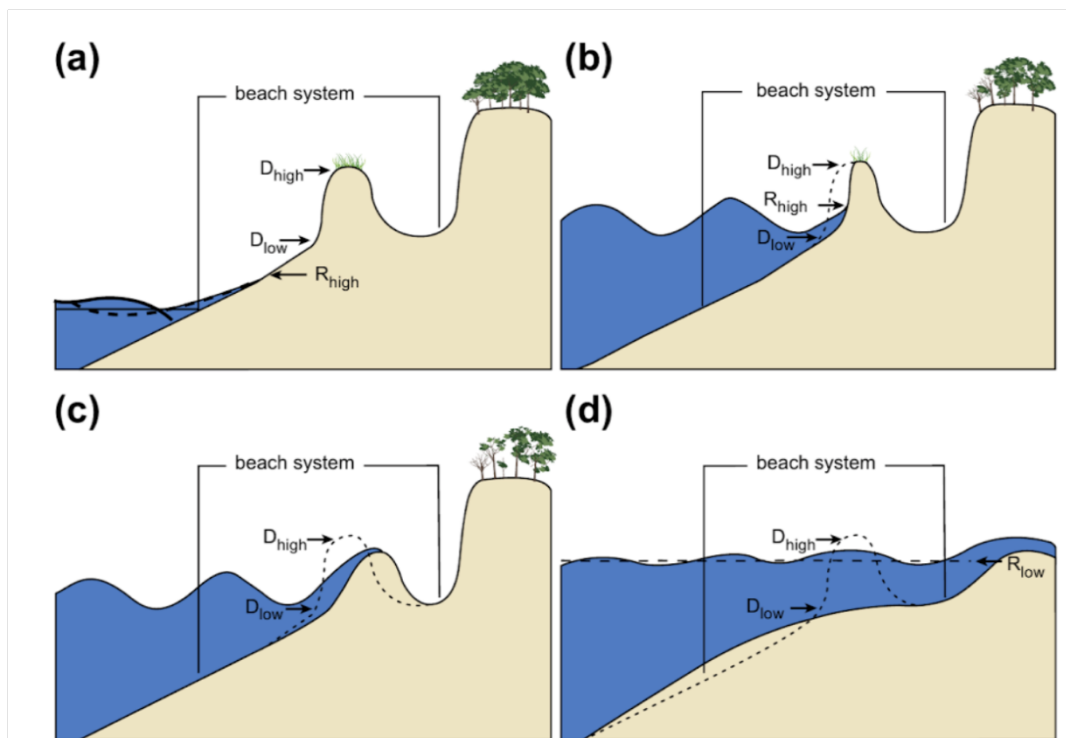


Figure 3.4: Sallenger's (2000) regimes and predictions of beach changes applied for barrier islands. (a) Swash regime: wave run-up confined to beach, temporary erosion, offshore sediment transport followed by non-storm return and no net change to the system. (b) Collision regime: wave run-up exceeds the elevation of the base of the dune, run-up collision causes erosion and occasionally net or (semi-) permanent dune retreat, depending on the sediment availability. (c) Overwash regime: wave run-up exceeds the dune elevation or beach berm, overtopping transports the sand landward to produce net profile change and eventually landward barrier migration. (d) Inundation regime: combined wave run-up and storm surge exceeds the elevation of low seaward dunes to inundate the entire beach; if the barrier is also narrow, the entire island may be inundated, which can result in net change and landward barrier migration landward.  $R_{high}$  is the maximum Runup elevation and  $R_{low}$  is the effective still-water level during a storm,  $D_{high}$  is the elevation of the dune crest and  $D_{low}$  is the elevation of the dune toe. (Credit: (USGS) United States Geological Survey, in: (Hansom et al., 2015))

Model studies and field observations have articulately shown that the presence of a high foredune reduces foreshore lowering and shoreline recession during a storm (in Pye & Tsoar, 2009; p: 336), which is especially important during storm surges. For those conditions, waves may begin to break close to, or even against (Pye & Tsoar, 2009) the dune line (Figure 3.5), making the seaward dune foot unstable and causing erosion or dune openings and allowing scarp formation and sediment loss from the dune. Nevertheless, among others, Wolman and Gerson (1978) argued, that a large catastrophic event may alter the landscape significantly, but the system may rebuild to the pre-event state under every-day processes that cause landscape change, provided positive sediment budget. Contrarily, even small landscape disturbances may persist for decades if there is weak capacity in the system to recover to the prior state. A general remark is that wave-induced dune erosion leads to beach accretion and bar development when the beach and surf zone slopes are relatively flat (dissipative conditions), but in case of a steep surf zone slope the dune and beach are eroded simultaneously and the sediments are carried away to deeper parts of the profile (van Rijn, 2010).

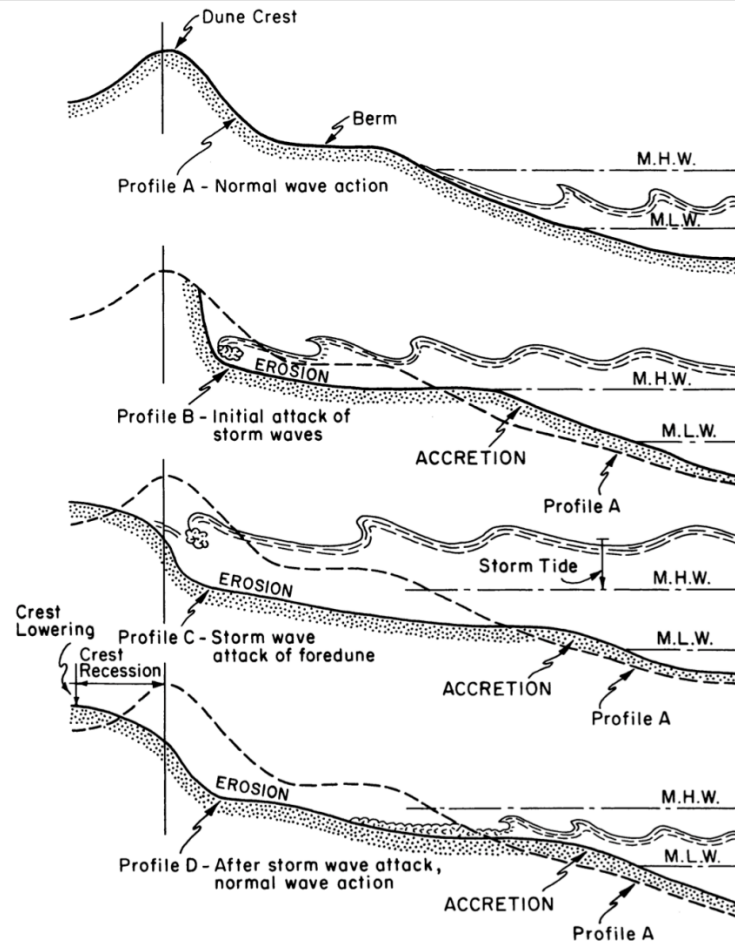


Figure 3.5: Schematic diagram showing the progressive effect of storm waves on a foredune/beach system. During the initial stages of wave attack, the average level of the foreshore is lowered and the berm is removed as sand is moved offshore (after CERC, 1977 in Pye & Tsoar, 2009).

Time and space relationships between the beach and the dune systems' sediment budget, are the foundation for foredune development and geomorphological evolution across the beach-dune profile (Psuty & Silveira, 2010). Coastal dunes develop as accumulating systems with very positive sediment budgets, i.e. input far exceeds output. Thus, a negative budget leads to a dissected dune system by erosion landforms: blowouts, deflation hollows and plains, reactivation dunes and scarping (Carter, 1991).

### 3.3. Dune formation/development and vegetation role

During onshore winds, sand is eroded from the beach and moves towards the foredunes mainly by saltation. Wolfe and Nickling (1993) recognized that the increased vegetation cover near the dune foot reduces wind velocity, blocks incoming grains and reduces the erodibility of the surface below it, because it acts as a friction element and slows down the wind enabling deposition to occur. As

a result, saltation usually fades out within a short distance from the first vegetation, leading to sedimentation over a width determined by wind velocity and vegetation density (Hesp, 1983, 1988; Sarre, 1989; Arens, 1996; Arens et al., 2001). The turbulence induced by vegetation and the upward velocities caused by the dune slope may also initiate grains transport in suspension (Arens, 1996; Arens et al., 2002). These grains may travel farther up the dune as they pass over the vegetation canopy, leading to deposition farther up the slope and near the crest (Arens, 1996; Arens et al., 1995; Hesp, 2002; Petersen et al., 2011; Ollerhead et al., 2013) (Figure 3.6). In addition, Hesp et al. (2009) and Petersen et al. (2011) postulated ‘modified saltation’, whereas storm winds may bend the foliage into their streamlines, reducing roughness and creating a secondary surface for saltation, allowing sand grains to proceed considerable distances downwind. Arens (1996) regarded that saltating grains will only reach the foredune if the surface is scarcely vegetated. However, field measurements on foredunes in monthly to yearly periods have shown transport and sand deposition (of large quantities) up the seaward slope of foredunes and over the crest onto the lee slope and beyond, even when vegetated by pioneer grasses (Arens et al., 2001; Kuriyama et al., 2005). Hence, airflow over a foredune is modified by both topography and vegetation (Keijsers et al., 2015). In general, a vegetated foredune induces flow deceleration upwind of the dune slope (Sarre, 1989; Wal & McManus, 1993; Arens, 1996; Davidson-Arnott & Law, 1996; Hesp, 1989 and 2002) and during onshore winds, wind is topographically accelerated due to flow compression over the seaward slope (Arens et al., 1995; Arens, 1996; Walker, et al., 2009). At the same time, vegetation roughness slows down the airflow, counteracting the topographic acceleration. In such events, it has been recorded that there was a marked speed up above the vegetation, which at times produced sediment entrainment within the canopy (Finnigan & Belcher, 2004).

Keijsers et al. (2015) reviewed that plant growth on the foredune is consecutively stimulated where an adequate amount of sand is deposited, while vegetation declines where tolerance limits are exceeded in either sedimentation or erosion. Hence, the pattern of sedimentation may define where vegetation thrives and where it subsides. Furthermore, variations in the tolerance to burial and exposure between species may contribute to the spatial distribution of plant species (Levin et al., 2008; Maun, 2009). Van Dijk et al. (1999) suggest in their modelling a correlation between plant and dune height, namely as plant height increases, dune height increases and dune length decreases, which was verified by field observations of Hesp (1989). Notwithstanding, as Bush and Young (2009) acknowledged, vegetation cover is a good indication of the relative stability of



coastal landforms. In general, the taller and thicker the vegetative growth, the more stable the site and the coastal geomorphic features.

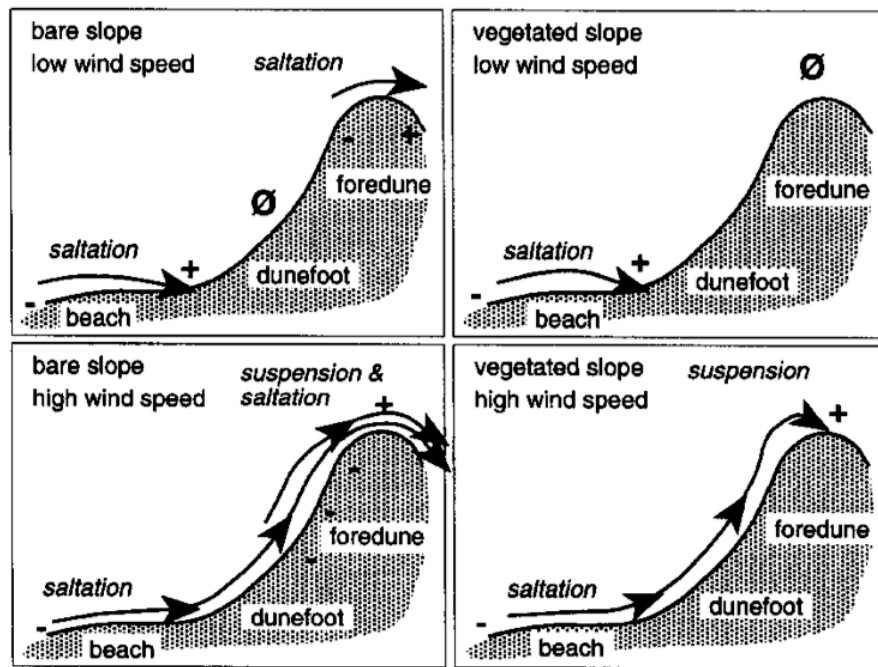


Figure 3.6: Scheme of sand transport by aeolian mechanisms over foredunes, for bare and vegetated foredunes, with different combinations of wind speed (high-low). + : potential deposition, - : erosion; Ø : no transport (Arens, 1996).

Vegetation in the dune area catches windblown sand and binds it to the dune. Without plants to trap the sand, the sand is blown away and the dune erodes or migrates. Plants in this zone are extremely enduring with special adaptations that allow survival. They provide vital protection for fauna that live in this zone, and for other flora further back in the dunes. The dune crest is also anchored by vegetation, which plays a secondary role as a passive roughness element, when interacting with wind flow, and thus preventing dune motion (Duran & Moore, 2013). Sand-fixing plants (e.g. *Atriplex* sp.) are responsible for stabilizing surfaces and sand-building plants (e.g. *Ammophila* sp. and *Elymus* sp.) are involved in accumulating sand (Carter, 1991). In conditions of dynamic equilibrium (erosion equals accretion)<sup>1</sup> (Feagin et al. 2005) the vegetation is mostly determined by environmental factors, as sea dynamics, sea proximity and sands mobility, which is expressed in specific plant associations, coverage and species compositions (Kim & Yu 2009). Contrarily, when beach faces severe erosive sea processes, very often the beach sediments and the foredune advance inland (Psuty & Silveira, 2010), overlapping the relatively stabilized dunes, in

<sup>1</sup> Such gradients are created as a result of spatial shift in elevation, climate, soil and many other environmental factors (Kark, 2013).

such situations their vegetation can mingle and coexist for a period of time. For the Portuguese coasts, it is acknowledged that native psammophilic flora and vegetation plays an essential role in the resilience and vitality of coastal social-ecological services (Feagin et al., 2010; Martins et al., 2013), for instance biodiversity maintenance (Til & Koojman 2007; Howe et al. 2009), sand fixation and dune construction.

### ***3.4. Shear velocity and threshold of sand movement***

As with all fluid flow, wind blowing across a surface is affected by friction with the bed, which leads to the generation of a boundary layer, in which flow speed is retarded by contact with the land surface and obstacles on it. Wind flow is affected by the topography of the bed over which it passes (Pye & Tsoar, 2009). Then the movement of sand by wind is caused by the transmission of impulse of the wind to the sand grains. Impulse (I) is the momentum,

$$I = m * U \quad (1)$$

with mass (m) and velocity (U) over time. The change of impulse results into a force per unit area parallel to the flow called shear stress ( $\tau$ )

$$U_{*t} = \sqrt{\tau/\rho} \quad (2),$$

where  $U_{*t}$  is the shear threshold velocity and  $\rho$  atmospheric density, that can be translated to “shear velocity”,  $u_*$  (Hsu, 1971)) (see Equation 5, p. 37)

When the shear velocity over a loose sand surface is slowly increased, a critical point is reached where some grains begin to move. This critical wind velocity, necessary to induce sand movement, is known as the fluid threshold velocity  $u_{*th}$  (Bagnold, 1941) or shear threshold velocity. This initiation of grain movement is explained by several theories, attributed to rolling (Bagnold, 1941; Malina, 1941; Chepil, 1959) or vibration of the particle before its “ejection” (Bisal & Nielsen, 1962; Lyles & Krauss, 1971) The initiation of grain motion is defined by the forces exerted on individual grains: a lift force, vertically upwards, constraining the horizontal movement by the adjacent grains and horizontally by a drag force acting in the direction of the flow (Figure 3.7 and 3.8) (Csahók et al., 2000).

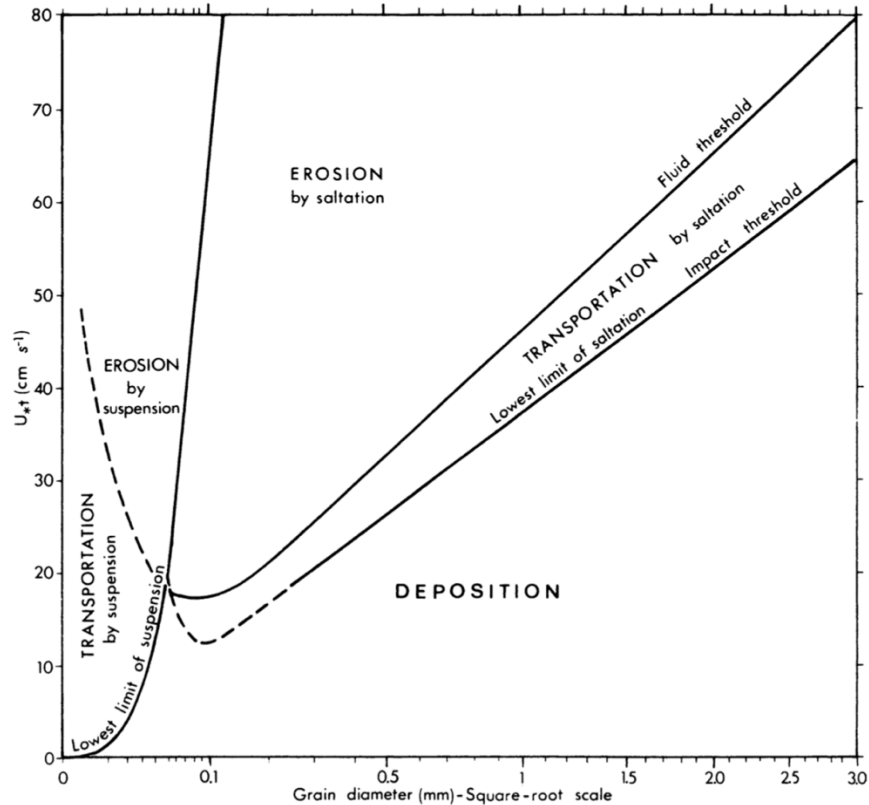


Figure 3.7: Variation of the fluid threshold velocity and the impact threshold velocity with grain size. The distinctions between the saltation and suspension modes of transport, and between erosion, transportation and deposition are also shown. (Data partly from Bagnold (1941) and Chepil (1945b) in Pye & Tsoar, 2009).

Arens (1996) concluded that the landward decrease in flux is shown to depend on wind strength: low wind speeds result in a sharp decrease, high wind speeds in a gentler decrease; during high wind speeds the sand is transported over a longer distance from the dune foot than during low wind speeds. The landward decrease in transport is not linear. An initially strong decrease, between dune foot and crest is thought to be related to the saltation process. In respect to suspended grains, between crest and back of the foredune, their content in the air decreases at a much slower rate, depending on the settling velocity of the grains. The transport of fine and medium grained sand in suspension appears to be a common process, operating when wind speeds exceed a certain critical level.

It is presently recognized that micro-scale changes in topography and vegetation cover presented to winds blowing onshore across the beach and foredune produce large departures in the velocity profile from the ideal log-linear form (Bauer et al., 1996; Walker and Nickling, 2003; Hesp et al., 2009; Weaver and Wiggs, 2011), making it impossible to make an accurate determination of  $u_*$ .

### ***3.5. Sediment Transport***

Foredune evolution is controlled by the local aeolian sediment transport regime, which is defined by the interaction of several factors including beach type, surface moisture content, wind regime, sand supply, sediment texture and density and spatial distribution of vegetation (Psuty, 1988; Hesp, 2002).

#### *3.5.1. Aeolian transport modes*

Sediment transport occurs by different modes defined by wind velocity and grain size. The layer of grains that move very close to the bottom is known as boundary layer. The bed load transportation within this boundary layer may be through saltation, in which grains move forward by a series of jumps, and surface traction, in which grains roll or slide along the surface, due either to direct fluid drag or the impact of saltating grains (Nichols, 2009, Pye & Tsoar, 2009).

Usually sand on the beach is transported in saltation (Arens, 1996). In "pure" saltation (Jensen & Sorensen, 1983), the grain trajectories are determined by the average wind profile, whereas in "modified" saltation (Nalpanis, 1985), the trajectories are modified by the turbulent characteristics of the wind. However, most of the upward momentum of the grains is received from frequent impacts with the sand bed.

Another major transport mode is suspension, the movement of usually smaller grains, lifted from the surface by a vertical gust, and transported over longer distances without any interaction with the sand bed (Arens, 1996; Pye & Tsoar, 2009). Turbulent airflow is able to keep a grain in suspension when the vertical fluctuating velocity component of the flow exceeds the settling velocity of the grain ( $w_f$ ) (Pye & Tsoar, 2009). So, movement of particles by the wind takes place by a combination of direct wind shear stress and atmospheric turbulence (Lancaster, 2009).

#### *3.5.2. Sediment transport factors*

As described by Pye and Tsoar (2009), the flow dynamics of sand movement can be explained considering wind flowing over a resting sand grain on a horizontal surface exerting two types of force on the grain: (a) a drag force acting horizontally in the direction of the flow, and (b) a lift force acting vertically upwards (Figure 3.8). Opposing these aerodynamic forces are inertial forces. grain's weight is defining isolated grains motion, whereas cohesion and friction are the most important for packed humid grains that act directly against the lift force. Then, the behaviour of a grain when acted on by a fluid is often more closely controlled by its mass, rather than by its

external dimensions. Mass represents a measure of the inertia of a body, i.e. the resistance that the body offers to a change to its velocity or position changed by the application of a force (Pye & Tsoar, 2009). Furthermore, the friction between the sand grains is also a transport impeding factor, as the densities of particles differ considerably depending on grain compaction or dilation, the fluid between the voids (water or air) and their elemental composition, size and heterogeneity (Pye & Tsoar, 2009; Stark et al., 2014).

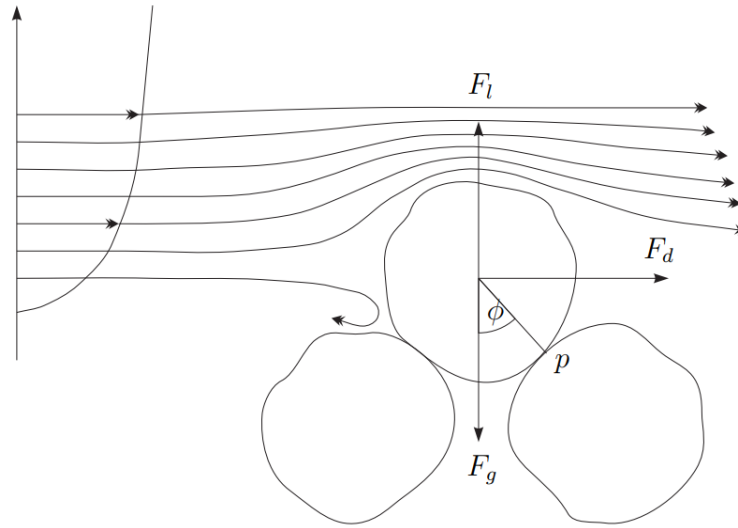


Figure 3.8: Schematic diagram illustrating the drag force ( $F_D$ ), lift force ( $F_L$ ) and gravitational force ( $F_G$ ) exerted on a static grain by wind flow, as the arrows indicate. On the upper left are the wind profile and the streamlines ensuing from it. The grain starts to roll when the drag and lift force exceed the gravitational force.

Cohesive forces are significant for soft beaches (grains smaller than 0.1 mm), thus particular factors as moisture derived from precipitation and waves or tides hamper sand transfer. After wetting, moisture is retained by sand as a surface film, especially at points of grain contact resulting in tensile force between the water molecules and the sand grains (Chepil, 1956; Bisal & Hsieh 1966). Adding to the aforementioned the unsteady and non-uniform nature of coastal wind regime (Bauer et al., 1998; Davidson-Arnott et al., 2005) researchers have found poor agreement between measured and predicted sand flux on beaches (e.g. Svasek & Terwindt, 1974; Bauer et al., 1996; Davidson-Arnott & Law, 1996; Jackson and Nordstrom, 1998; Sherman et al., 1998).

Beach width and fetch are also worth mentioning components of sand transfer. At narrow beaches with onshore winds, the total sediment transport rate across the dune line will be less than that predicted for a wide beach because of the constraint imposed by the fetch distance (Navarro et al, 2015). By fetch is referred the downwind distance from the leading edge of the transport to any general point of interest on the beach (Bauer et al., 2009), is an additional varying factor of

sediment flux. It has been proven, by several simulations of flow over foredunes in computational fluid dynamics (CFD) modelling, that the critical fetch distance<sup>2</sup> ( $F_c$ ) exerts an important controlling effect on the amount of sand supply to the foredune. However, the proportion of the sediment delivered to the dune relative to the amount eroded from the beach is influenced dominantly by the angle of wind approach, and not by the fetch distance. So, when the angle of wind approach becomes more oblique, the downwind portion of the beach closest to the dunes, experiences enhanced sand transport rates. Yet, the total amount of sediment supplied to the foredune is decreased relative to that during cross-shore transport, as most of the sand is lost to the downwind margin of the beach (Walker et al., 2017).

## 4. Study Area

### *4.1. Geographical and geomorphological setting*

The study area lies within Ancão Peninsula, being part of the Ria Formosa coastal lagoon system, which is located in the Algarve region in south-western Iberian Peninsula (Figure 4.1). Ria Formosa consists of a coastal lagoon bordered by five barrier islands and two peninsulas, Ancão Peninsula being the western and Cacela Peninsula the eastern boundary of the system. The lagoon connects to the sea by six tidal inlets (Figure 1.1): two relocated inlets (Ancão and Fuseta inlets), two artificially opened and stabilized inlets (Faro-Olhão and Tavira inlets) and two natural inlets (Armona and Lacém inlets) (Ferreira et al., 2016). The backbarrier is characterized by large salt marshes, sand flats and a complex network of natural and partially dredged channels, covering  $8.4 \times 10^7 \text{ m}^2$  (Andrade, 1990). Ria Formosa has a distinct triangular shape extended for 55 km, possibly related to the existence of a shallow shelf bounded by a relatively steep slope on the inner continental shelf (Dias & Gonzalez, 2000).

Ancão Peninsula (Figure 4.1) has a variable length of 8.5 to 12.8 km (approx.) and width of 50 to 200 m (Ferreira et al., 2016) and is positioned in a NW-SE direction. Its variable length is attributed to considerable morphological changes that the peninsula has undergone due to shoreline retreat, inlet migration and relocations and beach nourishment. Thus, its natural length has varied, as it was dependent on the Ancão Inlet position and migration. In a recent morphological analysis of

---

<sup>2</sup>  $F_c$  is the critical fetch distance related to the maximum sediment transport delivered by aeolian processes, as described in the conceptual model of Bauer and Davidson-Arnott (2003).

Achab et al. (2014) the profile was characterised as steep with a beach face slope of  $\tan \beta \approx 0.14$  (a less steep slope of 0.11 in average was stated by Ferreira et al. (1997)). During storm events, the erosion affects mainly the beachface and backshore, and the beachface slope decreases to  $\tan \beta \approx 0.07$  (Achab, 2014). Nevertheless, Vousdoukas et al. (2012) asserted that in general the profiles recover from erosion in a few days.

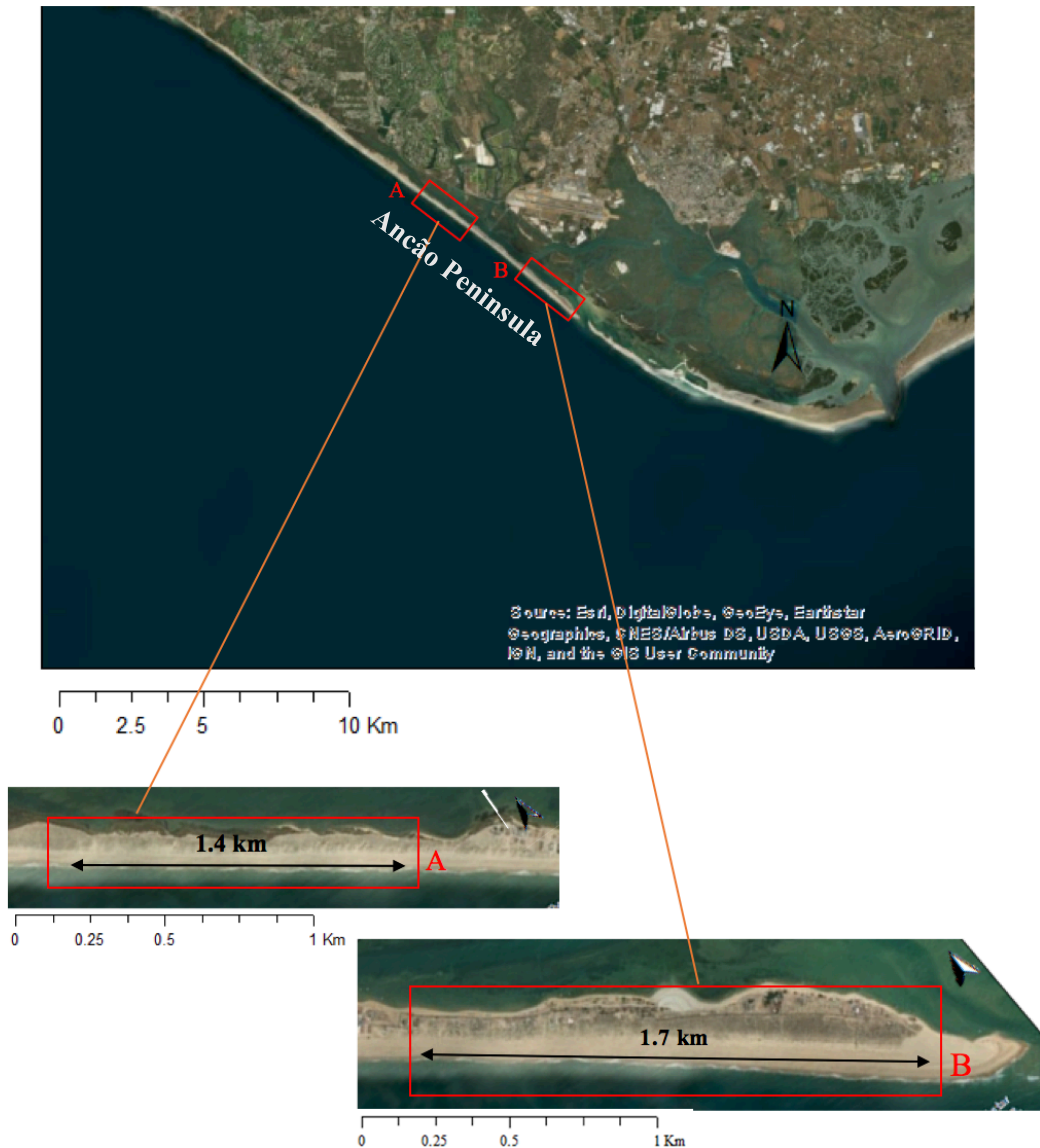


Figure 4.1: Close up view (upper panel) of the study area of Ancão Peninsula, including the two parts of interest (sectors A: western and B: eastern) at the lower panels (map: [www.bing.com/maps](http://www.bing.com/maps)).

An additional factor to be remarked affecting Ancão Peninsula is coastal erosion, which was amplified after 1970s due to updrift construction of the Vilamoura jetties, riprap seawalls and

extensive groin field in front of Quarteira (Figure 1.1) (Dias & Neal, 1992; Ferreira et al., 2016). Thereafter the sand supply was downdrift reduced. The remarked erosive trend was responsible for shoreline retreat rates reaching in some locations values of 1 to 2 m/yr in the last 50 years (Pilkey et al., 1989; Bettencourt, 1994). The littoral drift southeast of Quarteira was impacted causing coastal recession and property damage, thus several beach nourishments have been carried out from local and national authorities in Vale do Lobo (8 km west of Ancão; Figure 1.1) to mitigate coastal erosion, namely in 1999, 2006 and lastly in 2010 (Ferreira & Matias, 2013). Beach and dune nourishment took place also along the Ria Formosa barrier islands for dune preservation and recovery purposes (April 1999-July 2000) (Ramos & Dias, 2000; Ferreira & Matias, 2013). Aeolian transport processes promote dune construction and regularly causing the burial of roads and house yards, whereas overwash has promoted property damage and barrier breaching (Almeida et al., 2012; Achab et al., 2014, Ferreira et al., 2016; Popesso et al., 2016). Foredune erosion has caused the destruction of houses, dwells and roads located at the shorefront. In order to diminish the vulnerability of the frontal dune ridge to coastal erosion, overwash and breaching, the Park Authority has put into practice management plans that include beach and dune nourishment which proved to be successful with respect to the proposed objectives (Dias et al., 2003). Ancão Peninsula can be divided in three sectors, west, central and east, in reference to the location of Praia de Faro (as the human occupied part is locally referred) in the central part. The study area focuses on two sites of interest, located within the western and the eastern part of Ancão Peninsula and extend approximately 2.6 km, namely 1.4 km at the eastern sector and 1.2 km at the western sector (Figure 4.1). The sites demonstrate high morphological diversity; the western part is characterised by stable foredunes and dune bluffs (Dias, 1988). More specifically, as descriptively portrayed in Ferreira et al. (2006), in the western sector (Figure 4.2), the peninsula presents principally a continuous ridge, which is mostly unoccupied except for a few bars and restaurants near the attachment to the mainland. An erosion scarp was defining the transition from the dune to the beach, as beach profiles of 2000 and 2001 showed, signifying shoreline retreat processes (Achab et al., 2014). Nevertheless, the beach and dune nourishment of 1999-2000 (Ramos & Dias, 2000) supported the recovery of the profile and the respective scarp is not existent anymore. In this segment, there is a large breach in the dune ridge that corresponds to the location of a relict ephemeral tidal inlet opened during the first half of the 20<sup>th</sup> century. Nowadays, the surface of this breach is completely vegetated and not overwashed. At Praia de Faro section



(central), the dune has been lowered or even destroyed and the human occupation is dominant. For that reason, overwashes are more frequent in this sector, resulting to severe consequences (Pilkey et al., 1989; Ferreira et al., 2006; Garcia et al., 2010; Rodriguez et al., 2012).



*Figure 4.2: Perspective of the western side of the peninsula. The early vegetation zone is quite narrow and well defined and the ridge is distinct and continuous with some evidence of ancient dune scarping.*

The central part includes also the Praia de Faro settlement, which is the only location accessible by car among the Ria Formosa barriers. Along the 3-km-long extent of this coastal segment the dune ridge has been almost completely destroyed by the construction of residential, tourist and recreational infrastructures. To prevent property damage, some parts of the oceanfront of this developed site have been artificially stabilised with revetments. These structures have inhibited further shoreline retreat, but are frequently overwashed (Ferreira, 2011) when high-energy stormy waves coincide with spring high tides (Dissanayake et al., 2015).

The eastern sector consists of lower and wider foredunes and accretion is indicated by a wide vegetated backshore (Ferreira et al., 2016). To the east of Praia de Faro (Figure 4.3), the peninsula has a low-density population consisting mainly of fishermen, most of whom reside at the lagoon margin. The eastern sandy spit next to Ancão Inlet, is the only area along the eastern sector of the

peninsula that is periodically overwashed due to its low-lying topography.



*Figure 4.3: Dune setting in the east sector at a stable dune position. The subtle undulations are evident. Praia de Faro settlement (central sector) is visible at the top-right corner of the picture.*

The beach of Ancão Peninsula was classified as Low Tide Terrace Beach (Martins et al., 1997; Vila et al., 1999) and is often reflective during high tide and intermediate during low tide (Ferreira, 2011). It has also presented a variable shoreline evolution with retreat at the western part (-0.8 m/yr), almost no variation at the central part and small accretion (+0.4 m/yr) at the eastern end (Ferreira et al., 2006). Sediments until 5-m depth are very homogenous, consisting of 80-90% of quartz along the barrier island system (Achab et al., 2014). Sediments from sampling along the peninsula were impacted by period (pre/after storm conditions) and profile (location) as grain size analysis as indicated by Achab et al. (2014). The results showed for Ancão Peninsula a mean grain size varying from 590  $\mu\text{m}$  to 790  $\mu\text{m}$ , while the modal class ranged from medium to very coarse sand. However, excluding the presence of coarse sediments, attributed to replenishment operations, the sampling at “natural” profiles, revealed a mean grain size of 560  $\mu\text{m}$  to 650  $\mu\text{m}$  (Achab et al., 2014).

#### **4.2. Oceanographic setting**

Tides in the area are semi-diurnal with an average tidal range of 2.8 m and 1.3 m during spring

and neap tides respectively, reaching a maximum of 3.5 m in spring tides. The dominant incident wave direction is W-SW (71% of the year), however E-SE directions, corresponding to waves generated by local winds, occur during 27% of the year (Costa et al., 2001). Mean annual significant offshore wave height ( $H_s$ ) is 1.0 m and the mean peak period is 8.2 s. The most significant storms (offshore  $H_s > 3\text{m}$ ) that affect the Ancão Peninsula are events from W-SW (Costa et al., 2001). Net longshore drift, which is considered the main sand supplier for this coastal system, is eastward directed, being nourished by updrift cliff erosion (Dias & Neal, 1992, Vila-Concejo et al., 2003), that is mostly taking place westwards in the western zone of Olhos de Água-Vilamoura. Estimates of longshore sediment transport feeding Ancão Peninsula vary according to authors (Vila-Concejo et al., 2003) ranging from  $6 \times 10^3$  to  $3 \times 10^5$  m<sup>3</sup>/yr (Achab et al., 2014; Popesso et al., 2016).

### ***4.3. Ancão Inlet***

Ancão Inlet is a small migrating inlet that has an average width of 300 m (Vila et al., 1999) with dynamic evolution in its morphology and position (Andrade, 1990; Vila-Concejo et al., 2002). The inlet undergoes a cyclic eastward migration (Weinholtz, 1964; 1968 and Esaguy, 1986 in Vila et al., 1999; Dias 1988; Pilkey et al., 1989; Popesso et al., 2016) until a limiting location where the infilling processes begin, and eventually force the shift to its earlier position or at the western part of the peninsula where a new inlet opens (Weinholtz, 1964; 1968 in Vila et al. 1999). Vila-Concejo et al. (2002) analysed the historical development of the Ancão Peninsula inlet from 1947 until 1996 and found that Ancão Inlet underwent two eastward migration cycles during this period. The eastward migration trends were very similar for both cycles, with the inlet showing an initial stage of readjustment (characterised by low migration rates), followed by a stage of high eastward migration rates, until reaching a limiting position; while migrating, Ancão Inlet maintains a stable cross-sectional area. This was distinguished as a high-energy migration pattern by Vila-Concejo et al. (2002; 2004). Due to coastal management measurements, the inlet was relocated 3.5 km westwards in June of 1997, to improve water exchange at the western part of Ria Formosa lagoon system (Dias et al., 2003; Ferreira, 2011). Since then the inlet has been migrating 80 m/yr to the East (Pacheco et al., 2007). In the winter of 2009/2010 the inlet experienced a migration jump<sup>3</sup> of about 300 m eastwards and until 2010 it was displaced more than 1 km to the east from its

---

<sup>3</sup> A new inlet opening has naturally formed after a storm, whereas the former inlet has closed.

relocation position (Ferreira, 2011). Finally, the most recent relocation took place in 2015, near the relocation position of 1997 (Popesso et al, 2016).

#### **4.4. Vegetational setting**

The littoral zone of Ancão Peninsula is comprised by coastal plant ecosystems belonging, according to its biogeographic and bioclimatic features, to the Iberian Atlantic Coast section and more specifically to the Algarviense sector (Asensi & Diez-Garretas, 2017) as represented in Figure 4.4. Asensi and Diez-Garretas (2017) reviewed the coastal dunes in the broader region that follow the general scheme of dune vegetation profile structure in which communities are replaced from sea level to inland according to ecological gradients like mobility, influence of sea wind or increasing organic matter. Specifically, the most seaward zone, where marine organic deposits are accumulated, is colonized by annual halo-nitrophilous plants such as *Cakile maritima* or *Salsola kali*, *Honckenia peploides* and *Polygonum maritimum*. These species form irregular and discontinuous communities on mobile sands with high salinity. The most widespread association in this territory is the *Honckenyo-Euphorbietum peplis*, which also can colonize other places in the innermost shifting dunes, when the typical communities occurring there are degraded. Another halo-nitrophilous community (*Polygono maritimi-Elytrigietum athericae*) can also develop in contact with the shifting dunes. On embryonic dunes usual plants are *Calystegia soldanella*, *Eryngium maritimum*, *Euphorbia paralias* or *Honckenya peploides*. Herbaceous communities of *Ammophila arenaria* are often formed at mobile (white) dunes. *Ammophila arenaria* is a hemicryptophyte species with long rhizomes that stabilizes the sand, allowing other dune plants to grow, such as *Calystegia soldanella*, *Eryngium maritimum*, *Euphorbia paralias*, *Medicago marina*, *Otanthus maritimus*, *Pancratium maritimum*. More inland, behind the mobile dunes (foredunes), some factors, for instance the decrease of wind strength, the low salinity of sands, and increase in organic matter, lead to an increasing diversity of plants, mainly chamaephytes, such as *Crucianella maritima*, *Euphorbia portlandica*, *Helichrysum picardii* etc. The grey dunes (secondary dunes) are colonized by the *Linario polygalifoliae-Corynephorum canescentis* community of Medium coverage formed by chamaephytes, hemicryptophytes and geophytes, like *Corynephorus canescens*, *Linaria polygalifolia*, *Euphorbia portlandica* etc.

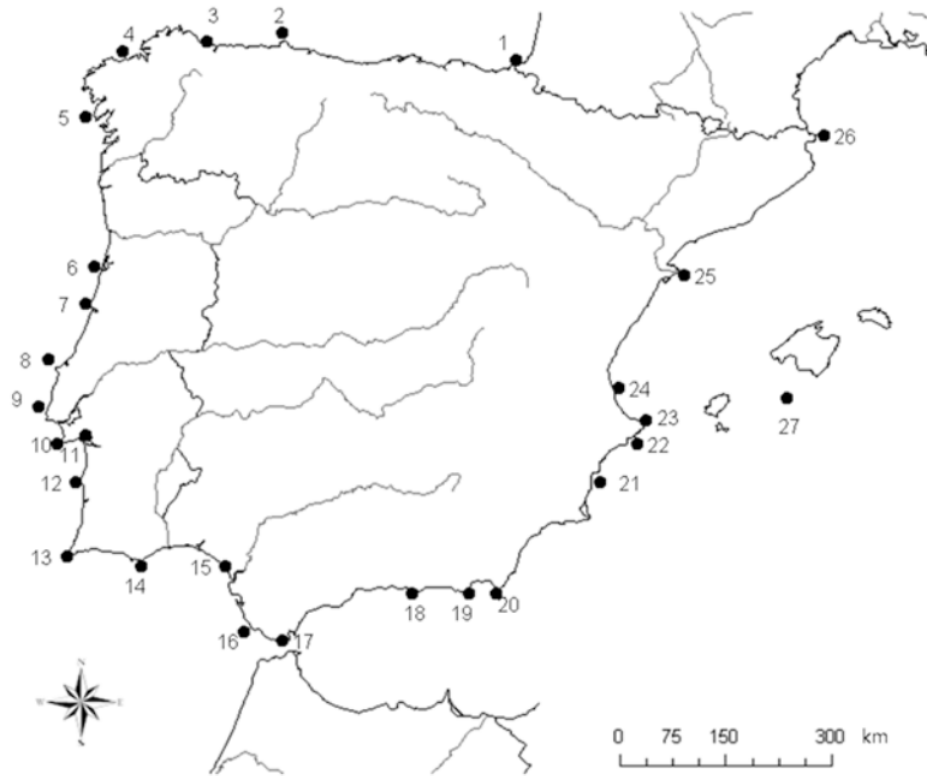


Figure 4.4: Map of the Iberian Peninsula coastline divided in stretches of specified bioclimatic and biogeographic features. The study area lies within the 'Iberian Atlantic Coast' section that stretches between Ria de Aveiro, Portugal (6) and Punta de Tarifa, Spain (17). Adapted from Asensi & Diez-Garretas, 2017.

## 5. Methodology

The analysis of the dune system and its development will focus in the western and eastern sectors of Praia de Faro in Ancão Peninsula (Figure 4.1 and 5.1). These sectors were selected as representative in terms of geomorphological variability of foredunes in the broader area of Ria Formosa after a preliminary assessment of the dune morphology through field visits and analysis of recent aerial photographs of the area. Aiming to investigate the dune morphology and the ongoing changes since the 1960's, a holistic approach has been adopted, where different aspects will congregate to elucidate the dune activity and its current form. These aspects refer to:

- current dune system state and morphology, evaluated from: a. field visits during September 2016-March 2017, b. use of GPS profiles and Digital Terrain Models (DTMs) and c. designation of dune zones and their maturity, according to the respective vegetational species.

- sediment transport potentials estimation by use of empirical formulas to ensue potential rates of aeolian sediment transport in Ancão Peninsula in the last twenty years.
- overall changes in the dune system: a. vertical and horizontal alterations derived from the profiles and DTMs, b. calculation of volumetric dune changes in distinct locations and c. investigation of shoreline evolution of the peninsula since 1952.

### 5.1. Dataset and data acquisition

The ascertainment of dune morphology along the Ancão Peninsula was carried out by using an extended dataset, presented in Table 1.

Table 1: Unified applied dataset with all constituents used for the investigation of the dune system state, development and sediment transport potentials.

Data	Year	Resolution	Acquisition	Details	Common profiles positions
Lidar	2009, Nov	0.23-0.5 m	European Project, MICORE	6 profiles: P0-P3, P5, P7 (extracted, 4 on the eastern sector, 2 on the western sector)	
Lidar	2011, May	2 m	Direção Geral Território (DGT)	6 profiles: P0-P3, P5, P7 (extracted, 4 on the eastern sector, 2 on the western sector)	
UAV	2016, Oct	30 cm	CIMA, University of Algarve	4 profiles: P0-P3 (extracted on the eastern sector) <sup>4</sup>	
RTK-GPS	2016/2017		CIMA, University of Algarve	2 profiles: P5, P7 (on the western sector)	
Aerial Photographs	1952, 1972, 1976, 1989, 2001, 2014		DGT, IGEOE (Instituto Geográfico do Exército)	Shoreline extraction	
Sediment	2016/2017		CIMA, University	5 profiles: 2 on the	

<sup>4</sup> The UAV survey could be conducted only for the eastern part due to legal permission issues.

sampling			of Algarve and the present dissertation	western sector, 3 on the eastern sector. The sediment sampling locations coincide on the profiles P0, P2, P5 and P7 that can be depicted in Figure 5.1 and one additional profile, G1, at the inlet, which is shown in Fig. 5.5.
Vegetation identification	2017, February & March	5m x 5m quadrats	CIMA, University of Algarve	7 transects (3 on the eastern sector, 4 on the western sector)
Wind data	1997-2016		Instituto Português do Mar e da Atmosfera (IPMA)	Sediment transport potentials evaluation

The geographical representation of the aforementioned data from Table 1 is given in Figure 5.1. Wind data and aerial photographs refer to the entire area and are therefore not illustrated in Figure 5.1.

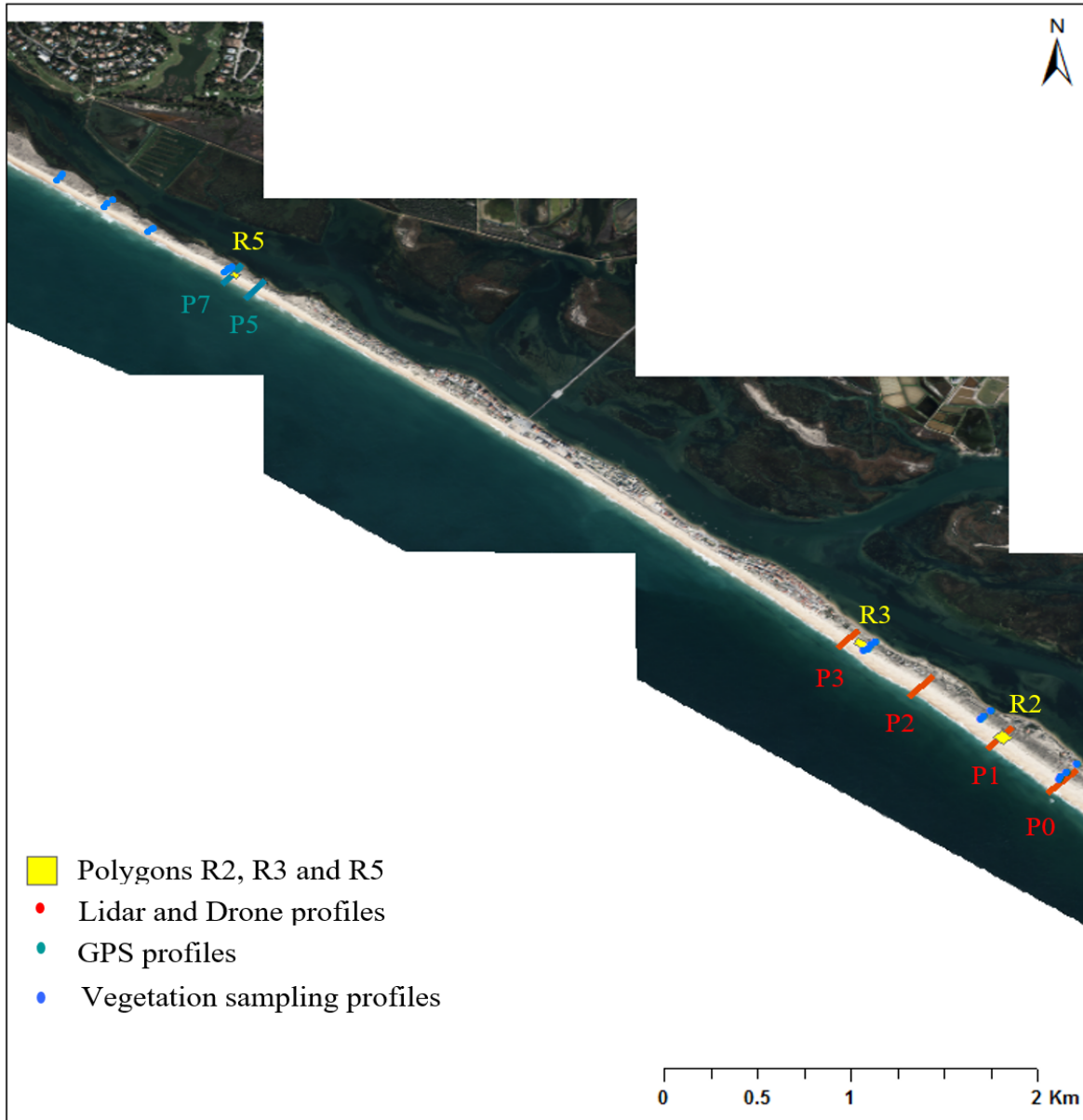


Figure 5.1: Overall illustrative map of the used dataset (Orthophoto of 2014).

## 5.2. Evaluation of dune morphology and morphological changes

The methodological topics presented in this section will be investigated and compared to determine impacting factors and evaluate the dune system development.

### 5.2.1. Dune morphology characterisation

The dune zones were distinguished initially on the field by their morphological characteristics: the most seaward sparse hummocks are considered as embryo or incipient dunes. Landwards, the more distinctly formed, elevated hummocks or dis-/ continuous dunes are designated as the first



foredunes. The next onshore placed dune crests are respectively considered the second or third (where applicable) dune ridges or mature foredunes. The in-between depression is characterized as an interdune area. In this way, the detailed topographical variations will be examined, where most of the profiles coincide with the vegetation sampling profiles.

The cartography of the dune belt was carried out in a GIS environment using the ArcGIS software to acquire information about the dune morphological zones and features: dune width, elevation, stoss slope, crest elevation, crest mapping, dune crest width.

The dune width extended from the early vegetation hummocks until the lee side vegetation, without considering the salt marsh type of vegetation. Regarding the eastern area, the stoss slope was defined as the slope starting at the dune toe of the backdunes reaching the dune crest. The backdunes were the highest foredunes with the most distinct ridge. At the western area, the stoss slope was calculated again from the dune toe to the dune crest of the first foredune (seaward) and is presented in a  $\tan \alpha$  form. On the eastern side, due to the various hummock and incipient dunes in the foredune area, the dune crest (highest point of dune) was taken into account to compute the dune slope, although it is encompassed in the mature dune zone. The dune crest ridge was delineated in relation to the respective morphology, namely to the dune crest.

The current geomorphological characterisation of the western sector was based on recent aerial photographs (2014) and on the Lidar dataset (2011) (grid resolution of 2 m). For the eastern sector, the DTM from a UAV survey (October 2016) was utilized (30-cm grid resolution).

### 5.2.2. Evaluation of vertical and horizontal changes

The evaluation of changes in the vertical and horizontal dimensions were investigated for the period 2009-2016, using the following approaches (see Table 1 and Figure 5.1):

Firstly, cross-shore profiles at a 2-year time scale were extracted from the Lidar datasets of 2009 and 2011 (Figure 5.1). Subsequently, in the western sector, two *in situ* cross-shore profiles were surveyed using a RTK-GPS in July 2016. The profiles took place during spring low tide starting from the dune crest to the beachface. In addition, four cross-shore profiles were extracted from the digital terrain model obtained from a UAV survey in October 2016 (grid resolution of 30 cm) at the eastern area. The comparison of horizontal and vertical in the profiles was made using the 2016 UAV DTM for the eastern site and the two profiles of the RTK-GPS for the western part.

Lastly, the aforementioned cross-shore profiles (extracted and *in situ*) were compared for the time-scale of 2009-2011 and 2011-2016.

### 5.2.3. Volumetric analysis

Volumetric estimations have been carried out in two perspectives: firstly, the obtained results from annual sediment transport potentials have been converted in volume per meter ( $V$ ,  $m^3/m$ ) using the formula  $\rho = m/V$ , where  $m$  the sediment mass (transported by one linear  $m$ , expressed in  $kg/m$ ), derived from the theoretical calculations and  $\rho$  the quartz density ( $2650 \text{ kg/m}^3$ ). The formula is modified in respect to the density parameter by incorporating the porosity factor for quartz medium sized sands (0.4):

$$V = \frac{m}{2650 \times (1 - 0.4)} \quad (3)$$

These results are theoretical, as they express potentials and not actual measurements. They are not referring to a specified area in the dune zone and do not distinguish between the different sectors, since only one mean grain size was considered.

Secondly, a direct volume assessment was also performed using the obtained DTMs. The volumetric changes at three selected sites R2, R3 (eastern area) and R5 (western area), as shown in Figure 5.1, have been computed in ArcGIS for the periods 2009-2011 (for the western and eastern sector) and 2011-2016 (for the eastern sector). The calculations in volume ( $m^3/m$ ) have been carried out after extracting the changes in elevation from the Lidar 2009, Lidar 2011 and UAV 2016 datasets for the respective periods. The polygons were outlined within the dune area from pioneer vegetation until the dune crest, to estimate the growth (if any) of the active dunes and represent the vertical differences for those defined areas.

For volume measurements, the computation has been made with ArcGIS Tool (in 3D Analyst tools, under Functional surface  $\rightarrow$  Surface volume). Subsequently, the volume of the vertical difference in respect to the examined polygons has been divided by the alongshore distance of the polygon, to obtain the volume of sand transferred (per meter) in the examined polygon. Finally, the theoretical (formulas, estimated potentials) and actual (ArcGIS volumes) measurements of the corresponding periods (2009-2011 and 2011-2016) have been compared.

Changes in beach topography associated with storm action and human activities were not taken into account in terms of gain/loss of sediments and therefore any possible vertical changes were attributed merely to wind transport. In addition, the calculated volume results (in the polygons) represent sand volume considering there are no sediment losses outside of the limits of the polygon.

### 5.3. *Vegetation classification and mapping*

The identification of vegetation was carried out during field visits (February and March of 2017) and was supported by a coastal vegetation guide book of dune systems flora in Ria Formosa (Muzavor et al, 2010), a versed dune vegetation smartphone application (“Sand Dunes Guide”, Field Studies Council, 2012) and two websites (‘www.biorede.pt’ and ‘www.flora-on.pt, 2014’) that include data, among others, about the vegetation of Portuguese coasts. Across 7 Transects, non-contiguous quadrats of 5 m x 5 m were created at several positions (30 plots in total), namely at three profiles in the eastern and four profiles in the western area of Ancão Peninsula (Figure 5.1 & 5.2), having an in-between distance, along the peninsula, of approximately 400 m. Each quadrat was placed at the morphological locations based on geomorphological criteria, i.e. distinct morphological attributes (hummocks, dune toe, dune crest, lee side, or prominent grouped vegetational communities, noticeably differentiating across the beach profile, i.e. from sparse and low vegetation seawards to denser, woody and darker coloured species towards inland).

The vegetation species have been further on classified in accordance to EUNIS (EUNIS habitat classification, 2004) in habitat types (Table 2). This enabled the identification of vegetation zones and could explain dune maturity or dune state (also per zone). Consequently, this would further allow possible correlation between morphological and vegetational/habitat zones.

Initially, on the field, the distinct geomorphological zones along the profile (incipient dune, dune toe, dune crest, lee of dune) were identified and characterized, in order to proceed with the respective inventory of the identified species in the selected quadrats. Consequently, the vegetation density of each species was measured to obtain the total cover density within the selected grids. For this purpose, the cover of the species (or their communities, when applicable) was estimated as follows: firstly, on the field, for those species that have an erect physiology, therefore not occupying a considerable surface (e.g. *Elymus farctus*), the number of the plants was counted. Their surface was then calculated in an Excel Spreadsheet by multiplying the counted number by the area of stem (considered as circle) (A) of the respective species using the formula:

$$A = \pi \times r^2 \quad (4),$$

where r the radius of the stem. In cases of short (a few cm below the sand ground) species with leaves (e.g. *Pancratium maritimum*) occupying further area, the area coated by leaves (length x width) is added to the stem area, as corresponds to each species. Regarding the species that have denser roots (e.g. *Ammophila arenaria*) or develop a canopy (e.g. *Artemisia crithmifolia*) the area

was approximately estimated in the field by the surface as viewed from above. Finally, the density represented in percentage (%) is quantified by dividing the total area of the respective species with the quadrat area (25 m<sup>2</sup>), resulting in the cover density of each species. The sum of densities of all present species in a quadrat consists the total cover density this quadrat and will be reflecting the cover density of this vegetational and hence morphological zone.



Figure 5.2: Detailed map of vegetation sampling locations in eastern (up) and western (down) sector at seven selected sites.

The characterization of dune type or formation were furthermore discriminated based on habitat standards, as established by Natura 2000 (European Environmental Agency, Ria Formosa code: PTZPE0017), which facilitated the characterization of the dune types in terms of vegetation. Table

2 displays the classification of the applicable habitats in the surveyed study areas and Figure 5.3 illustrates a typical beach environment with EUNIS code characterised environments.

Table 2: EUNIS habitat type classification (within the Natural Park of Ria Formosa) in dune systems of the surveyed areas according to EU Habitats Directive (92/43/EEC) (*European Environmental Agency (EEA)*).

<b>Habitat type code</b>	<b>Habitat type</b>	<b>Description</b>	<b>Main representative species</b>
<b>1210</b>	Annual vegetation of drift lines	Formations of annuals or representatives of annuals and perennials, occupying accumulations of drift material and gravel rich in nitrogenous organic matter	<i>Cakile maritima</i> , <i>Eryngium maritimum</i> , <i>Euphorbia paralias/peplis</i> , <i>Polygonum spp.</i>
<b>2110</b>	Embryonic shifting dunes	Formations of the coast representing the first stages of dune construction, constituted by ripples or raised sand surfaces of the upper beach or by a seaward fringe at the foot of the tall  Dunes	<i>Elymus farctus</i> , <i>Eryngium maritimum</i> , <i>Euphorbia peplis</i> , <i>Honkenya peploides</i> , <i>Medicago marina</i> , <i>Otanthus maritimus</i> , <i>Pancratium maritimum</i>
<b>2120</b>	Shifting dunes along the shoreline with <i>Ammophila arenaria</i> ('white dunes')	Mobile dunes forming the seaward cordon or cordons of dune systems of the coasts	<i>Ammophila arenaria</i> , <i>Calystegia soldanella</i> , <i>Cutandia maritima</i> , <i>Cyperus capitatus</i> , <i>Eryngium maritimum</i> , <i>Euphorbia paralias</i> , <i>Medicago marina</i> , <i>Otanthus maritimus</i> , <i>Polygonum maritimum</i>

<b>2130</b>	Fixed coastal dunes with herbaceous vegetation ('grey dunes')	Fixed or semifixed dunes	<i>Artemisia crithmifolia/campestris</i> , <i>Armeria pungens</i> , <i>Carex arenaria</i> , <i>Crucianella maritima</i> , <i>Helichrysum italicum</i> , <i>Pancratium maritimum</i>
-------------	---	--------------------------	---

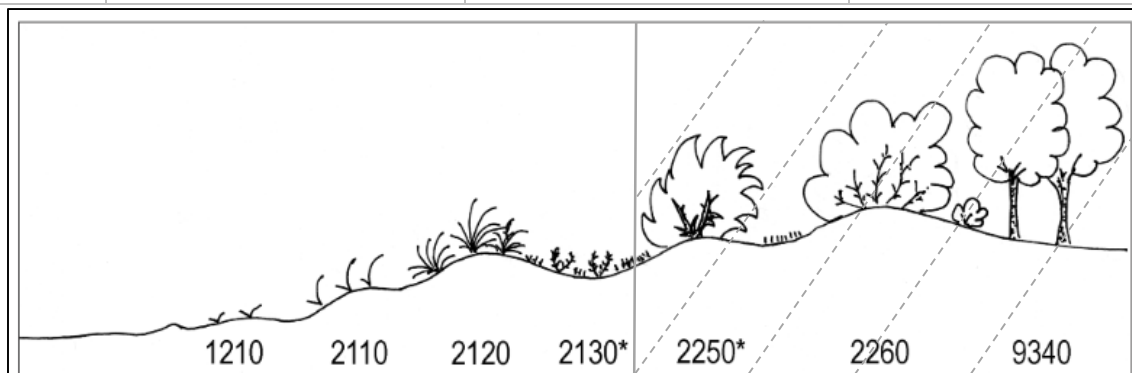


Figure 5.3: Scheme of a typical coastal zonation representing EU habitats complementing Table 2. In Ancão Peninsula the given developed habitat types extend until the fixed dunes (code 2130) (adapted from Prisco et al., 2012).

The dune types in terms of habitats will be characterized according to Table 2 and subsequently correlations with the observed morphological zones will be elucidated. According to Table 2, the species of habitat types 1210 and 2110, that are located most seaward, will be onwards referred as embryo dunes. In cases of absent hummock formation, the mention will be as incipient vegetation. Habitat type 2120 species are included in foredune formations, and more specifically in the first (seaward) foredunes.

Some species identified and located in the study area were not included in the EUNIS inventory (Table 3), and the designation of habitat zone was accomplished by “Flora-on” (Sociedade Portuguesa de Botânica, 2014).

Table 3: Supplementary table of existing species in Ancão Peninsula.

<b>Species</b>	<b>Habitat type</b>	<b>Corresponding to EUNIS habitat code</b>
<i>Silene nicaeensis</i>	Primary dune and/or bare places in secondary dunes	2120 2130

<i>Lotus creticus</i>	Primary dunes but also in	2120
	secondary dunes	2130
<i>Armeria pungens</i>	Primary dunes but also in	2120
	secondary dunes	2130
<i>Paronychia argentea</i>	Unspecified dune zone	
<i>Reichardia gaditana</i>	Unspecified dune zone	
<i>Carpobrotus edulis</i>	Unspecified dune zone	

**5.4. Textural analysis**

For the grain size characterization of the study area samples were collected at selected morphologies (at the beachface, backshore and embryo-dune) across five profiles (Figure 5.4). In total, 29 sand samples were acquired, representing the upper 5 mm of the surficial sediment. The sampling took place in distinct seasons (summer, fall and winter) within the period 2016-2017 at low tide during spring tides, at several profiles: G1, P0 and P2 in the eastern area, P5 and P7 in the western area (Figure 5.1). From each beach sample, an approximately 100 g portion was selected, dried and subsequently sieved using 0.5 phi intervals to determine grain size distribution. Textural parameters were furtherly measured using the Geometric Folk and Ward graphical measures technique (Folk & Ward, 1957) in GRADISTAT program (Blott & Pye, 2001). Additional textural parameters of sorting and skewness were also calculated. Finally, the general grain size description in the results was given based on Udden (1914) and Wentworth (1922). The results from the different profiles will accommodate to interpret possible sediment transfer patterns from the beachface to the dune and sorting processes.

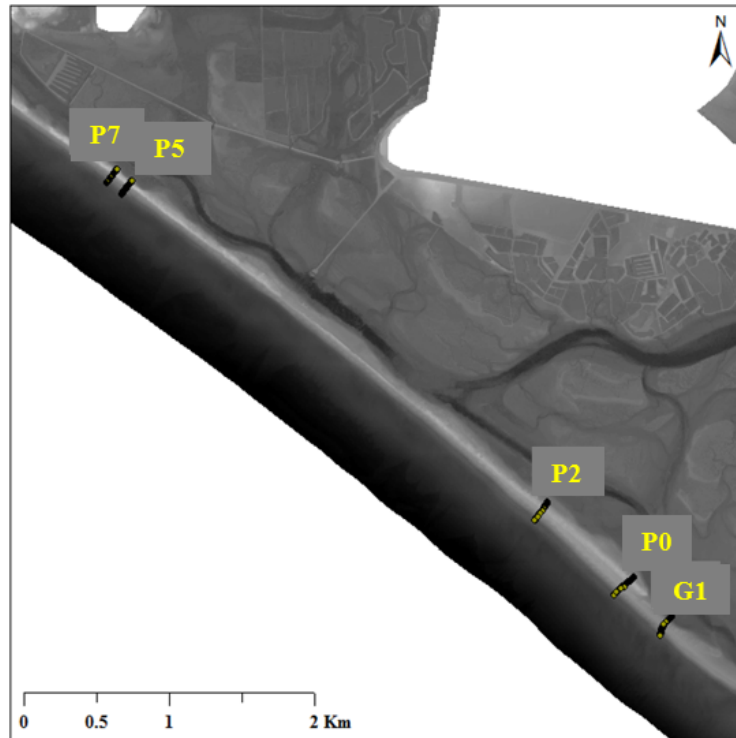


Figure 5.4: The profiles in Ancão Peninsula, across which the sand samples were acquired (beachface, backshore and dune toe), with the positions being obtained by RTK-GPS (photo from 2011 Lidar dataset).

### 5.5. Wind field regime

Wind data from the adjacent airport were used for evaluating the wind field regime. The dataset extends for the period of 1997-2016 with records of average velocity every 10 min (m/s). The wind record represents wind at 10 m above ground level and was provided by the Portuguese Institute for Ocean and Atmosphere. It must be noted that there is a gap in the records of November and December of 2013 and of the year 2014 regarding direction data, thus those data were not used for the analysis of the wind field regime, as wind direction was essential for the sediment transport potential approaches. To replace this time gap in order to have an integrated idea following computations, the average rate of 2013 and 2015 was used.

Consequently, wind data were filtered by directions, considering as favouring dune development winds, only onshore winds, which according to the alignment of the peninsula are within  $130^\circ$  and  $310^\circ$ . Hence, offshore and parallel to the dune ridge winds were eliminated (see detailed approach described in ‘Aeolian sediment transport potentials and dune changes’, section 5.6).



### 5.6. Aeolian sediment transport potential and dune changes

In respect to the investigation of sediment transport potentials, a simplified approach has been employed, whereas no further limiting factors (besides wind angle and grain size) have been applied (i.e. moisture factor, beachface slope, fetch distance etc.). Instead the transport potential was based on the grain size and the angle of wind approach.

Specifically, the aeolian sediment transport has been calculated using the results of the textural analysis, by applying two approaches, which will be subsequently described. Initially, the critical shear velocity ( $u_{*c}$ ), at which a sand particle starts to move, was calculated using the relative Bagnold formula (1941):

$$u_{*c} = A \sqrt{\frac{\rho_s - \rho}{\rho} g d} \quad (5)$$

where A is a constant coefficient (0.085 during active saltation), d is the sediments median diameter (m),  $\rho_s$  is the mass density of sediment (2650 kg/m<sup>3</sup> for quartz grains),  $\rho$  is the density of air (1.23 kg/m<sup>3</sup>), g is the gravitational acceleration (9.81ms<sup>-2</sup>).

Subsequently, wind speeds measured at 10 m were transformed into shear velocities applying the Prandtl equation (1904) that yields the logarithmic profile of the atmospheric boundary layer (Law-of-the-wall):

$$u_z = (u_* / k) \ln(z / z_0) \quad (6)$$

where  $u_z$  is the wind speed at the elevation z (10 m),  $u_*$  is the shear velocity,  $k \approx 0.4$  is the von Karman universal constant for turbulent flow and  $z_0$  is the roughness length of the surface defined by Bagnold (1941),  $z_0 = D_{50} / 30$ , where  $D_{50}$  is the median grain size diameter (m).

Equations 5 and 6 were also utilized for defining a windy event in the study area using additionally the mean grain size, as resulted from the beachface environment.

In the present study, potentials of sediment transport were calculated applying the model proposed by Lettau and Lettau (1977):

$$q = K \left( \frac{\rho}{g} \right) \sqrt{D / D_{ref}} u_*^2 (u_* - u_{*c}) \quad (7)$$

where q is the sediment transport rate in kg (m s)<sup>-1</sup>, K is an empirical coefficient (4.2), D is the diameter of the representative sand size (m) and  $D_{ref}$  is the reference median grain size (0.25 m).

Total sediment transport potentials and annual rates were estimated using beachface grain size, postulating that beachface sand is the sand supplier of the dunes. Two approaches have been

applied for these estimations. Firstly, the sediment transport potentials were calculated for the period 1997-2016 (excluding the 14 months of direction record gap) applying the Lettau-Lettau model (Equation 7), using the mean grain size of the beachface samples. Secondly, the sediment transport for each grain size class has been calculated and subsequently the percentages of weights for all sediment classes ( $\% X_i$ ), as obtained from the grain size analysis (beachface results), were multiplied by the respective sediment per class transport ( $ST$ ) and summed to obtain the total sediment transport value ( $\Sigma q$ ) (or correspondingly the sediment transport rates per year), as described in the formula below:

$$\begin{aligned} \Sigma q = & (\%X_{4000} \times ST_{4000} + \%X_{2800} \times ST_{2800} + \%X_{2000} \times ST_{2000} + \%X_{1400} \times ST_{1400} + \\ & \%X_{1000} \times ST_{1000} + \%X_{710} \times ST_{710} + \%X_{500} \times ST_{500} + \%X_{355} \times ST_{355} + \%X_{250} \times ST_{250} + \\ & \%X_{180} \times ST_{180} + \%X_{125} \times ST_{125}) \end{aligned} \quad (8)$$

The formula reflects the classes of grain sizes (in  $\mu\text{m}$ ) present in the grain size analysis, where the lowest limit of grain size class is 125  $\mu\text{m}$ . The highest grain size limit starts at 4000  $\mu\text{m}$  that is the critical grain size, at which initiation of sediment transport in respect to the wind field regime in the study area. Grain size classes below 125  $\mu\text{m}$ , are not expressed in the formula, as they are either weight negligible or not present.

Aeolian sediment transport potentials were defined by determining the wind direction range that promotes dune development (in horizontal or vertical accumulation) or dune formation, so the across and oblique wind ranges were utilized. For this, the direction of the peninsula was taken into account, which was measured  $-50^\circ$  in respect to North (or  $310^\circ$ ). Thereupon, a directional range of onshore winds coming from between  $130^\circ$  and  $310^\circ$  was defined for the calculation of sediment transport, as these are the ones facing the seaward side of the dune system. The angle between the wind and the perpendicular to the coastline ( $\alpha$ ) was defined and its cosine was applied to the sediment transport equation to result in the sediment transport values coming either from perpendicular or oblique wind directions (Equation 9). Hence, offshore directed winds and the alongshore wind components are eliminated.

$$q_n = q \times \cos \alpha \quad (9)$$

Consequently, to assess the variation of wind activity in the twenty-year period and thus the respective fluctuation in sediment transport potentials, wind annual rates have been computed and contrasted within the two decades.

### ***5.7. Shoreline evolution***

An analysis of the shoreline evolution was conducted in ArcGIS in an extent of 9.5 km along the peninsula, supported with aerial photos from 1952 to 2014. The results can be later used to correlate the shoreline movement with dune system activity. For this purpose, the following approach was adopted: the cartography of the pioneer vegetation was delineated, defining the limit between the beach-dune environment for five aerial photograph settings from 1952, 1972, 1989, 2001 and 2014. Then, by marking a baseline offshore, the variations between the vegetation lines were calculated in respect to the baseline, to extract later the shoreline evolution rates for the respective four periods. The vegetation line is a reliable coastal feature for identifying shoreline changes (Alves, 2007), as it reflects the erosional or accretional trends of the shoreline in a long-term scale (e.g. Dolan et al., 1991; Birmingham & French, 2017), thus it enables conclusions to be derived in relation to the dune system migration and development throughout the years up to present.

The used photos of 1952, 1972, 1989, 2001 were georeferenced using common reference points (minimum 30) with respect to more recent aerial photos. Additional aerial photos of in-between years (1947, 1958, 1969, and 1976) were also georeferenced to accommodate higher accuracy. The multiple images of each year, due to their partial spatial extent in representation of Ancão Peninsula, were subsequently combined into a mosaic photo covering the entire study area and when required a conversion of the coordinate system took place.

Additionally, to gain some supporting results the mark of the wet/dry limit on the sand, which was clearly identified as a significant tonal change (e.g. Crowell et al., 1991; Moore, 2000) for the same photographs was also mapped. However, this can be considered a less reliable indicator, since it is affected for instance by the wind/wave conditions, tidal stage (Mendez, 2007), beach slope and seasonal changes (Crowell et al., 1991). Subsequently, the variations in the position of the shoreline were calculated using the Digital Shoreline Analysis System tool (DSAS) (Thieler et al., 2009), by production of alongshore transects (every 20 m), to quantify the net shoreline movement (NSM, distance between the oldest and the youngest shorelines) and the linear regression rates (LRR, fitting a least-squares regression line to all shoreline points for each transect) for the

examined periods. Each line represents the vegetation/ wet-dry mark of the corresponding year. To end up with the safest results possible regarding the studied parameters (NSM and LRR), a threshold of five present lines was applied (representing the appearance of vegetation/ wet-dry limit in the five studied years). So, when there was no vegetation present due to reasons listed subsequently, this requirement was not achieved and the representation exhibits gaps, concluding to a final 42% of the analysed area. The fact of higher gap occurrence in vegetation in the western part is mostly owed to blowouts and in the eastern part due to human occupation. The central part is entirely occupied by human structures. The same criterion was applied for the results of the wet/dry beach mark proxy (transects 25 m apart), whereas a 75% of representation of the study area was obtained due to less discontinuities in the mark line.

Limitations regarding the mapping of the vegetation and wet/dry mark line arose and the relative details in respect to their handling are in sum noted below:

- In locations, where incipient vegetation was sparse, the delineation was a connective line between the pioneer vegetation. Occasionally, this distinction was accommodated by morphological attributes, e.g. mounds, between the beach/ dune limit.
- Discontinuity in vegetation is found in the western part due to wide blowouts mouths (>5 m) or total lack of vegetation due to human intervention (houses, walls, fences, parking lot etc.) in the central and eastern part, therefore the vegetation line is in those segments interrupted. So, for those occasions no vegetation was taken into account.
- Error is involved regarding the delineation of the pioneer vegetation in the older photos (1952) with lower resolution, whereas in higher resolution photos the new vegetation is clearly defined.
- The spatial range of the photos is not the same for all years. Therefore -and after the application of the five present lines requirement-, only the common transects within the same area were considered. This explains the 75% representation of the wet/dry line, that is related mostly to the dynamic morphology of Ancão Inlet area.
- Dune vegetation in front of walls and houses was also incorporated in the vegetation line.

Finally, the quantification of the shoreline evolution for each of the four periods was calculated by the end-point-rate method, where the distance between the two shorelines is measured (from the earliest to the most recent) and then divided by the time (years) elapsed between the successive shoreline positions (Crowell et al., 1999b). Therewith, the shoreline evolution rates (m/yr) will be

obtained to derive the shoreline trends (accretional/erosional) to further accommodate correlation with the dune system morphology. The computations are carried out per transect and in regard to the vegetation line. Statistically, the results of the data are not significant (typical  $\alpha=0.05$ ), as there are only five years examined and thus p-value is greater than the 0.05 significance level (p-value=0.878).

## 6. Results

### 6.1. Textural analysis

The spatial variation of the textural characteristics of 29 sediment samples is described in respect to particle size, sorting and skewness at the selected points across the beach profiles (beachface, backshore and dune/dune toe) alongshore the study area (G1, P0 and P2 at the eastern area, P5 and P7 in the western area).

The mean particle size of the samples has a wide range and varies between 340  $\mu\text{m}$  and 1023  $\mu\text{m}$  (0 and 5  $\phi$ ). The mean grain size for each distinct morphology is: 466  $\mu\text{m}$  at the beachface, 624  $\mu\text{m}$  at the backshore and 452  $\mu\text{m}$  at the dune. The majority of samples have a mean grain size of 340-630  $\mu\text{m}$  (medium and coarse sand) and are mainly moderately well sorted, symmetrically skewed and mesokurtic. The discrepancies of the three coarsest samples are owed to the presence of shell fragments and gravels.

Furthermore, the mean grain size distribution in relation to the sampled morphologies was examined, therefore samples were grouped into beachface, backshore and dune/ dune toe (Figure 6.1 and Figure 6.2).

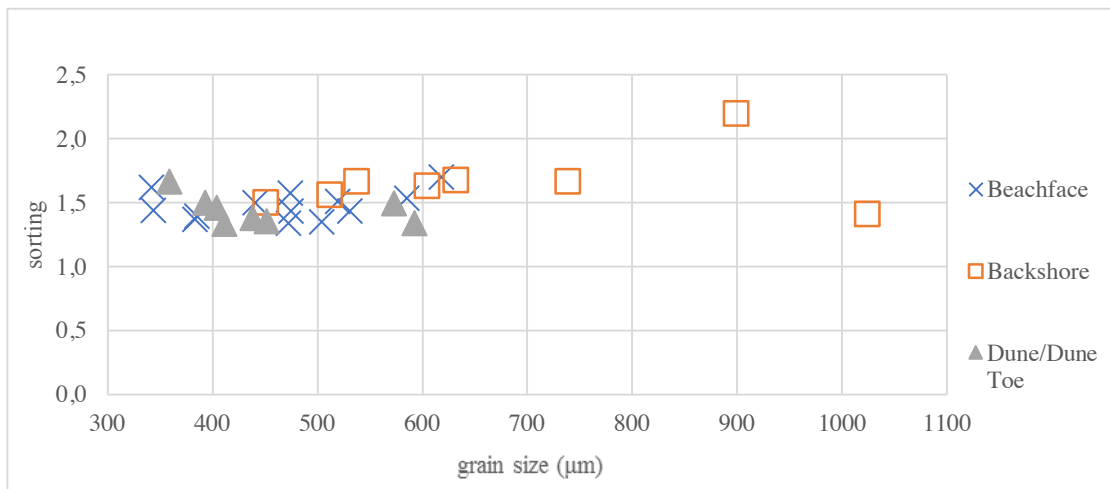


Figure 6.1: Mean Grain size ( $\mu\text{m}$ ) vs sorting per zone.

The results indicated variation of grain size in the distinct morphologies (Figure 6.2) (beachface, backshore of dune/dune toe) and sampling period. Profile P5 had coarse sand on the backshore and medium sand on the beachface and dune. Profile P7 showed a homogenous grain size, nevertheless only one sampling was considered. The beachface of P2 profile exhibits similarity in the grain size, however there are differentiations at the dune. Oppositely, at P0, the dune shows alike results in grain size, whereas fluctuation at the beachface and backshore is exhibited. At G1 profile, close to the inlet, the beachface and backshore mean grain size varies. In general terms, it is ascertained that the backshore accommodates the coarser sand. Additionally, the beachface and dune demonstrate a milder differentiation along the profiles, in contrast to the backshore. So, a trend can be observed, whereas the beachface and dune zones share particle groups of alike size and the in between zone of the backshore is enriched in coarser sands.

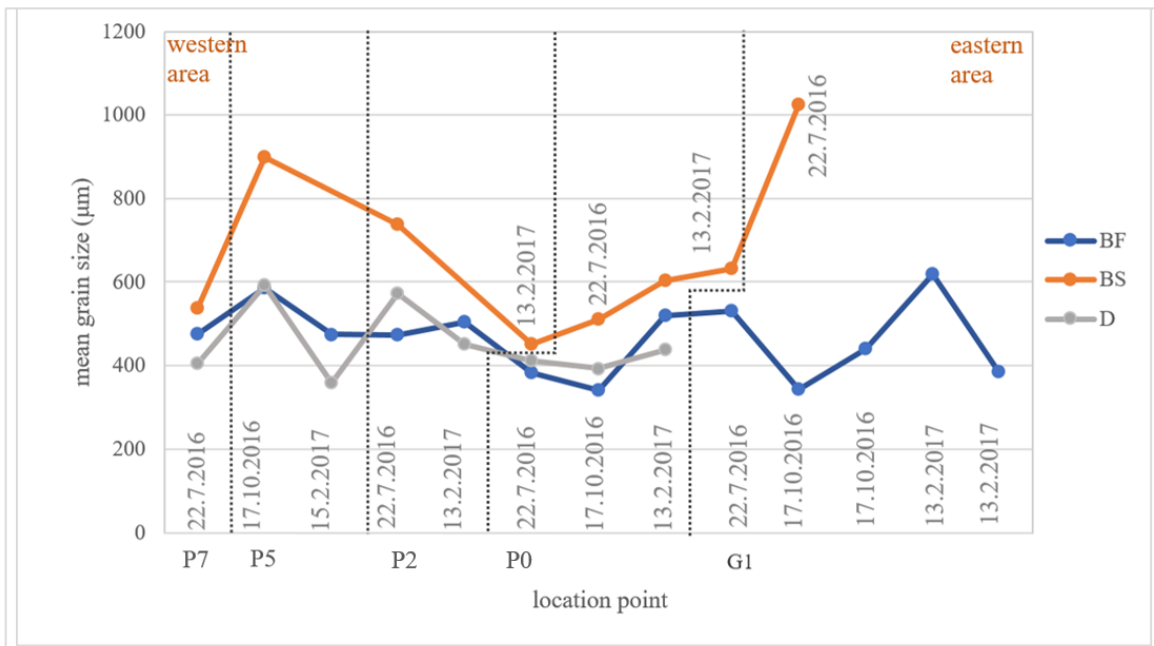


Figure 6.2: Grain size distribution per site and morphology of all samples in respect to their sampling date. The vertical dashed lines discriminate each profile. BF: beachface, BS: backshore, D: Dune toe/Dune

In respect to sorting parameter, the average sorting is 1.52, corresponding to moderately well sorted sand (Figure 6.3). The sorting per sampling site (G1: most eastern location, near the inlet and P7: most western location) shows no particular pattern, and only a few outliers are present (sites G1, P2 and P5), nevertheless it is slightly higher and tending to increase at the backshore. At the beachface and dune the sorting is similar and has a moderately better sorting (1.35), where mostly finer sands of 340-530 µm are accumulated, at the backshore the arrangement is medium

to coarse sands of 450-1023  $\mu\text{m}$  and the dune/dune toe are richer in finer sand of 360-450  $\mu\text{m}$ .

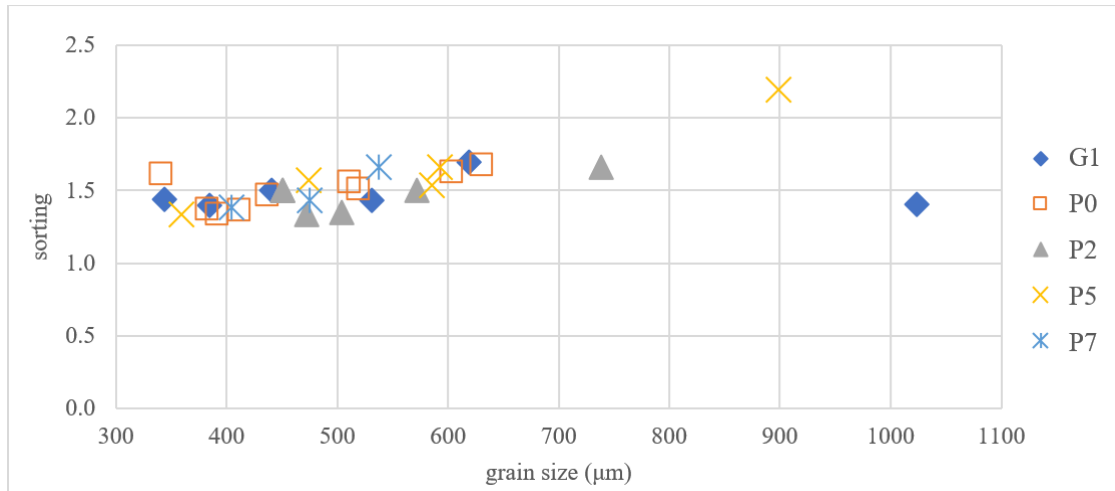


Figure 6.3: Mean grain size ( $\mu\text{m}$ ) versus sorting per profile for 29 beach samples of 2016-2017.

Finally, to apprehend the asymmetry deviation, the skewness at each position was plotted (Figure 6.4). The skewness of the overall sample population is mainly concentrated in a range between -0.1 and 0.2, which indicates a symmetric distribution with an inclination of skewness towards coarse sand. At the beachface skewness ranges from -0.1 to 0.17 (excluding an outlier at P2: -0.23, BF), characterizing an almost symmetrical distribution. Likewise, within a smaller range (-0.05 to 0.1) the dune sand skewness is symmetrical. On the contrast, the backshore, at which the coarsest sand was sampled, has only positive skewness (0 to 0.2) presenting fine skewed distribution, underlying the asymmetry of the coarser sediments of the backshore.

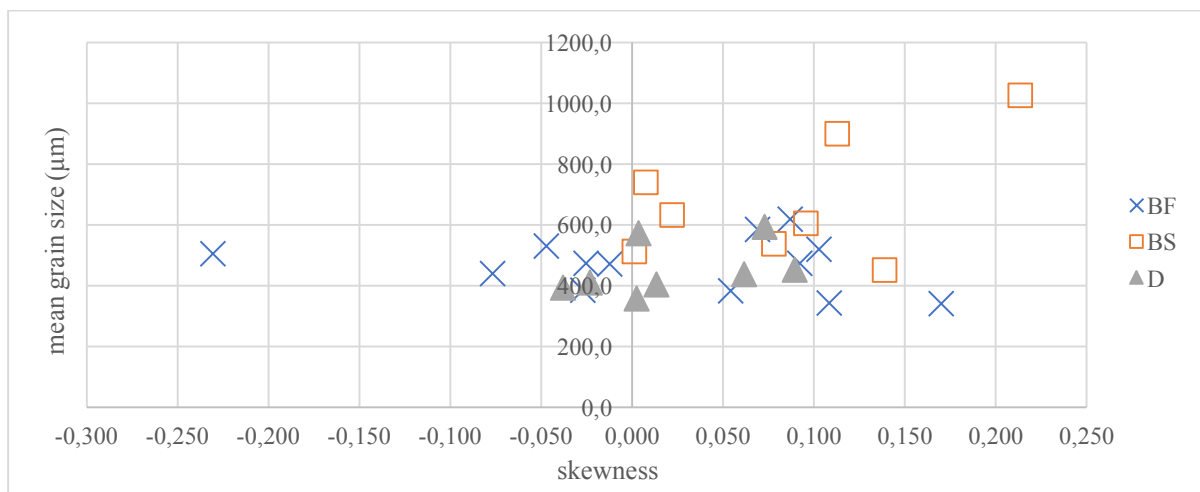


Figure 6.4: Skewness vs mean grain size per position plot for all sites.



At this point it is essential to state, that to estimate (when applicable) sediment transport potentials, (section 6.6.) a certain outlier, namely the backshore sample of profile P5, as well as the samples of the G1 profile, were excluded. More specifically, the backshore sample of P5 displayed a very coarse mean grain size of 899  $\mu\text{m}$  (Figure 6.2), which compared to respective backshore samples of previous years (from grain size data archive of CIMA research group of University of Algarve for Ancão Peninsula of the last twenty years), this was not a representative sample. It is approximately estimated that the backshore sand does not exceed the 600-700  $\mu\text{m}$  (Achab et al., 2014). Additionally, all data of G1 samples will not be included for further analysis, since no dune formation exists in that area near the inlet. Considering the particular location of the profile, namely in the vicinity of the inlet, the entire site is highly influenced by wave and tide action and cannot ascribe reliable grain size results. Nevertheless, it was regarded important to explore and present the grain size distribution along the entire peninsula, to hold an integrated aspect of the grain size spectrum in the study area.

### ***6.2. Wind field regime***

The wind distribution of the last 20 years (1997-2016) indicated NW and SW dominant directions of winds in the study area, as depicted in Figure 6.5. Low intensity velocities (<5 m/s) prevail, moderate velocities (5-10 m/s) are more frequent from southwest directions and intense winds of 10-15 m/s are mostly from WSW and E. Wind speeds above 15 m/s were present in the study area, however occupied only a minor fraction (approximately 53 h) of the total 20-year record.

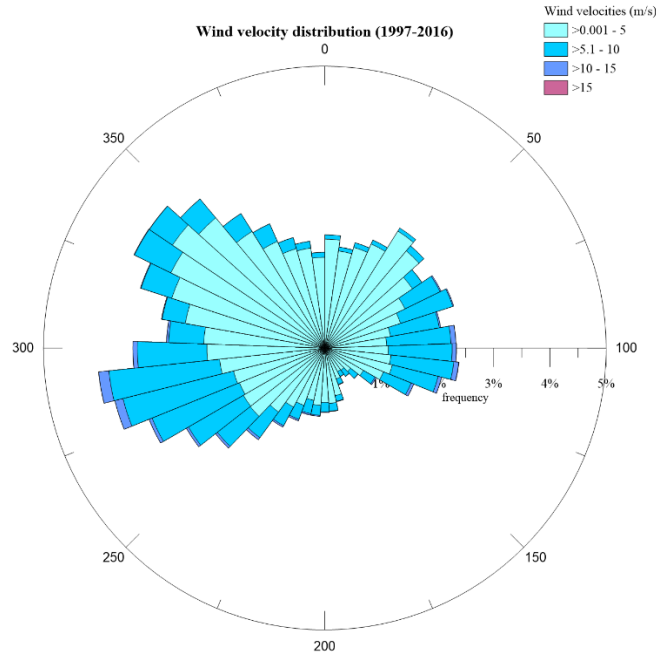


Figure 6.5: Wind rose showing the speed and frequency of wind blowing for the study area.

The dominant directions of the favouring winds for dune development are designated by WSW and NW conditions, as shown in Figure 6.6a. Those winds represent the 45% of the total wind in the period of examination. Furthermore, a ‘windy event’ for the study area is defined by determining the threshold velocity for sediment movement initiation (Equation 5) using the mean grain size at the beachface (466  $\mu\text{m}$ ). This resulted in a value of  $u_{\text{cr}}$  of 8.9 m/s. In Figure 6.6b, the wind intensity above  $u_{\text{cr}}$  is shown (for the filtered direction range) being dominantly from WSW. The windy events covered a 3.7% of the favourable direction events and 1.7% of the total events in respect to the initial dataset.

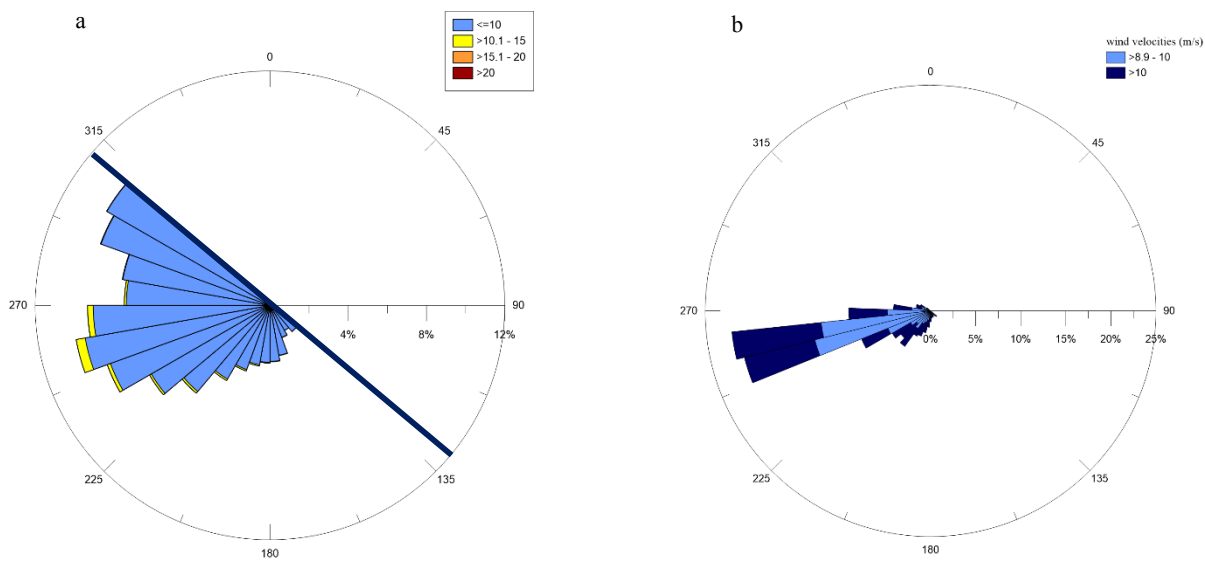


Figure 6.6: a) Wind velocities distribution of favourable directions (1997-2016). The dark blue line represents the shoreline orientation. b) Wind velocities direction above the threshold ( $>8.9$  m/s).

In Figure 6.7 the sum of windy events ( $>8.9$  m/s) for each month is presented in the twenty-year period (each 10-min record represents one event). Additionally, the average velocity of the corresponding month is also plotted, taking into account solely the favourable wind direction. The windy events are not concentrated in the winter months (December, January and February), but were also occurring during the entire year, namely most frequently in autumn and spring months, (marked months in Figure 6.7). The highest mean velocities of 1998 were marked and that December the highest velocities in the 20-year span have occurred. However, the frequency of windy events was not correspondingly high, namely 84 windy events. Intense average velocities were also recorded in 2002 and 2003, especially in the winter months (November 2002 until February 2003), but with constrained frequency of events (approximately 180 events of 10 minutes ( $\sim 10$  days)). In 2008 and 2009 the most considerably frequent windy events took place in April (450) and December (522) respectively, accompanied by average velocities of approximately 11 m/s. Furthermore, February of 2010 was also characterized by high number as well, namely 420, windy events (10.8 m/s).

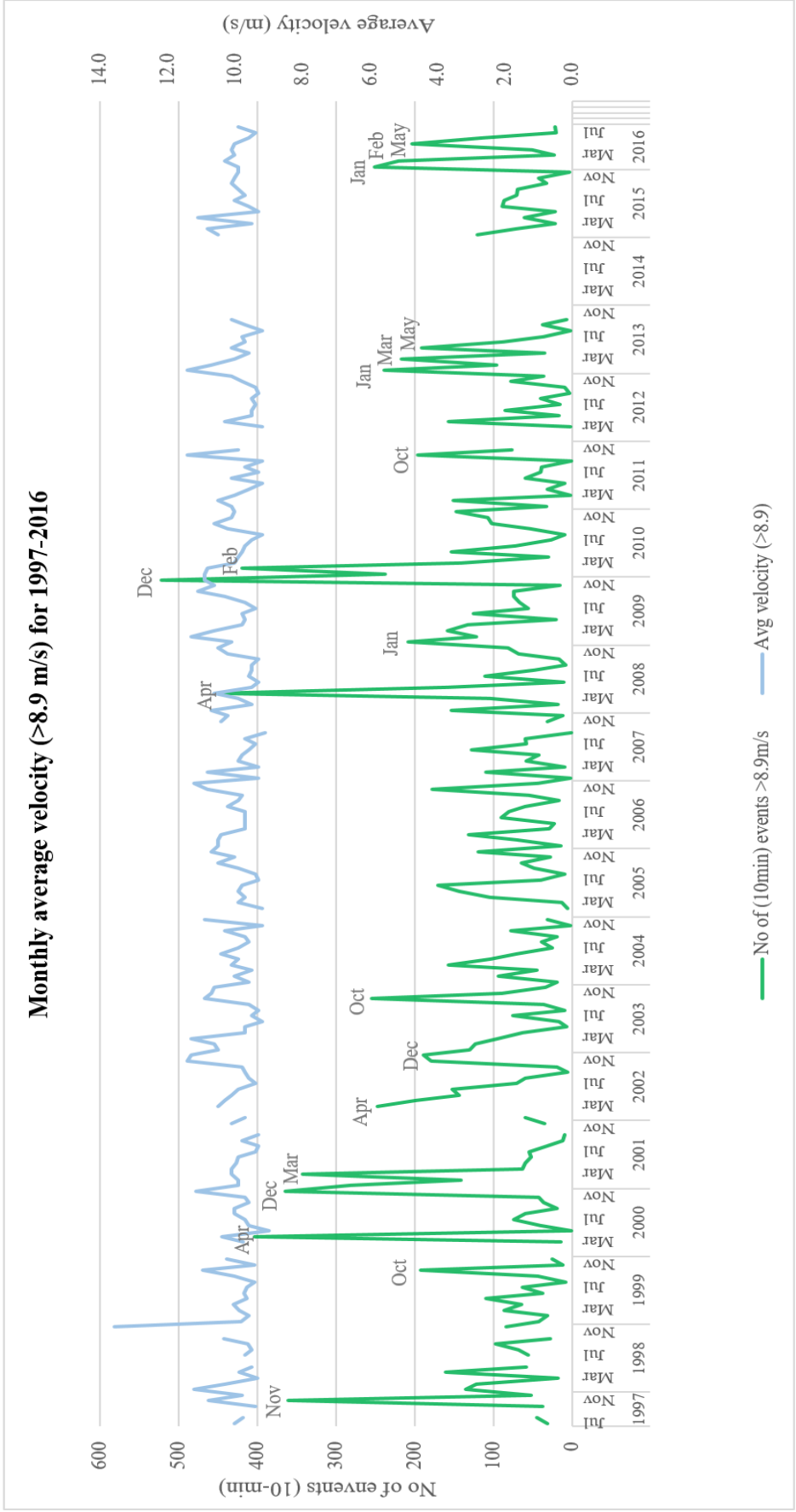


Figure 6.7: Average monthly velocities for events above the threshold (8.9 m/s), in blue, and number of these events per month (in green) for the 1997-2016 period. The gaps in the graph line represent either absence of windy events in the corresponding month or as referred in the 'Methodology' section for November and December 2013 and for 2014 a deficiency of the direction data. On the graph, the months with more than 180 windy events are noted.

### 6.3. Dune morphology

In the western area, there is one distinct ridge with three morphological zones: dune toe, dune crest and lee side. Low incipient hummocks are present only in the most western site, Transect 8 (Table 4). Regarding the eastern sector, the morphology is more complex. Transects 3 and 4 showed five pronounced zones, while six are present in Transect 2. Additionally, also distinguishable from, in Transect 2 concurrently with six dune zones, the peninsula width is wider, and in Transects 2 and 3 the incipient vegetation area is more extended seaward opposed to Transect 4. On the other hand, Transects 2 and 3 were kept intact from human occupation. Table 5 summarizes the morphological units at each site in the eastern area of the peninsula, along a dune transect. The morphological differentiation between the eastern and western sector is evident, nevertheless at both sides the vegetation was changing along with the present corresponding morphology at each area, either in species introduction/absence or in density (total/per species coverage).

Table 4: Morphological zones of distinct dune habitats at the selected transects in the western area. The (-) sign signifies the absence of that morphological zone at the specific transect. The numbering of the morphologies starts from the shore. Transect 5 is the most eastern transect in the western area (near the bridge) and Transect 8 is the most westward.

<b>Transect 8</b>	<b>Transect 7</b>	<b>Transect 6</b>	<b>Transect 5</b>
-	-	-	Embryo dune
Dune toe	Dune toe	Dune toe	Dune toe
Crest	Crest	Crest	Crest
Lee side	Lee side	Lee side	Lee side

Table 5: Geomorphological zone classification with distinct dune habitats at the selected transects in the eastern area. The numbering of the morphologies starts from the shore. The (-) sign signifies the absence of that morphological zone at the specific transect.

Transect 4	Transect 3	Transect 2
-	-	Embryo dune
-	-	Crest 1
Dune 2 toe	Dune 2 toe	-
Crest 2	Crest 2	Crest 2
-	-	Dune 3 Toe
Crest 3	Crest 3	Crest 3
Lee side	Lee side	Lee side

Subsequently, analysing the Lidar datasets of 2009 and 2011, the surveyed cross-shore profiles and the UAV dataset of 2016, six profiles (four at the eastern area: P0-P3, and two at the western area: P5 and P7) were extracted (Figure 6.8). The cross-shore profiles extend from the dune to the beachface and their levels are relative to mean sea level (MSL), as presented below (Figure 6.9 and 6.10).

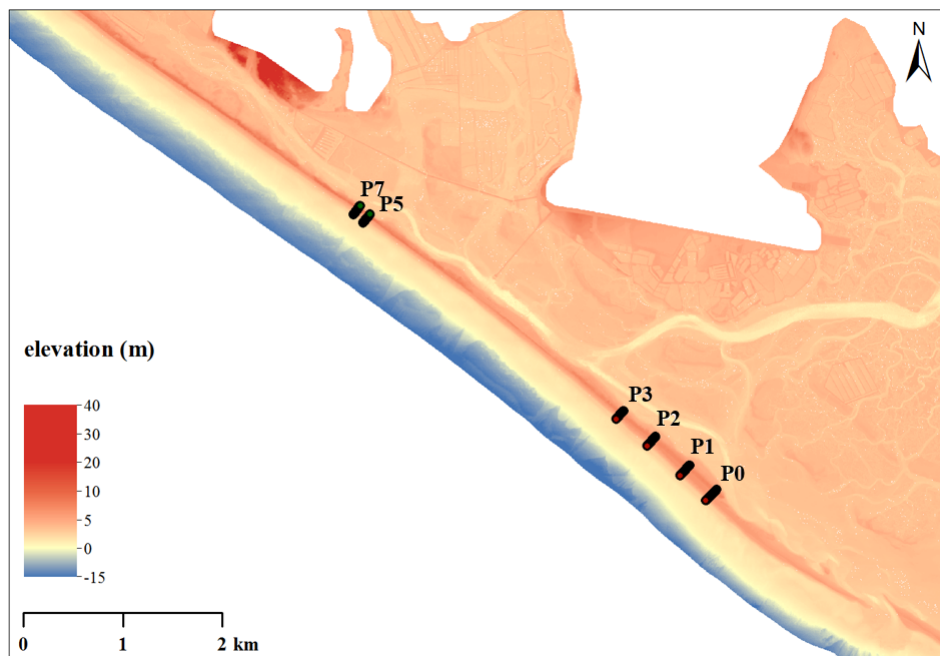


Figure 6.8: Location of the six extracted profiles in the study area (Lidar Dataset, 2011).

At the eastern area (Figure 6.9), the profiles reveal in general terms no significant vertical accretion, when examining the dune crest from 2009 until 2016. Restrained deposition on the dune crest is presented in profile P2 occurring after 2009. Vertical growth is also more notable in the backshore and foredune area of profiles P0 and P1 (adjacent to the inlet) from 2009 to 2011. Additionally, horizontal growth on the foredune slope since 2011 is apparent in P2. In profiles P2 and P3 the foreshore shows erosion in 2011 and 2016, but is very likely to have been constructed by wave deposition.

At the western area (Figure 6.10), for profiles P5 and P7, the alterations are minor. In profile P7 the stoss side exhibits small deposition seaward occurring gradually from 2009 till 2016. No notable alterations are present but only in the berm and beachface of both profiles. It is remarked in profile P1 that the UAV survey is a few centimetres above the Lidar level, even at the dune and backshore. This can be attributed to the survey itself and not necessarily to a true variation.

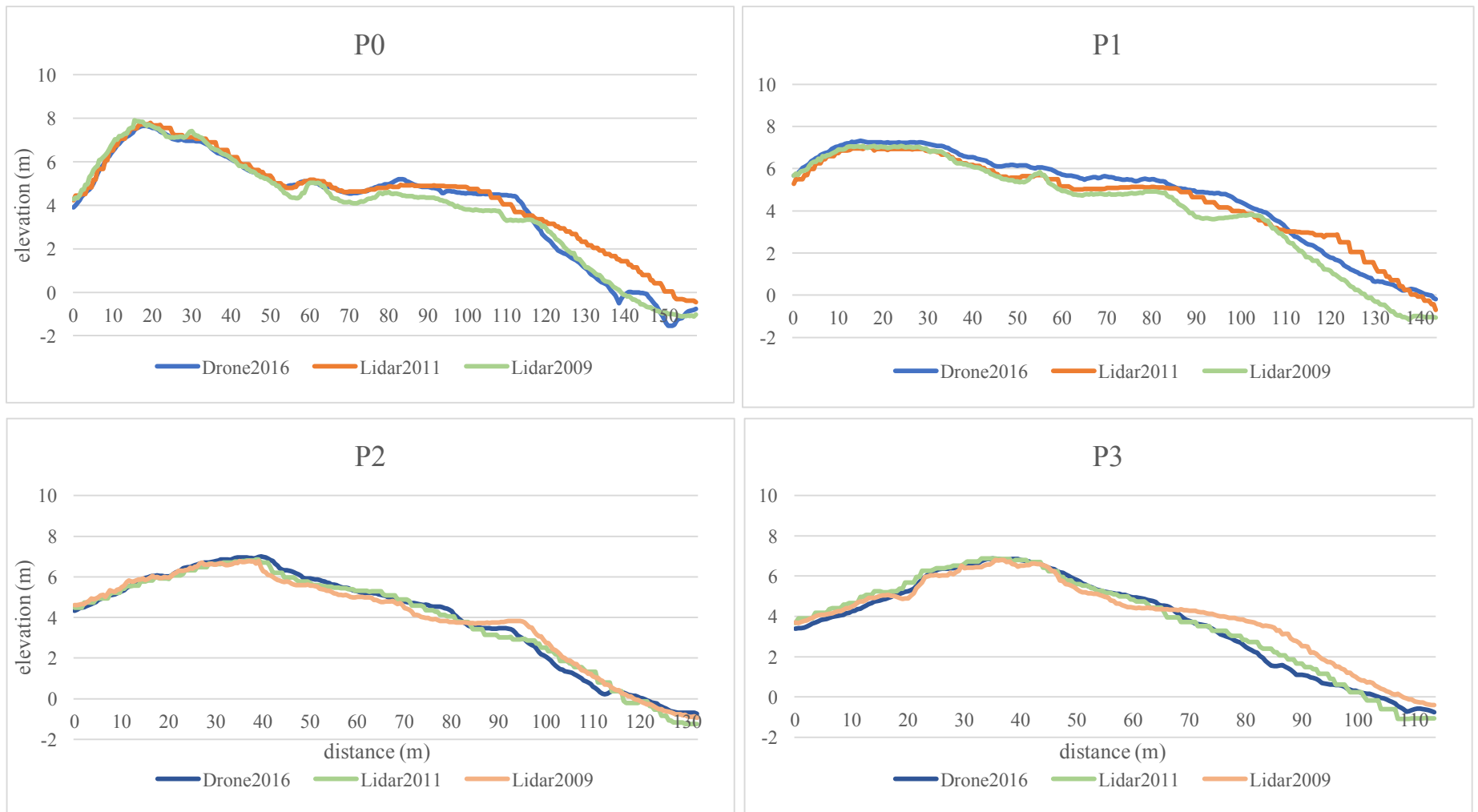


Figure 6.9: Cross-shore profiles at four selected sites in the eastern area of Ancão Peninsula extracted from Lidar datasets (2009 and 2011) and DTM (2016).



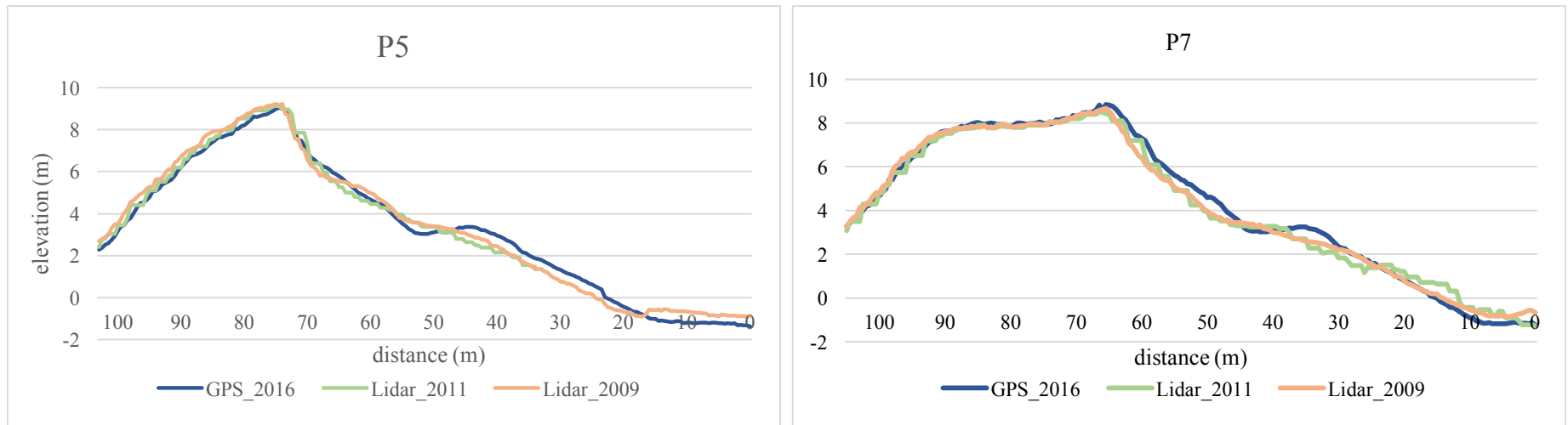


Figure 6.10: Cross-shore profiles at two selected sites in the western area of Ancão Peninsula extracted from Lidar datasets (2009 and 2011) and RTK-GPS surveyed cross-shore profiles (2016).

The dune width varies along the peninsula. In the eastern area ranges from 80 to 120 m near the inlet, whereas in the western sector 30 to 50 m is the general extent. In respect to the dune ridge elevation, as extracted from the UAV dataset (2016), in the eastern area, the dune average height is 7 m and it doesn't exceed the 8 m (above MSL) (Figure 6.9 and 6.11). The crest ridge, considering an elevation above 6 m, has an approximately width of 43 m. The eastern sector presents very smooth undulations that gradually elevate. The secondary dune crests are not well discriminated neither in shape nor in elevation (in respect to foredune area) (Profiles P1-P3), which is more apparent in the central part of this side. Approaching the inlet (Profile P0), the foredune dune crest is relatively clearer formed and the hummocks of the primary dune are colonizing the area closer to the shore. Considering the highest dune crest, the mean dune slope was  $\sim 0.1$  (P0:  $\tan \gamma \approx 0.08$ ; P1:  $\tan \gamma \approx 0.06$ ; P2:  $\tan \gamma \approx 0.12$  and P3:  $\tan \gamma \approx 0.15$ ). The beach width extends from the wet-dry limit to the most seaward hummocks averagely at 32 m, and it increases near the inlet to  $\sim 45$  m.

On the other hand, employing the 2011 Lidar dataset, almost the entire ridge of the western area is above 8 m and reaching the 10 m. The ridge is distinct and continuous above the 8-m elevation, with a width of 35-37 m between the 6 m contours. The colouring scale in Figure 6.11 indicates the dune elevation, where in the eastern area a smoother gradient from the dune crest to the dune toe or interdune area exists (from 7 m to 6 m). On the contrary, the slope is steeper in the western part throughout the ridge (from 8 m to 6 or 5 m height) (also Figure 6.10). The mean dune slope on the western area was  $\sim 0.5$  (P5:  $\tan \gamma \approx 0.65$  and P7:  $\tan \gamma \approx 0.41$ ). The beach width on this sector is narrower, namely approximately 23 m (distance from the wet-dry limit until the dune toe vegetation).

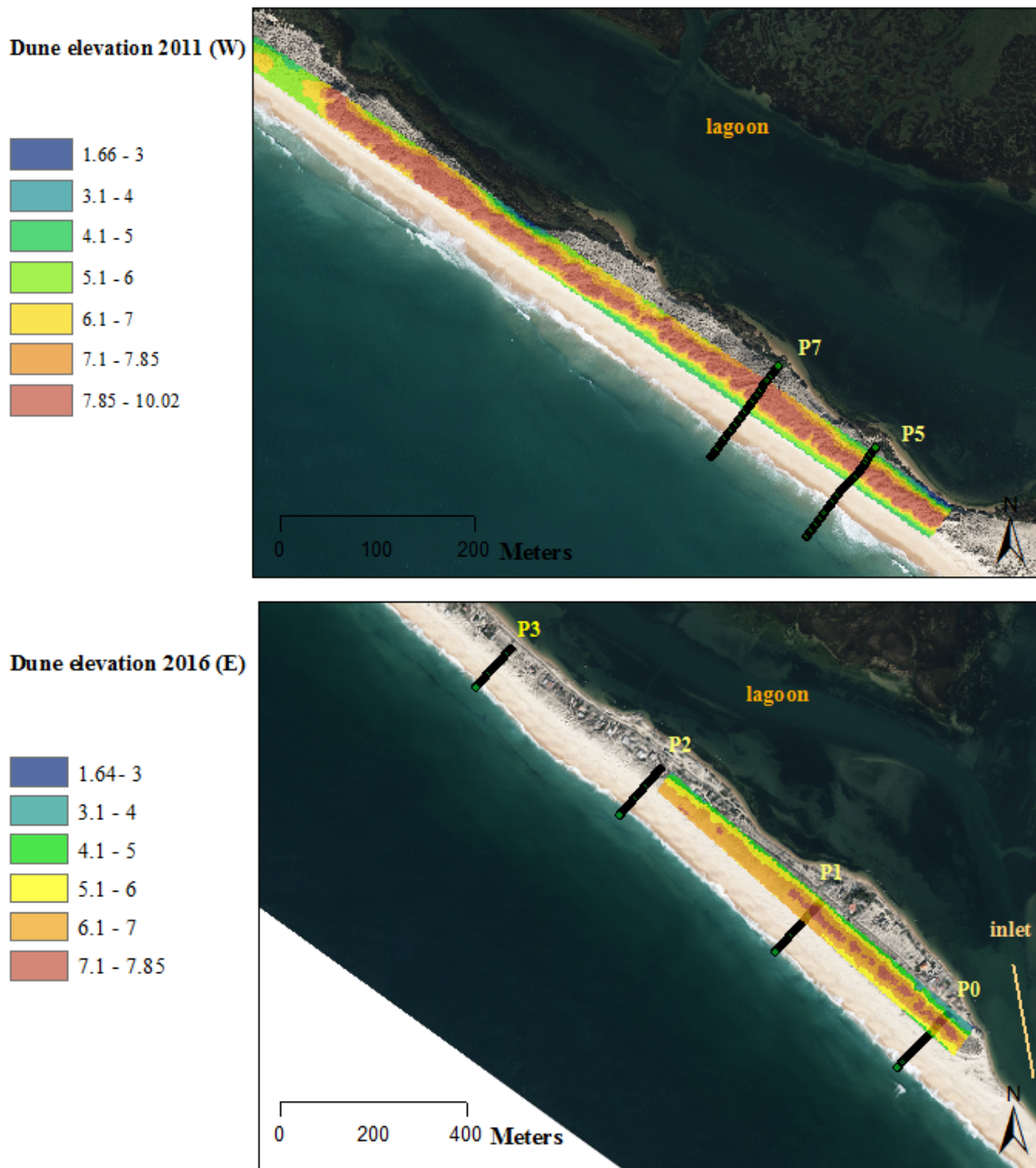


Figure 6.11: Dune ridge elevation at the eastern (upper panel) and western (lower panel) areas. The primary dune area is not depicted, rather the height of the dune ridge is emphasized. The studied profiles are depicted as well for each side respectively.

#### 6.4. Shoreline evolution

##### a. Vegetation line proxy

A net shoreline retreat between 1952 and 2014 is shown for the western part of the peninsula that varies from -5 to -10 m. The retreat is eastwards near the central area intensified up to -30 m, as

depicted in Figure 6.12. It must be noted that net retreat was reported for parts with no human occupation.

At the eastern sector, for the displayed transects, a shoreline progradation from +10 m up to +62 m near the inlet is noted. Apart from the small fragment of transects with low positive progradation, where human presence was active during the years of study, the remaining part was maintained or even conservation measures were implemented (fence placement or vegetation implants).

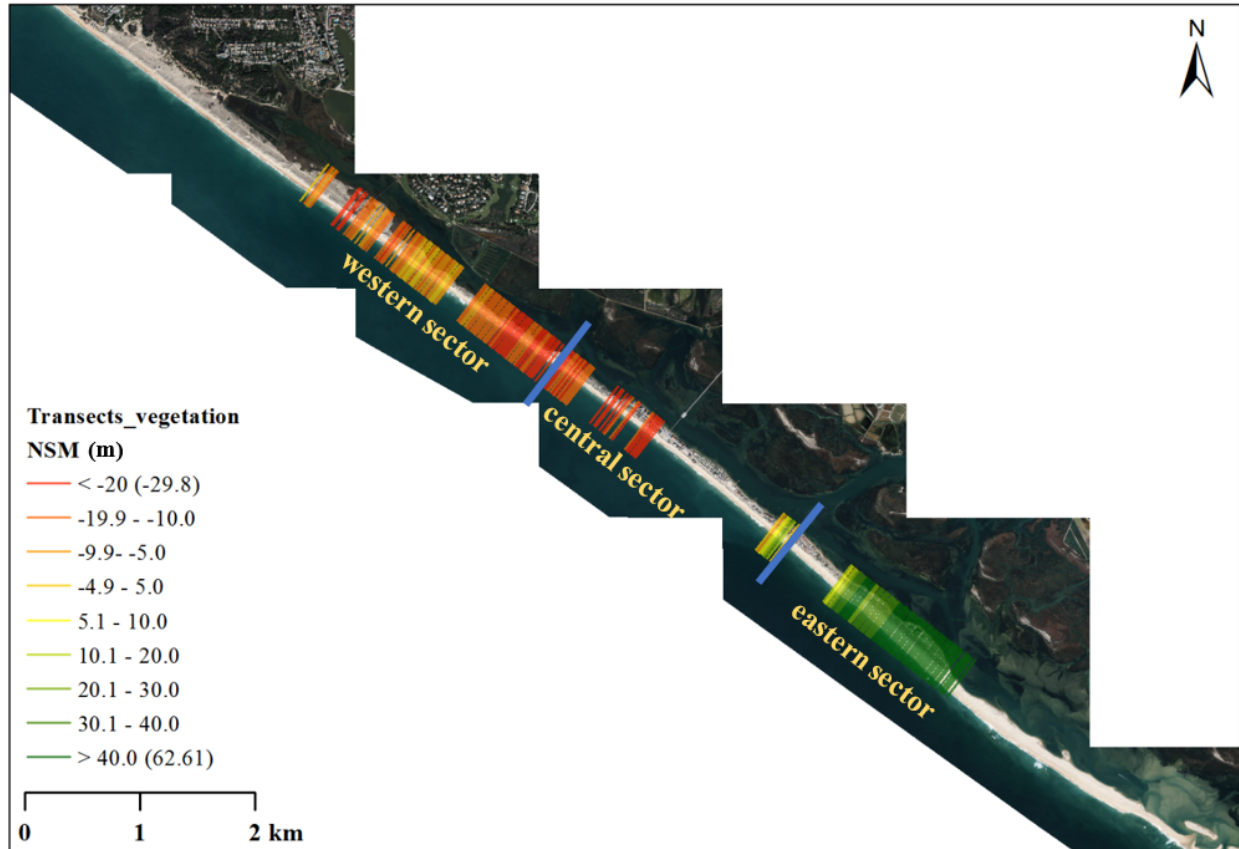


Figure 6.12: Net shoreline movement (NSM) between 1952 and 2014, using the dune vegetation line proxy (Orthophoto of 2014).

The linear regression rate of change for the same period reveals in total a negative slope for the entire western side of the peninsula (Figure 6.13). More specifically, a sharp negative rate corresponds to the east part of the western site (retreat of -0.20 to -0.47 m/yr), which are partially areas of human occupation. A gentler, but still negative rate ( $< -0.20$  m/yr) is also present covering an extended segment at the western site. For the occupied central area, the results were not adequate due to the variations in vegetation presence between the examined years in consequence of the human interventions that have been taking place on the beach. Contrarily, the eastern area has positive rates that get higher adjacent to the inlet (+0.60 to +0.95 m/yr).

However, it must be clarified that the deviations in shoreline development have not followed a linear path neither in space nor in time, as it will be revealed consequently. The shoreline of the study area presents an inconsistent development in terms of progradation or retreat that are not linearly evolved between the periods of investigation. By examining the linear regression per transect alongshore the peninsula, it was attempted to obtain a straightforward first deduction of the erosional or progradational trend at sites.

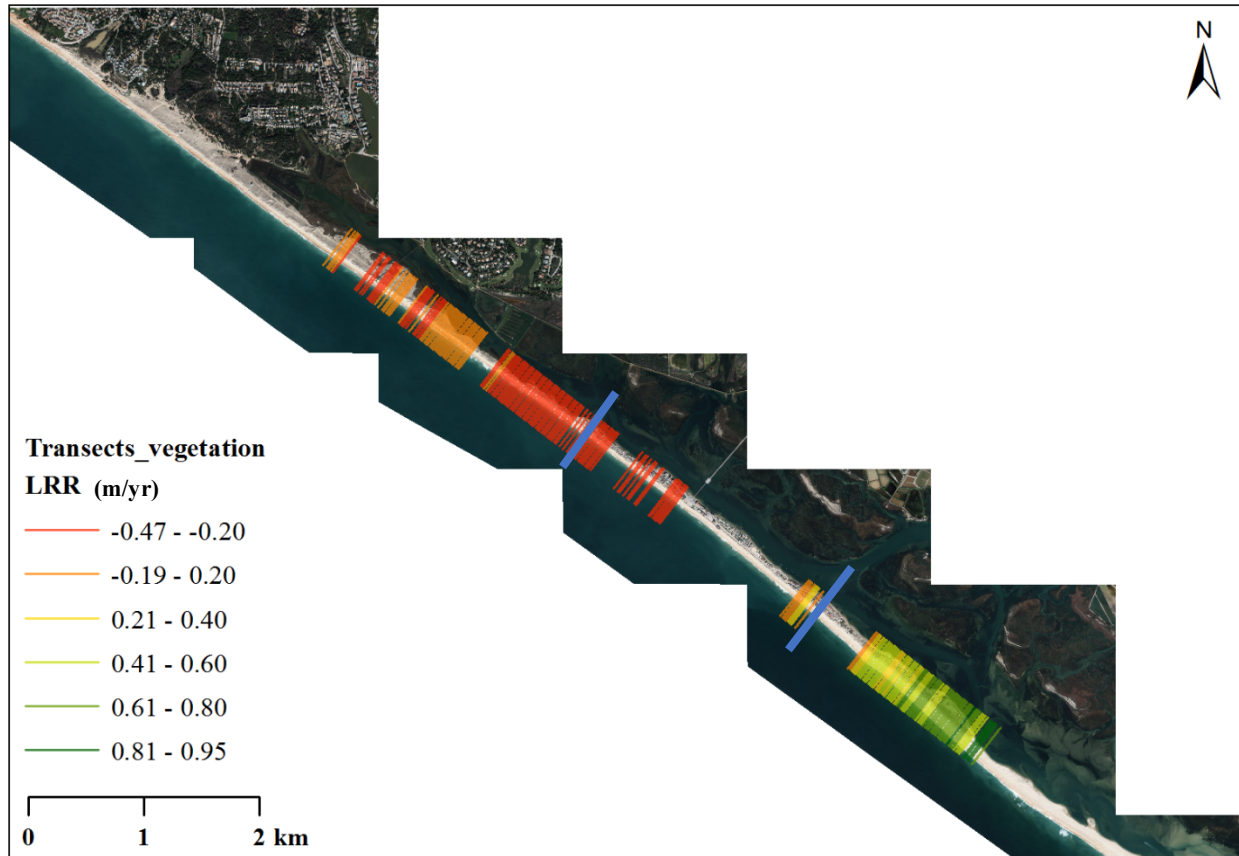


Figure 6.13: Linear regression rate variation (vegetation line approach) between 1952-2014 (Orthophoto of 2014).

Finally, to obtain a clearer aspect of shoreline movement trends between the years of examination and to investigate the causes involved, a graph with the respective movement rates per year for the periods of study is plotted (Figure 6.14). For an overall assessment of the evolution, the studied area of the peninsula is divided in three sectors, considering the distinguished zones of the western (transects: 1-169) and eastern (transects: 325-393) sites of unoccupied area and the central zone (transects: 171-296) of the human residencies. It is evident, that the shoreline movement has not developed in a linear manner neither in space nor in time. The shoreline evolution presents a varying behaviour in the different main sectors (western, central and eastern) and the

corresponding trends are not constant during the analysed periods. In particular, when examining the first period of 1952-1972, the western sector presents no dominant movement in the shoreline, whereas some shoreline retreat occurred in the central part, and in the eastern part there is a trend of 1 m/yr progradation. In the next period, 1972-1989, the most western part was not shifted, but towards the central part (transect 121-183) a retreat of almost 1 m/yr was noted. A slighter erosion was apparent in the central part and in the eastern area there was a contradictory condition, namely retreat and then closer to the inlet accumulation. Later, between 1989 and 2001 the entire western sector was retreating, besides a restricted segment, while on the other hand the eastern area is mostly advancing or constant shoreline at specific segments is retained. Lastly, from 2001 to 2014 fluctuations of slight erosion and progradation were taking place in the western and central parts. The eastern area was accumulating increasingly towards the inlet with +1 to > +4 m/yr rates. So, in general terms in the western zone the shoreline was either dynamically stable or under erosion and the eastern area was mostly under accretion conditions.

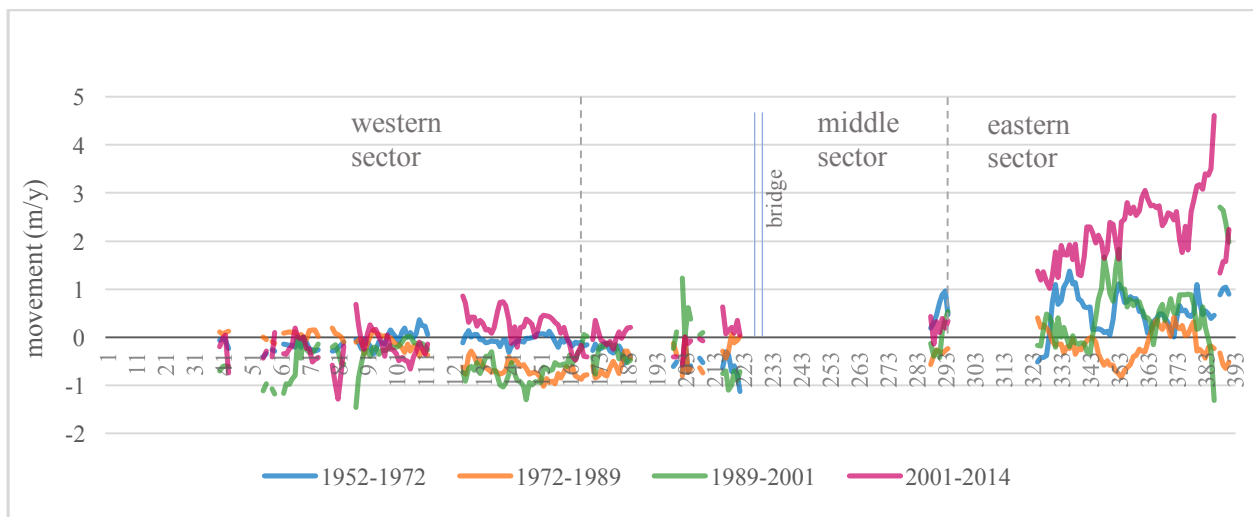


Figure 6.14: Shoreline movement rates per year using the vegetation line proxy, for the analysed periods.

The average evolution rates per period, in respect of the vegetation line marker approach, have been calculated and presented in Table 6. The rate results indicate, along with Figure 6.14, the divergence in retreat or advance trends between periods and sectors. For the first period of 1952-1972, the western area remains stable, the middle sector presents a small retreat of -0.26 m/yr, whereas the eastern area is prograding half a meter per year. The trend has changed in the next period and an overall erosion in Ancão Peninsula was taking place, with the central sector being the most affected one. In the following period, the erosion is concentrated in the western sector,

with an increased rate of -0.54 m/yr, in contrast to the eastern area where an accumulation of an equal rate is occurring. Lastly, in the most recent period, both western and central area have remained constant, however the eastern area was significantly accumulating by over +2 m per year.

Table 6: Average annual evolution rates for the western, middle and eastern area of Ancão Peninsula in four distinct periods of examination.

	<b>1952-1972</b> (m/yr)	<b>1972-1989</b> (m/yr)	<b>1989-2001</b> (m/yr)	<b>2001-2014</b> (m/yr)	<b>Average</b> (m/yr)
<b>Western sector</b>	-0.01	-0.33	-0.54	-0.03	-0.20
<b>Central sector</b>	-0.26	-0.42	-0.22	0.05	-0.25
<b>Eastern sector</b>	0.52	-0.17	0.54	2.25	0.79

A general aspect of evolution in Ancão Peninsula from 1952 until 2014 could be given by the average annual rates, although there is no linearity of the beach erosion/progradation in the three distinct sectors, and it is evident that only the eastern part has been considerably accumulating by almost +0.8 m/yr, whereas the rest of the peninsula is retreating about -0.2 m/yr. Thereafter, the shoreline movement was not evolving linearly during the years. Additionally, the distinct coastal sectors of the peninsula (western, central and eastern) showed even for the same period a dissimilar shoreline evolution behavior, due to different reasons.

b. Wet/dry mark line proxy

The net shore movement results using the wet/dry mark indicator are generally in agreement with the previous results of the vegetation line proxy. However, the values of the movement change are considerably lower in the accretion areas.

The net shoreline movement exhibits similar results as previously, with the strongest erosion value in the western and central part and accumulation in the eastern part, intensified towards the inlet (Figure 6.15). The progradation movement results are more conservative compared to the respective of the vegetation line proxy. DSAS analysis showed that linear regression rate is also consistent with the linear regression rates resulted from the vegetation lines, presenting almost the same rate values for the corresponding sections of the peninsula (Figure 6.16). However, the  $r^2$ , in general, acquired from the tide lines is weaker in respect to those of the vegetation lines, especially for the eastern area (Figure 6.17). It is also apparent that the strongest  $r^2$  is related to the central

intervened sector, and part of the western area. The relatively low  $r^2$  values are expected, as no further information regarding the tide phase are available, thus no corrections with respect to high/low tide could be made. Notwithstanding, the correlation coefficients are for both indicators statistically not significant.

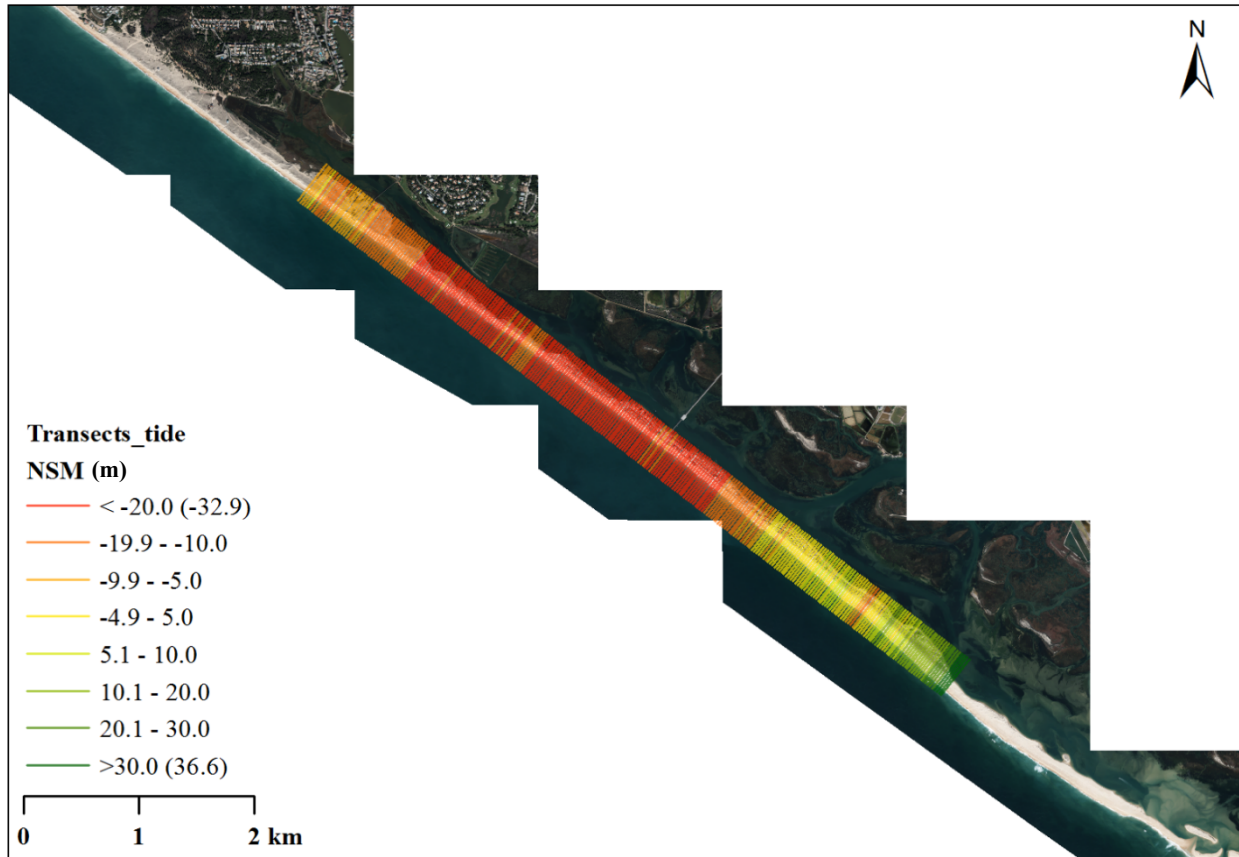


Figure 6.15: Net shoreline movement (NSM) for 1952-2014 period using the tide mark line approach.



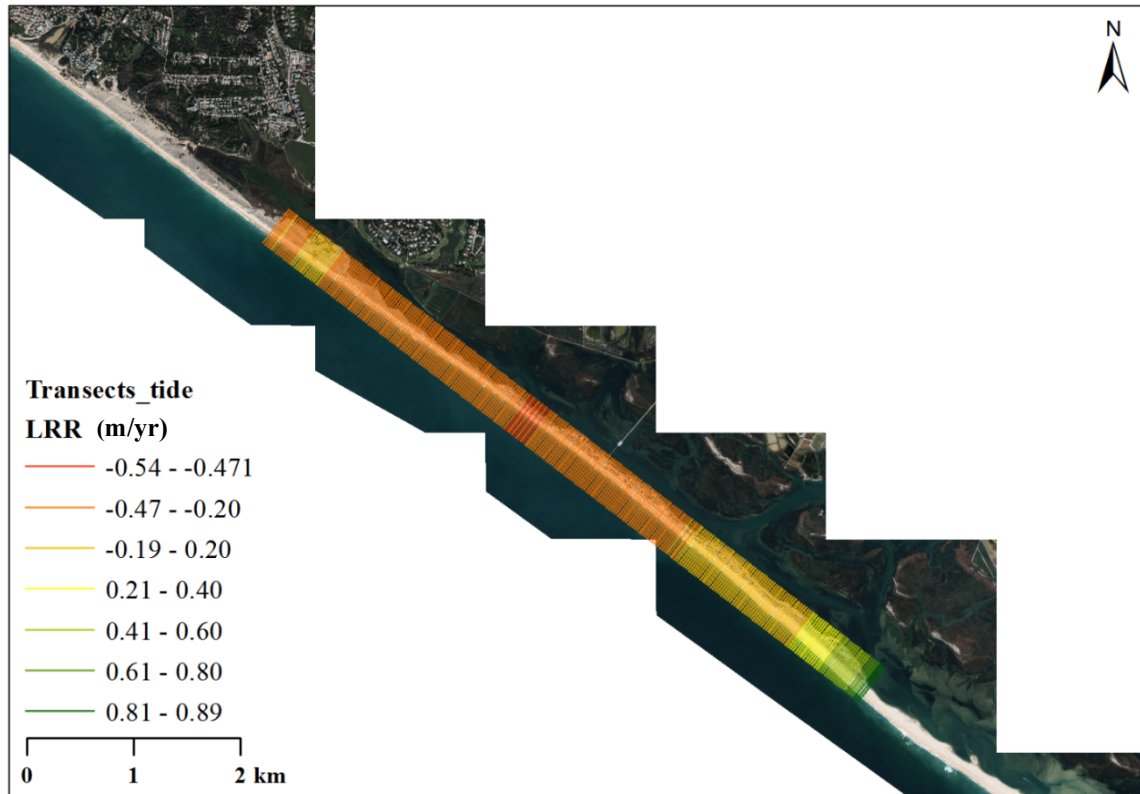


Figure 6.16: Linear regression rate using the tide mark line approach for 1952-2014 period.

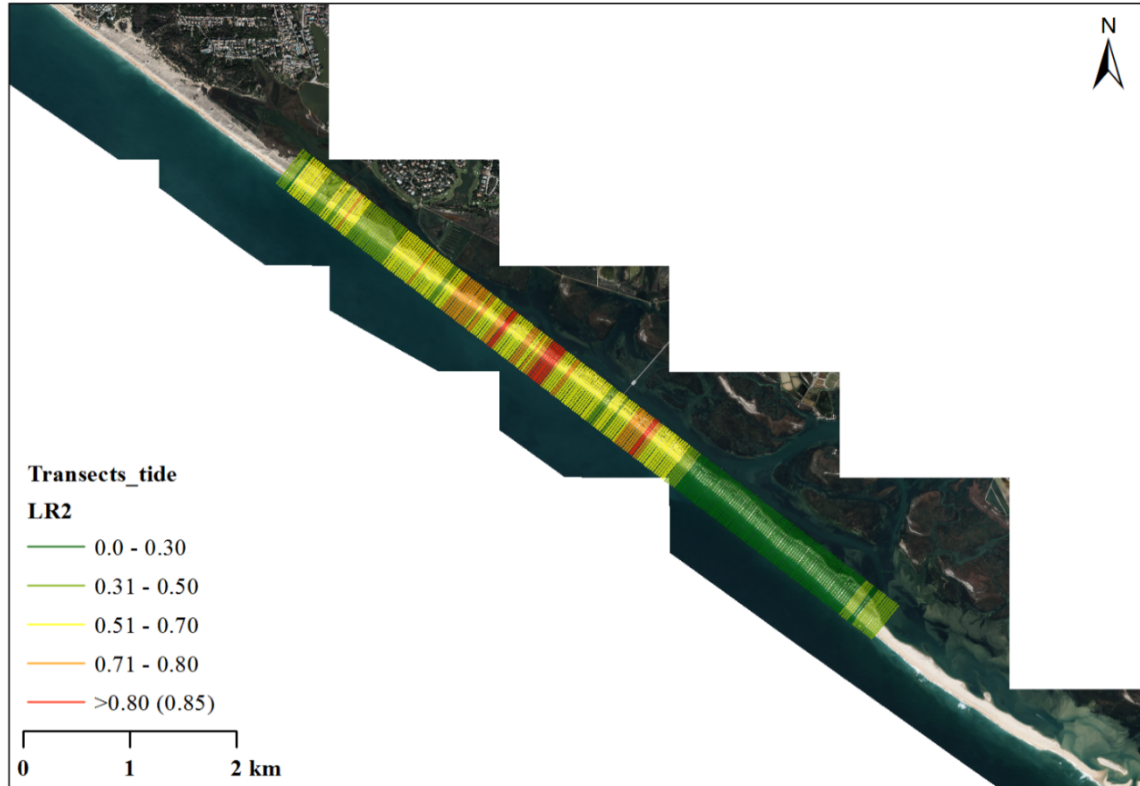


Figure 6.17: Representation of the correlation coefficient ranges (no threshold application).

### 6.5. *Vegetation identification and mapping*

The vegetation species at selected transects in both eastern and western area were identified and counted, to obtain information about biodiversity and cover density in the dune system. Since the morphology defined the zones along the dune profile at each transect, it was requisite to examine the vegetation species and cover density correlation to those distinct zones. The vegetation species were modulating from one zone to the next. This diversity was also varying not only per vegetation species at each zone, but also in coverage of each species as well as total coverage at each separate zone was differentiated landward (see Annex 1).

In detail, in the eastern area grids at three selected transects, primarily based on morphological, criteria were used for species identification and their cover density (Table 5 and Annex 1). The embryo dunes in Transect 2 covered 2% and hummocks at Transects 4 and 3 had few and sparsely vegetated species and similar cover density (0.6%). At ‘dune 2 toe’ of Transects 4 and 3 the species had similar presence, yet the overall coverage was twice as high in Transect 3 (5%). At Transect 2, the elevation was unvarying and hence the dune toe was lacking. The crest of the first foredune (‘Crest 2’) at all sites was alike in species and presenting high biodiversity (nine to eleven species) and medium density (T4: 10.2%, T3: 6.5%, T2: 8.4%). At the crest of the second foredune (‘Crest 3’), although the present species were the same in number and type, the density was diverse, namely in Transect 4: 12%, in Transect 3: 32% and in Transect 2: 19%. At Transect 2, the ‘dune 3 toe’ and the crest of the third and more mature dune were clearly separated, and it was recorded that the crest was more abundant in species and density (42% and 63.5%, respectively). However, the cover density between the mature ‘Crest 3’, is not similar in the three sites and is increasing eastwards (T4: 12.1%, T3: 32.1% and T2: 63.5%). Finally, the lee zone was covered by a comparable number of species (10-13 species per site), but it was by far denser at the most eastern Transect 2 (T4: 12%, T3: 15%, T2: 53%).

In terms of vegetational species, in Transect 4, the vegetation identification on the seaward hummocks showed very limited coverage (less than 1%). *Calystegia soldanella* was the most frequent species, belonging however to shifting dune habitats (code 2120). The dune toe has mainly *Pancratium maritimum* and *Medicago marina*, which are suitable species for this zone. At the first foredune crest (‘Crest 2’) *Artemisia crithmifolia/ campestris*, that corresponds to fixed dunes, is a dominating species of almost 7%. At the third foredune crest *Crucianella maritima* and *Artemisia crithmifolia/ campestris* coexist and equally occupy again 7%. The total coverage

between the two crests hardly differs (crest 2: 10.2%, crest 3: 12.1%). The lee side exhibits low coverage of 12 %, of which the 7% is constituted by *Artemisia crithmifolia/ campestris*.

Transect 3 was also discriminated in five zones, as Transect 4. Once more, the incipient vegetation consisted of less than 1% and mainly by *Silene nicaeensis*, that fits to primary dunes (2120). The same species occupies also the dune toe (2.2%) with *Medicago marina* (1.2%), a suitable species for this zone. Although it is also prevailing on the first dune crest ('Crest 2') (2.4%), *Medicago marina* can exist in both embryonic (2110) and shifting dunes (2120). However, in the second dune crest ('Crest 3') the coverage and the species diversity differs. *Artemisia crithmifolia/ campestris*, that belongs to fixed dunes vegetation, is dominating in 30%, whereas other species have a poor presence. The lee side exhibits noticeably lower coverage (15%), again occupied by *Artemisia crithmifolia/ campestris*.

Close to the inlet, Transect 2, the zones appearing were six. Firstly, the embryo dunes were constituted by *Eryngium maritimum* (1210) and the in total coverage was greater (2%) than the corresponding habitat zones of Transects 2 and 3. Additionally, it should be marked that this habitat is occurring seaward (Figure 5.2). The first dune crest ('Crest 1') is occupied by *Ammophila arenaria* (6.5%), characteristic of that dune zone. Yet, at the second crest the coverage is increased (19%) and mostly by presence of *Medicago marina*, another typical species of 2120 habitat. In the middle of the transect a dune toe of a third crest was distinguished. This dune toe was greatly covered (42%) by *Medicago marina*, typical in this environment, and *Artemisia crithmifolia/ campestris*. The third dune crest had even more increased coverage (63%) of dominant *Artemisia crithmifolia/ campestris* (42%). Lastly, the lee side was largely vegetated (53%) again by *Artemisia crithmifolia/ campestris* (39%). The biodiversity of numerous species, besides *Artemisia crithmifolia/ campestris* is retained in this last morphological series -from the dune toe of the third crest to the lee side-, it is however particularly restricted. The only species that have coped to extend their coverage is *Crucianella maritima*, *Medicago marina* and *Lotus criticus*.

In the western area (Figure 5.2 and Table 4) the morphological and thus vegetational zones are less, compared to the eastern, as shown in Table 4 (see also Annex 2). Embryo vegetation was present only at the most western part, where *Elymus farctus* was principally the only species, however covered less than 2%. The following zones of the dune toe, the dune crest and the lee side were present at all transects, yet each location of the same zone exhibited diverse density. In particular, the dune toe vegetation of Transect 6 exceeds importantly the corresponding coverage

of the other investigated sites (T6: 10% and T5, T7, T8: 0.7-2%). The dune toe zone at all sites present a similar species number (seven or eight of species). Transect 8 (most western site) has the denser crest with 41% coverage, whereas Transects 5-7 are occupied with 18-24% of vegetation. In terms of biodiversity all sites of dune crest host eight to ten species, however Transect 7 presents half of species number. Diverse results are demonstrated similarly for the lee side, namely Transect 5 (most eastern) has almost 60% coverage and westwards the density gradually decreases at Transects 6 and 7 approximately to 25% and at Transect 8 to 12%. Despite that, the biodiversity showed constantly presence of eight species present.

The western area exhibited mainly three morphological zones. In Transect 5 the dune toe is scarcely vegetated (1.7%) by *Medicago marina* (1%), which is inherent of shifting dune habitats. The vegetation at the dune crest (18%) is described by typical species of fixed dunes (*Artemisia campestris* and *Armeria pungensi*, 7.5%). The lee side is dominated by *Artemisia campestris* in most of its coverage (34%), which is a characteristic species of grey dunes, as well as *Armeria pungens* and *Paronychia argentea* that are also occupying the back-zone of the foredune (8% and 10% respectively).

In Transect 6 at the dune toe, there are more species present compared to the respective zone of Transect 5, (and are covering a greater area, 10.1%), however the prevailing species (*Lotus creticus* and *Ammophila arenaria*) attributes more shifting foredunes rather than the embryonic. The dune crest, as well as the lee side, host mainly species correlated to fixed dunes (*Artemisia campestris* and *Armeria pungens*).

Transect 7 has an almost bare dune toe and the dune crest is scarcely vegetated by *Lotus creticus*, but also hosting in a small percentage of *Armeria pungens* that belongs to secondary foredunes. Then, the lee side is prevailed by *Artemisia campestris*, which is in agreement with the typical vegetation in that habitat.

Finally, in Transect 8 four habitats are existing, the most seaward is presenting an *Elymus farctus* community, however not very extended in the profile length (embryonic habitat approximately 7 m of cross-shore length). The dune toe except for the presence of *Elymus farctus* has relatively high percentages of *Lotus creticus*, *Artemisia campestris* and *Armeria pungens* that belong to fixed or semifixed dunes. The crest is densely covered and almost dominated by *Artemisia campestris*. Oppositely, low coverage was noted on the lee side, whereas *Armeria pungens* occupies the greatest percentage.

## 6.6. Aeolian sediment transport potentials estimation

The two approaches, i.e. of a. one mean grain size and b. weight percentage of all grain size classes (Equation 8) have been employed for the calculations of sediment transport potentials by wind, and are the following:

### 1. First approach: one mean grain size from beachface grain size results

A mean grain size of 466  $\mu\text{m}$  was obtained for the beachface environment and this defined a threshold velocity of 8.85 m/s and a threshold shear velocity of 0.27 m/s. For all computations, the cosine of the angle has been applied on the sediment transport results from Lettau and Lettau formula (Equation 7), to obtain the final sediment transport that is directed merely to the backshore.

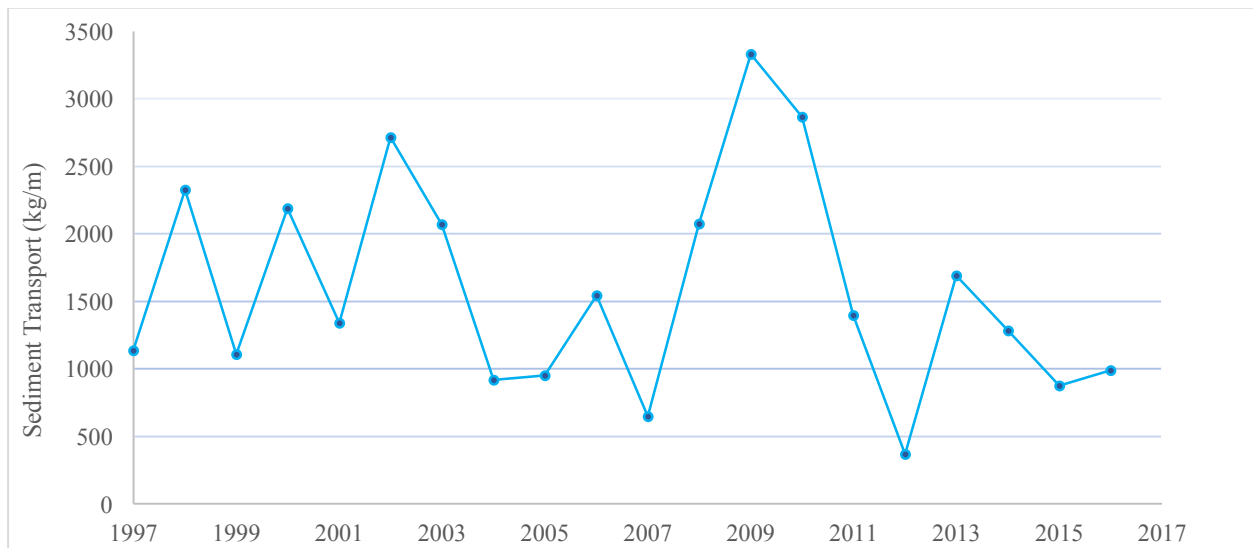


Figure 6.18: Annual sediment transport potentials for 1997-2016 by use of one mean grain size (beachface environment) and the cosine of the angle of wind perpendicular to the shore. For the 11<sup>th</sup> and 12<sup>th</sup> month of 2013 and for 2014 the sediment transport potentials were not calculated and thus not presented, due to gap in the data. The plot is presented in kg/m and m<sup>3</sup>/m.

The total sediment transported for the twenty-year period of study was 30532.6 kg/m. As it was shown from Figure 6.7, the wind distribution was diverse for each year (and month) and this was apparently reflected on the annual sediment transport potential. Figure 6.18 demonstrates the potential annual transport rates (with average approximation used for year 2014) and it is evident that the years with the most influencing winds and hence sediment transport potentials, are years 2002, 2009 and 2010. The mean annual sediment transport potential rate was estimated on 1.00 m<sup>3</sup>/m (or 1590.8 kg/m).

2. Second approach: theoretical sediment transport for each grain size class and consequent application of weights percentages

In this approach the percentages of weights, as derived from the grain size analysis for the beachface environment, have been applied to the theoretical calculation for the sediment transport potentials again in an annual scale (Figure 6.19) using for simplicity reasons the granulometric results of the western area (the respective results of the eastern area showed minor difference). The results are alike when compared to the previous approach, the percentages of weights resulted in somewhat higher values. The total sediment transport potential was 36741.4 kg/m and the mean annual potential sediment transport rate 1.16 m<sup>3</sup>/m (or 1837.07 kg/m).

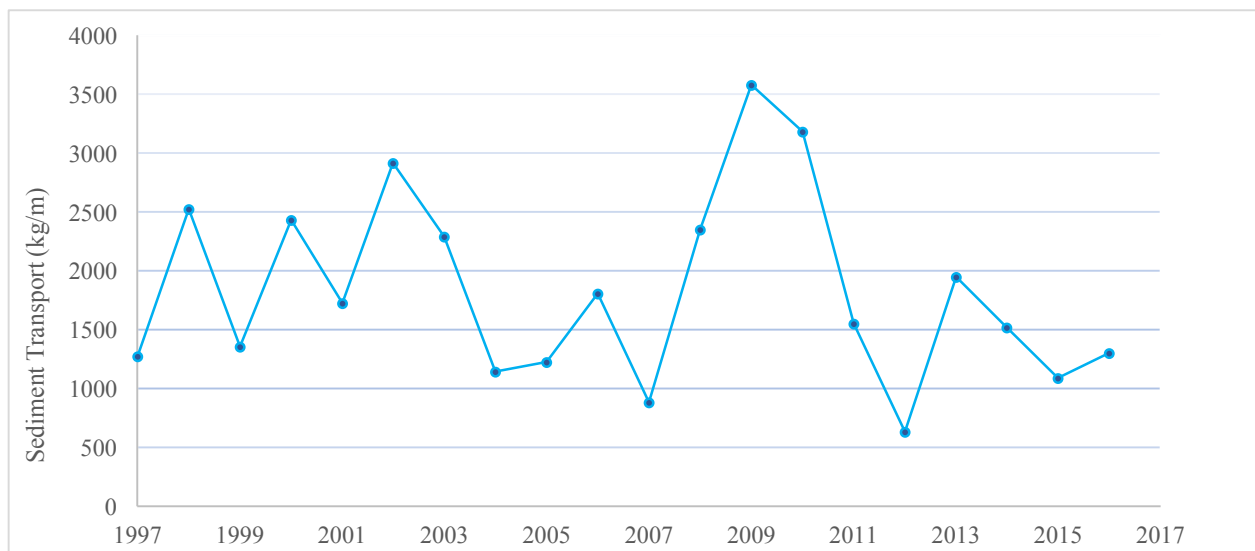


Figure 6.19: Annual sediment transport potentials using the percentages of weights presented for the western area.

### 6.7. Volumetric changes

The vertical and volumetric changes in the foredune as extracted from the Lidar (2009 and 2011, for western and eastern area) and UAV (2016, for the eastern area) datasets were obtained, which will be compared to the results derived from the two ‘theoretical’ calculations. Three polygons (one in the western, R5 and two in the eastern area, R2 and R3) were utilized for those measurements (Figure 5.1) and were drawn covering the embryo dune and foredune area, to gain results regarding the contribution to the dune development. The first measurement period was conducted for 2009-2011 and the second for 2011-2016. The following graphs (Figure 6.20; 6.21 and 6.22) will demonstrate the vertical differences and how these were distributed in the selected polygons.

In the first graph, R5 (Figure 6.20) there is a minor vertical reduction of -0.20 m in total on this dune area in both its high and low positions, and as can be seen from the elevation subtraction, the sediment accretion was concentrated on the dune toe (up to +0.65 m), whereas the dune crest was approximately -0.2 m lowered during the two-year period of 2009-2011.

### R5 polygon 2009\_2011

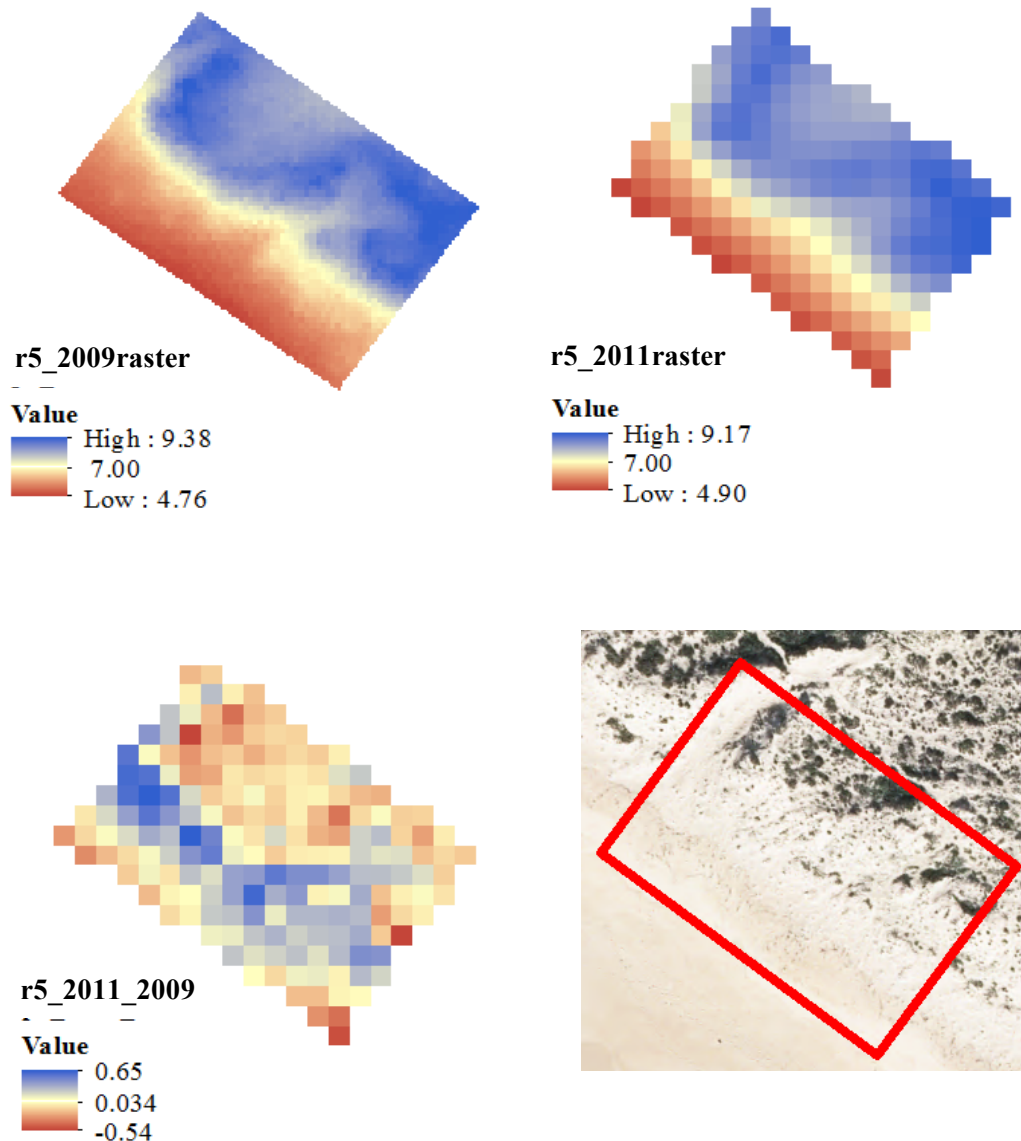


Figure 6.20: Polygon R5 of the western area. The elevation of the specified surface is displayed for 2009 and 2011 in the top panels. The vertical difference for this period is presented in the bottom left polygon. Lidar dataset of 2009 had a higher grid resolution compared to the 2011 dataset, hence the representation of raster polygon (top right) for 2011 is poorer.

Polygon R3 in the eastern area (Figure 6.21) is likewise showing a similar reduction of -0.17 m at its high positions, but the lower points have elevated in 2011. In 2016, the surface condition seems alike to 2009. Comparing in detail the 2009-2011 period, an accretion of up to +0.6 m is presented at constrained fragments on the dune crest and backwards on the tip of the lee side and on the embryo dune (early vegetation zone). The narrow foredune zone and the dune crest was more affected with erosion up to almost -0.5 m. The picture in 2016 is however different. The accumulation is more extended on the embryo dune and crest and where elevation between 2009 and 2011 was occurring, namely at the end of the crest (upper right margin), in 2016 erosion has taken place.

Again, the same representation is demonstrated for an additional polygon, R2, in the eastern area (Figure 6.22). The case is very much related to the condition of R3 surface for the years 2009 and 2011. In particular, there is a general reduction compared to the lower fragments from 2009 to 2011 and an unimportant vertical increase of +0.10 m. Additionally, in 2016 the highest and lowest points are slightly increased. The pattern in R2 site is matching the R3 vertical differences for the periods 2009-2011 and 2011-2016, whereas for the first period of study (2009-2011) most of the accumulation has taken place in the embryo dunes and first foredune hummocks, especially the most eastern part. For the second period (2011-2016), the accretion has shifted to the western part of the polygon and a bit backwards, that is in the wider embryo dune area and the first dune crest. The erosion is concentrated at those places where it was accreting in 2009-2011. Towards the secondary dune crests the erosion remained almost constant.



### R3 polygon 2009\_2011\_2016

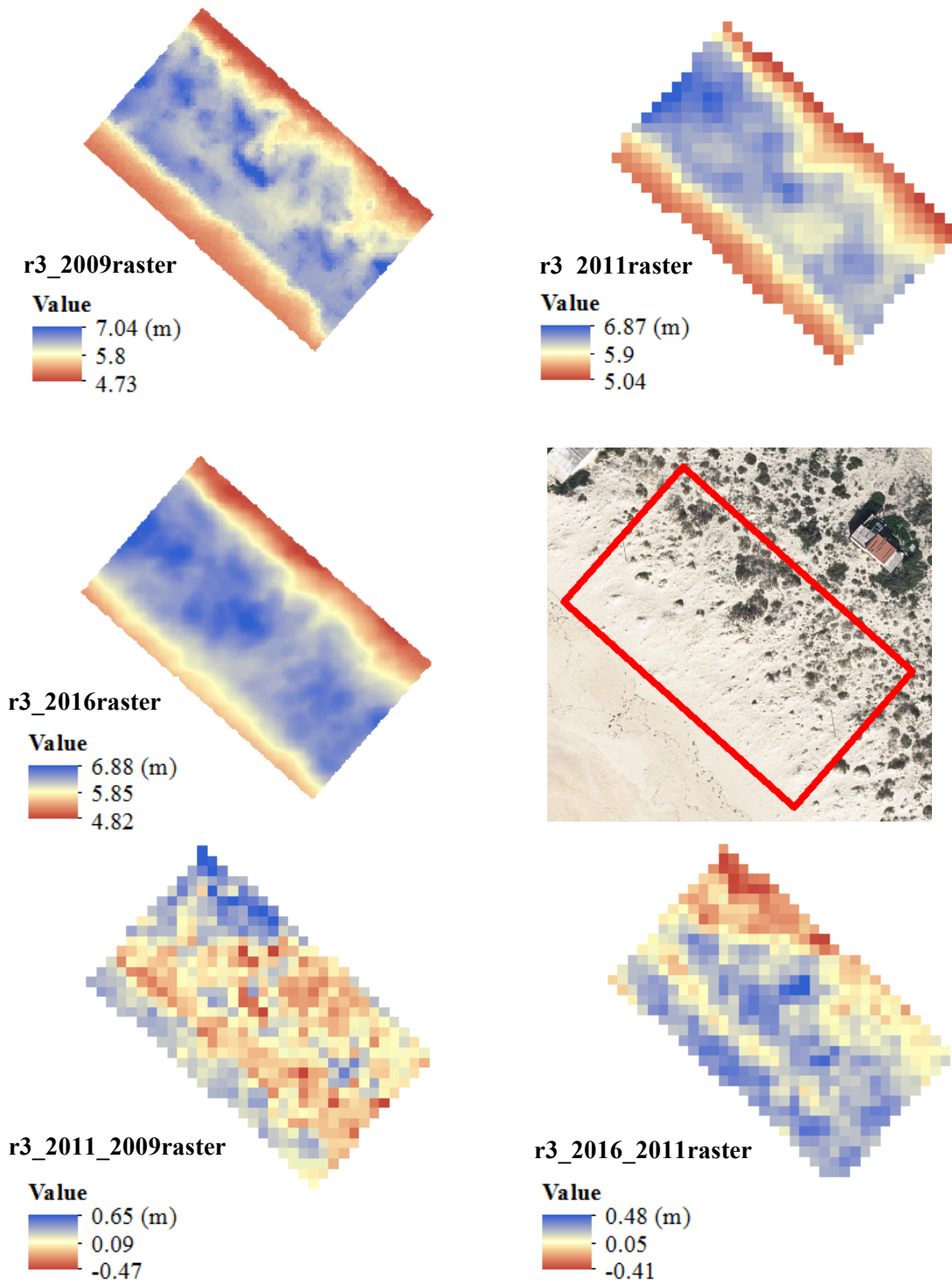


Figure 6.21: R3 polygon for the eastern area is demonstrated for years 2009, 2011 and 2016. The vertical difference is presented in the bottom polygons for periods 2009-2011 (left) and 2011-2016 (right).

### R2 polygon 2009-2011-2016

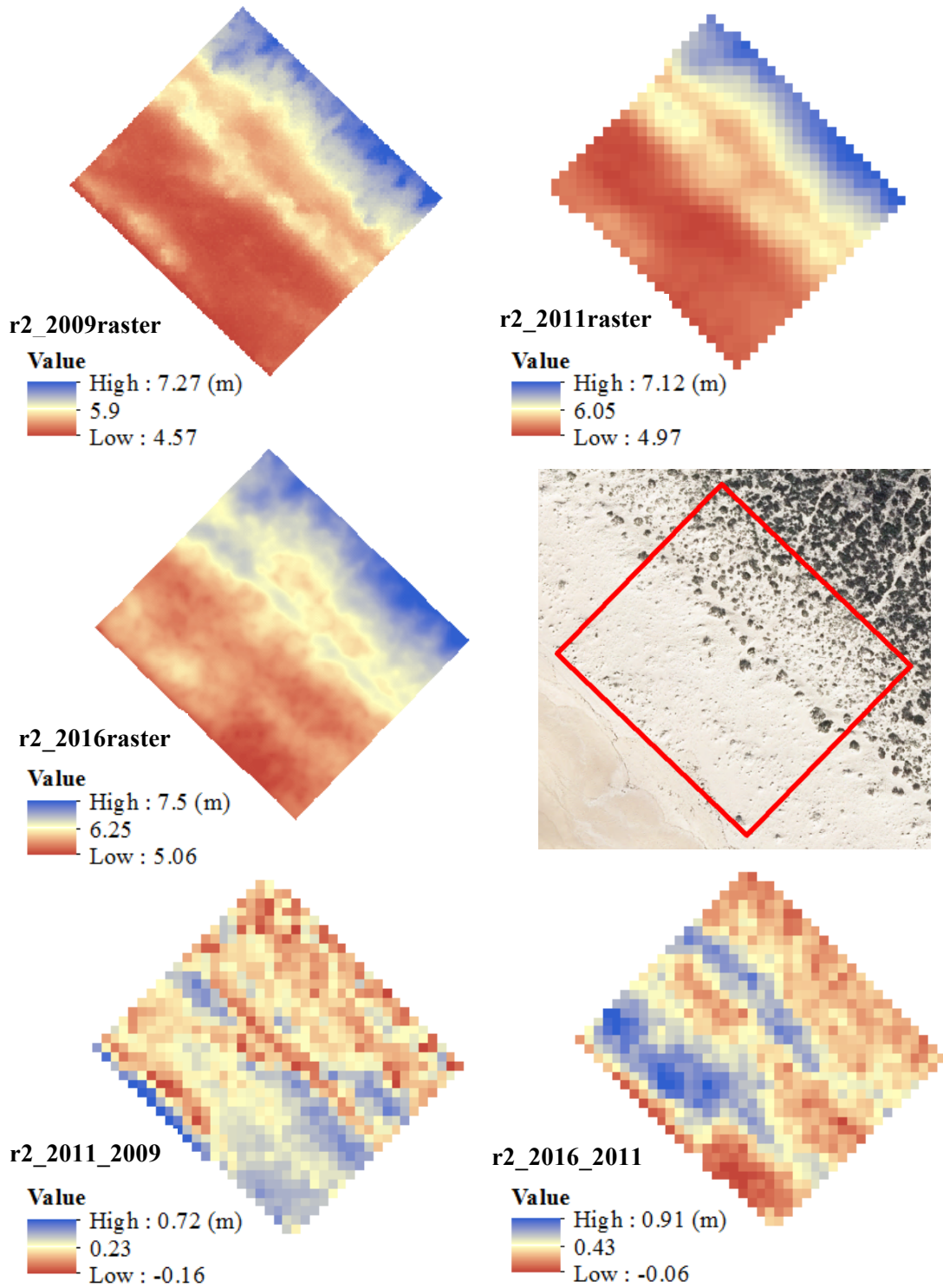


Figure 6.22: Surface vertical elevations for polygon R2 for the 2009-2011 (down left) and 2011-2016 period (bottom right).

Finally, to have a volumetric aspect as well, the difference in volume for the selected sites and the corresponding periods have been calculated (Table 7) and compared with the computation results of the two methods based on the sediment transport equation (Table 8). For comparison reasons in Table 8, the sediment transport potential (in  $\text{m}^3/\text{m}$ ) and rates (in  $\text{m}^3/\text{m}\cdot\text{y}$ ) derived from the two theoretical approaches are contrasted to the calculated volumes from the Lidar and UAV datasets for the corresponding years, i.e. regarding the first period of examination from 1<sup>st</sup> November 2009 until 30<sup>th</sup> May 2011 and for the second period from 1<sup>st</sup> May of 2011 until the 30<sup>th</sup> October 2016. The overall volume results of the three polygons are apparently indicating for both periods of examination that the most eastern polygon is concentrating the higher sediment accumulation and decreases towards the most western polygon, having the lowest sedimentation. Moreover, in the east sector there is high discrepancy of polygon R3 with regards to the R2 polygon.

Table 7: Volumetric difference as resulted for the respective polygons and periods.

	R5_vol_diff ( $\text{m}^3$ )	R3_vol_diff ( $\text{m}^3$ )	R2_vol_diff ( $\text{m}^3$ )
Along shore distance (m)	34.5	61.5	34.5
<b>2011-2009</b>	75.48	193.32	654.21
<b>2016-2011</b>		283.93	1161.54

Table 8: Comparison table of results from formula estimations (two methods of calculation) and from the Lidar and UAV datasets for volumes and average annual transport rates. For the period 2009-2011 computations, the percentages-of-weights approach was applied using the grain size results of the western area, as R5 site (of western area) was included. Conversely, for the period 2011-2016, the results of the eastern grain size analysis were used.

<b>2009-2011</b>					
	percentages of weights approach	mean grain size approach			
	general ( $\text{m}^3/\text{m}$ )	general ( $\text{m}^3/\text{m}$ )	R5 ( $\text{m}^3/\text{m}$ )	R3 ( $\text{m}^3/\text{m}$ )	R2 ( $\text{m}^3/\text{m}$ )
2009	1.00	1.01			
2010	1.93	1.80			
2011	0.29	0.24			
<b>total</b>	<b>3.22 (<math>\text{m}^3/\text{m}</math>)</b>	<b>3.05 (<math>\text{m}^3/\text{m}</math>)</b>	<b>2.2</b>	<b>3.1</b>	<b>18.9</b>
<b>average</b>	<b>1.25 <math>\text{m}^3/(\text{m}\cdot\text{yr})</math></b>	<b>1.18 <math>\text{m}^3/(\text{m}\cdot\text{yr})</math></b>	<b>0.85 <math>\text{m}^3/(\text{m}\cdot\text{yr})</math></b>	<b>1.20 <math>\text{m}^3/(\text{m}\cdot\text{yr})</math></b>	<b>7.32 <math>\text{m}^3/(\text{m}\cdot\text{yr})</math></b>

2011-2016					
	percentages of weights approach	mean grain size approach			
	general	general	R5	R3	R2
2011	0.80	0.64			
2012	0.52	0.23			
2013	1.43	1.06			
2014	1.13	0.81			
2015	0.83	0.55			
2016	1.02	0.62			
<b>total</b>	<b>5.73</b>	<b>3.91</b>		<b>4.6</b>	<b>33.7</b>
<b>average</b>	<b>1.07 m<sup>3</sup>/(m.yr)</b>	<b>0.73 m<sup>3</sup>/(m.yr)</b>		<b>0.86 m<sup>3</sup>/(m.yr)</b>	<b>6.32 m<sup>3</sup>/(m.yr)</b>

The theoretical findings of volumetric changes regarding 2009-2011 period, match the actual results of the Lidar dataset for polygons R5 (western sector) and R3 (eastern sector), compared to results of both approaches. The divergence is largely exceeded for the most eastern polygon R2 (six times), not only in comparison to the results of the formulas, but also with respect to polygons R3 and R5. However, as R2 polygon coincides with profile P1 (Figure 5.1 and 6.9), this surprisingly high discrepancy could be attributed to survey quality problems and is probably not reflecting the real accumulation.

The equations results regarding R3 polygon were also in good agreement, showing similar outcomes with the UAV dataset results for 2011-2016 (acquired only for the eastern area). A discrepancy in terms of R2 polygon is again revealed, exhibiting again nearly six times greater sedimentation rate, opposed to the formula results and the R2 polygon. It is also worth to remark that the volume rates of R2, and hence of near the inlet area, of period of 2009-2011, are notably higher to the corresponding rates of 2011-2016. Overall, the results evidence higher accumulation rates in the first examination period 2009-2011 in respect to 2011-2016.

## 7. Discussion

Within this study the potential of aeolian sediment transport in Ancão Peninsula and its effect on the dune system development were approached from different aspects to spherically ascertain its evolution over the past decades. For this purpose, textural analysis, vegetational habitats, onshore wind regime, sediment transport potentials, shoreline evolution and dune morphology have been explored. These parameters combined, aim to enlighten in what extent the dune activity of Ancão Peninsula is controlled by the aeolian sediment transport and furthermore, which complementary factors are contributing to its current morphology.

### *Textural analysis and wind forces*

Initially, textural analysis was a required step to define the critical grain size for potential sediment transport with the provided wind conditions. Simultaneously, by determining the threshold velocity, a windy event was established for the study area. In addition, by examining the mean grain size per morphology in the beach profile (beachface, backshore and dune) conclusions regarding the transfer patterns once sand is provided on the beachface are allowed. The sedimentary analysis indicated that there are overall minor differences between the eastern and the western sector (Figure 6.1). The estimation of sediment transport potentials was mostly investigated from the beachface to the backshore to ascertain the amount of new transferred sand available for foredune enhancement. Investigating the aeolian sediment transport potentials from the beachface to the backshore along Ancão Peninsula, geomorphological differences between the two sectors cannot be attributed to grain size. Backshore zone had in general coarser sediment and shells, compared to beachface and dune samples, that may have been deposited on the sand surface directly by wave/tide action or they may have been exposed as a result of erosion by storm waves or wind, resulting in the development of a lag deposit (Davidson-Arnott et al., 1997). Additionally, the beachface and dune morphologies are consisted of fine sediments (Figure 6.2). Consequently, aeolian transfer of the finer sediments from the beachface to backshore, lay a coarser bed layer of sediments bare at the backshore that cannot be transported with the existing wind field regime (Figure 6.6b) further on to dunes. Hoonhout and de Vries (2016) described how the spatio-temporal variation in bed surface properties influences the aeolian sediment transport, namely spatial variations occur naturally in coastal environments, for example coarse material or

strandlines that cover erodible surface reduce the sediment availability. Roughness density can explain on the other hand the instantaneous variations in time and changing consequently sediment transport capacity. Such properties can be hereby explained by the concept of an initial reduction of sediment supply to the beachface, which is consisted by medium and fine sand and is transferred further on to the backshore, where the medium sand resides on the surface (Figure 6.2). Since the threshold velocity is hence increased, mainly the finer sediments are winnowed and transported inland, reducing the transport capacity. As a result, the transport rate is impacted and the backshore has been likely in an armoured state over time, due to shell fragments and non-erodible sediments (Neuman et al., 2012). This suggestion is furtherly enhanced by the sorting results of the granulometric analysis, where each morphological zone (beachface, backshore and dune) is well sorted (all results within range of 1.50-1.52, excluding the outliers; Figure 6.3) for all three sampling dates (July, October, February) implying that this concept of fine sand transferred from the beachface to the backshore and winnowed from the backshore to the dune and exposing a coarser backshore surface can be a regular condition in the beach profile. The dune granulometric results also support this sediment transfer path since dune and beachface grain size classes coincide (Figure 6.2).

#### *Wind field regime and sediment transport potentials*

At first, from the wind record of the last two decades it is clearly inferred that the peninsula is not affected by frequent windy events, and at the same time the dominant wind velocity is below the threshold velocity (8.9 m/s) (see Figure 6.6 and Figure 6.7). It is therefore expected, considering the mean grain size of the beachface (466  $\mu\text{m}$ ), that sediment transport capacity is low. Nevertheless, the occurring windy events followed in some extend a periodic trend and not only in specific years but also in distinct months throughout the entire year. Subsequently, the years with the most numerous windy events were integrated with the years that resulted in the highest sediment transport potentials to ascertain how the frequency of windy events affects the potential of sediment transfer. Comparing the two relative figures of the events with monthly velocities  $>8.9$  m/s and their corresponding frequency in Figure 6.7, it appears that 1998, 2000, 2001, 2008, 2009 and 2010 are the years with the majority of windy events. On the other hand, only 2002, 2009 and 2010 show high potential transport rates (Figure 6.18 and 6.19). In terms of comparison between the two examining periods, 2009-2011 and 2011-2016, the first period yielded higher rates of

transport potentials than the latter, since it was consisted by more frequent windy events occurring in 2009 and 2010.

Examining the windy events on these 'yielding' years, they were concentrated in one or two months, but simultaneously during at least three of the months, the monthly mean wind velocities were above 10.5 m/s. On the contrary, during the remaining years the windy events prevailed only in one or two months, where the majority of the average monthly velocities blew near the threshold velocity. The corresponding calculations, in terms of potential transport confirm that the annual theoretical sediment transport for the years 2002, 2009 and 2010 (Figure 6.18 and 6.19) is the highest, whereas very strong winds (>11 m/s) marked in 1998, 2003, 2011 and 2013 during a single month did not accommodate respectively high transport rates. As Table 9 indicates, years 1998, 2009 and 2010 had a combination of high mean velocities and high frequency of windy events. When comparing years 1998 and 2001, the first had the highest mean windy event velocities resulting in high sediment transport potential, whereas 2001 had very high sum of windy events that was not respectively reflected in the potential transport. At the same time, even between 2000 and 2001 the mean velocity of the year 2000 overcomes only by 0.1 m/s the mean velocity of 2001 and it even has lower frequency of windy events compared to 2000. It is nevertheless resulting in significantly higher average transport rates. More detailed, presented also in Figure 6.7, in 2000, 403 windy events occurred in April with a mean monthly velocity of 10.4 m/s and in December 365 events with mean velocity of 11.2 m/s. In contrast, in December 1998 the mean velocity was 13.6 m/s, but only 84 windy events took place in that month and the rest of the months had high wind velocities (9.3 to 9.9 m/s) combined with few windy events (approximately from 20 to 160 events). In addition, as an example, in 2002 numerous windy events with ~10.1 m/s velocities in April, March and May (from 145 to 250) and November and December (~11.4 m/s and ~190 events) resulted in one of the highest transport rates. An ensuing assumption could hence be that persistent and relatively high velocities are more effective than concentrated and intense windy events lasting some hours or a few days. Future on-field measurements of volume changes in monthly and annual rates could enlighten this suggestion, since the applied formula yields results only as a function of wind velocity.

Table 9: Comparison table of average annual velocity of windy events, sum of windy events (10-min) each year and annual estimation of potential sediment transport.

year	average annual velocity > 8.9 m/s	sum of windy events	average potential sediment transp. (m <sup>3</sup> /m)	
1997	9.9	527	0.71	data from July until December
1998	<b>10.3</b>	827	1.46	
1999	9.9	718	0.70	
2000	9.9	1055	1.38	
2001	9.8	1085	0.84	
2002	<b>10.2</b>	<b>1326</b>	<b>1.71</b>	
2003	<b>10.1</b>	936	1.30	
2004	9.9	6.85	0.58	
2005	9.8	750	0.60	
2006	<b>10.2</b>	790	0.97	
2007	9.8	512	0.41	
2008	9.8	1231	1.31	
2009	<b>10.3</b>	<b>1577</b>	<b>2.09</b>	
2010	<b>10.1</b>	<b>1502</b>	<b>1.80</b>	
2011	9.9	639	0.88	
2012	9.6	445	0.23	
2013	10	949	1.06	
2014	-	-	~0.81	no data for the entire year
2015	10	691	0.55	
2016	9.9	903	0.62	data from January until August

Overall, the sediment transport potentials don't signify prompt growth or in general a dynamic dune system, so the sand input based on the wind theoretical calculations is rather low. Regarding the sediment transfer potentials estimated with the two approaches (mean beachface size and sand weight percentage per class), the annual sediment capacity rate results, from a methodological perspective, indicate negligible differences (Figure 6.18 and 6.19). Therefore, in the particular study area with the existing granulometric data, the application of a more detailed calculation didn't contribute to conclusions on how the entire spectrum of grain size classes affects sediment transport. Nevertheless, it must be noted that the beachface sediment results used, had a normal distribution (skewness: -0.1 to 0.17, Figure 6.4). It could be hence suggested, that the mean grain size can be applied to obtain sediment transport potentials when granulometric data tend to have a



symmetrical distribution, and obtain safe results. On the other hand, when the granulometric analysis indicates asymmetry, the use of the entire grain size distribution (percentages approach) may be more appropriate.

Furthermore, the wind regime is not following a specific pattern, i.e. windy events occur in both winter and spring months. And in a more general aspect, in the 20-year investigated period windy years show a relative periodical behaviour, i.e. for each high annual average velocity year corresponds, relatively, a following low in average velocities year. Such variations are inducing variations in the volume of sand transported and on dune morphology (Hesp, 1983). Nonetheless, due to low frequency of windy events, extreme alterations on the morphology and elevation of the dune system are not anticipated. Accounting for all the above, the existing wind field constitute a mild to low influence factor for dune development.

An additional remark is that the rates of theoretical estimations are in very good agreement with the rates of actual Lidar and UAV measurements (Table 8) for both examining periods, but for R5 (western) and R3 (westward eastern) polygons. Nonetheless, these estimations express a generic overall assessment of sediment transport potential, where no additional impacting factors (e.g. beach slope, moisture, fetch distance, roughness, etc.) are taken into account.

#### *Vegetation habitat mapping and dune system correlations*

Initially, it was a necessity on the field for practical purposes to distinguish the morphological zones with regards to vegetation habitats and consequently to fulfil the vegetational identification. Simultaneously, this would allow the correlation and investigation of compliance between the morphology and the vegetation habitats. It was also attempted to use identified vegetational communities as bioindicators of coastal conditions and changes (Lomba et al., 2008).

From the vegetation species analysis in respect to the species presence in the distinct habitat zones, it can be asserted that the dune system of Ancão Peninsula is divided in two sectors, a more mature, the western and a partially dynamic, the eastern. Initially, in the western area only the most western site exhibits limited early vegetation (EUNIS code: 1210) and in conjunction to absence of embryonic foredunes this is rendered to erosion influence (Lomba et al., 2008; Attore et al., 2012; Ciccarelli, 2014). In addition, the embryo vegetation was in the western sector merely concentrated on the dune toe and constrained in a few meters length, that signifies beach restriction (Martins et al., 2014). In general, the present vegetational habitats are explaining their position in this sector

only in some extend, and in particular only at the dune toe. This complies also with the current morphology, i.e. the absence of hummocks. Subsequently, on the dune crest species *Armeria pungens* and *Artemisia campestris* are being introduced to the dune toe and colonizing the dune crest, which is not constituting their original habitat.

So, at the dune toe, it is suggested that the confined sedimentation (or sediment renewal deficiency) is not allowing the development of new embryo hummocks and consequently fixed dunes' species can be introduced even at the dune toe. The frequently formed escarpment (Achab et al., 2014) as well as other studies on the area, e.g. (Ramos & Dias, 2000; Ferreira & Matias, 2013; Ferreira et al., 2016; Lira et al., 2016) verifies the dune system's retreat on this sector. On the dune crest the species hosted, belong both to the shifting and fixed dunes. Mingling of these species can be justified by restricted accretion at the dune crest, revealing the stabilization of the crest's substrate (Martins et al., 2014), a prerequisite for chamaeephtic species, as *Artemisia crithmifolia/campestris*. This is indicative of erosional beaches, which could be explained when sand saltation and accumulation action is primarily occurring between the crest and lee side and thus the vegetation of the two zones is mixing (Martins et al., 2014). Conclusively, the dune system in this sector is unfolding an advanced level of maturity with a concurrent inclination to dynamic erosion. On the other hand, the eastern sector is comprised in all sites by embryonic habitats vegetated even with low density coverage. In this most seaward zone however, in Transects 4 and 3, most hosted species correspond to vegetation of shifting dunes (2120). At the same time, the dune crests in these sites are colonized by *Artemisia crithmifolia/campestris* found on fixed dunes, implying development ceasing and mainly a more mature dune zone. However, Transect 2 near the inlet, incipient hummocks are more seaward formed and an additional foredune zone has developed, hosting the corresponding species (*Eryngium maritimum* and *Ammophila arenaria* respectively) for these zones. These habitats are in agreement with the morphological zones, which reveals that this location in the dune system is under ongoing development. It can be inferred that the dune system is advancing as a consequence of delivery of new sediment to the backshore. The peninsula's broadest width at this most eastward section should also be accounted for this progradation, providing therefore a longer accommodation space, apparently supported by the positive sedimentation rates on this peninsula part.

Furthermore, within the present study it is suggested that additional factors are impacting species interior movement, as limited sediment supply. In that sense, the lack of sand renewal in the

foredunes and secondary dunes, induces bed surface stabilization and permits herbaceous plants to populate. Also, when shifting dunes species, for instance *Ammophila arenaria* are found more inland, this can also be caused due to strong colonization capacity, resistance and resilience to environmental perturbations and stress conditions (Martins et al., 2014) of the species and not necessarily due to sea erosion. An additional agent could be in this case the sediment transport, where the sand from foredunes transferred inland superimposes the existing sand layer, carrying biochemical properties to secondary dunes and allows its adaptation. Sparse density or low biodiversity in interior dune habitats can also contribute to species penetration and occupation of space, enhancing species migration in an inland direction. Respectively, a long term and constant state of a dune system with no significant sedimentary changes, provided efficient offshore winds, could also cause species movement from the secondary dunes to foredunes, governed by lack or constriction of sediment renewal in the primary dunes. This suggestion is contrasted with Martins et al. (2014), where primary species are migrating to foredune zone, insinuating sea water penetration, which is ultimately considered as a high bioindication potential of sea erosion. In addition, based also on the work of Lomba et al. (2008; 2005) and Ciccarelli (2014) vegetational communities, vs. individual species, are much stronger bioindicators of environmental conditions and changes for both short and long-term changes. Thus, when a species or a group with certain features colonize an extended surface, e.g. show high density, a community is formed. So, in terms of communities, in the western sector, where the dune crest vegetation is dominated in mostly by *Artemisia spp.* and *Armeria pungens* (2130), fixed dune vegetation species, it can be inferred that this is a mature dune ridge and under continuous erosion phenomena. The absence of phytosociologic features (embryo dune vegetation species) is enhancing the regression phase of the dune system in this sector (Lomba et al., 2008). On the eastern sector, in Transect 4 the most seaward crest ('Crest 2', Table 5), is colonized by *Artemisia spp.* and *Crucianella maritima* (2130), a fixed dune vegetation community, instead of shifting dunes vegetation, although embryo hummocks are formed. Hence, complex coastline dynamics can be inferred on that part. In Transect 3, ('Crest 2', Table 5) *Medicago marina* and *Pancratium maritimum* (2110) communities prevail on the seaward crest, and initiation of embryo dunes formation is signified. Near the inlet, in Transect 2, where shoreline progradation is most evident *Ammophila arenaria* and other shifting dune vegetation species (2120) are occupying the seaward crest ('Crest 1', Table 5) and thus new foredunes are supported, indicating an accretional phase.

Although it is not within the scope of this study, the following remark was appraised to be included. In relation to the dunes' habitat ecology, noticeable during field visits and supported later from the vegetation coverage results, is the appearance and domination of *Artemisia crithmifolia/campestris* in both sectors of the study area. This species tends to colonize and consequently to diminish the existence of other species in a habitat/morphological zone. The biodiversity at the time of the vegetation identification (February and March 2017) was suddenly confined when passing to more upland zones. This could entail prospective impediments to new hummock formation especially in the western sector. Considering also the limited appearance of sand-fixing (surface stabilization) and sand-building (sediment accumulation) plants (Carter, 1991), the shrubby physiology of *Artemisia crithmifolia/campestris* can further hamper sediment accumulation and tends to possess on its environment.

#### *Sand volumes, sediment supply, shoreline evolution and dune activity*

The dune vegetation line across the peninsula was used as a reliable indicator of shoreline evolution (Moore, 2000; Boak & Turner, 2005; Alves, 2007). Due to its response of accretion or erosion on the order of months to years, long term trends in shoreline are more apparent contrary to higher frequency changes of wet/dry lines (Hoeke et al., 2001) and it was thus trusted to extract shoreline movement rates. Movements in shoreline are well reflected in the dune system that is shifting accordingly, as the periodic evolution rates illustrate in Table 6, based on the vegetation line in each corresponding aerial photo employed. Additionally, the fact that vegetation delineation across the peninsula's beach is constituted by incipient perennial species, hence not affected by seasons, enhances the use of vegetation line as an indicator for shifting trends of the dune system. Nevertheless, such distinct link between shoreline and dune migration is allowed at large time scales (years, decades), which include a number of hydrodynamic events that reform the dune or affect the dune toe position (Pruszek et al., 2011). At smaller time scales (weeks, months), migration of the shoreline on sandy beaches is not always associated with the simultaneous evolution of the dune formations (Pruszek et al., 2011), and shifts can be temporary, owed to wave action. Within this context, shoreline evolution rates can represent dune system migration only in the long term (Crowell et al., 1993). It is then expected, that shoreline and dune shifts are reflected by approximately the same rates. With the existing conditions, in the western sector, where the beach is narrow and eroded, the variability of the shoreline positions can also be related to a change

of the dune toe position. However, in the eastern sector with a wider beach, shoreline trends and the dune toe can be mutually independent, as also stated in Pruszek et al. (2011).

The shoreline evolution rates in each period of investigation in conjunction with the mild wind field regime, suggest that Ancão Peninsula is highly affected by the eastward alongshore sediment supply. It was evident that after the jetties construction in Vilamoura (in early 1970s) the littoral drift was affected (Ferreira et al., 2016; Lira et al., 2016), delivering less sediment to the peninsula which reflected on an erosive period (period 1972-1989, Figure 6.14). It seems that the entire peninsula was impacted, as the western and central sector were eroding by -0.33 and -0.42 m/yr respectively and the eastern area indicated a milder erosion of -0.17 m/yr (Figure 6.14 and Table 6). The later periods shoreline rates (1989-2001 and 2001-2014), after the Vale do Lobo nourishments (Ferreira & Matias, 2013), contributed to shoreline stabilization in the western sector, but accretional trends were noted on the eastern (Figure 6.14 and Table 6). It can be hence insinuated that Ancão Inlet is a great impact factor on the coastline of this sector. Furthermore, this is supported by the fact that a new embryo and foredune ridge are formed hosted by incipient dune vegetation on the most eastward part of the eastern sector (Costas et al., 2017). Thus, the inlet has an effect at the dune system's morphology, nevertheless in its vicinity. This sand accumulation can be related to the formation of submerged sand banks that act as sediment trap to littoral drift and are associating to the inlet ebb delta development (Ferreira, 2011; Pacheco et al., 2011). In the next analysed period (1989-2001) the peninsula was also under shoreline retreat in the western sector, underlining the ongoing impacts of interruptions in the littoral cell (Taborda et al., 2005; Lira, et al., 2016) from the Vilamoura constructions. Especially, in period 2001-2014 the western area demonstrated further stabilisation and even some positive sedimentation rates at parts, governed by the 2010 updrift nourishment. On the contrary, the eastern sites had the highest sedimentation rates in this period, especially in the inlet vicinity, which was reflected with a new foredune dune ridge and developing incipient hummocks. In average, along the peninsula the range of shoreline evolution rates (linear regression rates, Figure 6.13) for 1952-2014 was between -0.47 to 0.95 m/yr. In Lira et al. (2016) for 1958-2010 the rates were indicating only erosion, namely a range from -2.0 to -0.2 m/yr. This discrepancy could be in some extend attributed to the shorter period of examination, as the supplementary updrift nourishment of 2010 has positively impacted the Ancão Peninsula. Additionally, in Lira et al. study (2016) the foredune toe line was used as a

shoreline indicator, that can be more dependent to wave processes and indicative more for erosion and not accretion (Stafford & Langefelder, 1972).

Assessing the dune development by the shoreline movement rates extracted by the aerial photographs, they reflect medium term evolutionary changes, as classified from Crowell & Leatherman (1993), of 62 years, whereas the volume results from the Lidar and UAV datasets, are demonstrative for a smaller temporal scale of six years. In the study area, the aeolian action indicates low depositional rates, considering, that the period when the volume results were extracted (2009-2016), is within a non-erosional period and after a recent nourishment.

The present conditions in the western sector of the peninsula suggest that after the updrift nourishments starting in 1998 between Quarteira and Vale do Lobo until the recent in 2010 (Ferreira & Matias, 2013), the beach capacity for sand retention has relatively increased, therefore shoreline is currently stabilised and dunes were therefore preserved, nevertheless due to a steep foreslope and narrow backshore, the beachface is lacking the capacity to retain the sand and is susceptible to wave impact (Costas et al., 2017). Therefore, beach growth and subsequent dune development are expected to be limited. In support of this, volume results of R5 polygon (Table 8) show low but positive sedimentation rates. On the other hand, the eastern sector with gentler beach face slope and wider beach width, is positively impacted by the sediment retention at the ebb delta (Ferreira, 2011), and is showing ongoing but mild development, provided the existing wind power and grain size. Worth noticing is that volume rates of R2 polygon (Table 8) are very high in respect to R3 rates for 2011-2016, although no particular high transport potentials were marked in that period. This can be partly attributed to accretion from wave action in the upper berm area (Figure 6.22) and not merely to aeolian accumulation. Simultaneously, this explains the higher sedimentation in 2009-2011 from aeolian transport, achieved due to more frequent windy events in respect to 2011-2016, where lower rates have been marked after 2011 owed to windy events deficiency.

The development of embryo dunes in the east-most area in the eastern sector can be used as a supplementary geoindicator (Lomba et al., 2008) of the dune system progradation. Furthermore, as Ancão Inlet is in an ongoing eastward migration (Vila et al., 1999; Pacheco et al., 2007) that progressively elongates the peninsula, there is a constant effect of sedimentation in the eastern side positively impacting approximately 2 km adjacent to the inlet (Ferreira, 2011). As a result, the dune system development is expected to be influenced in a dynamic manner, mainly controlled by

the inlet's position. In Ferreira (2011) the beach volume results at the berm in profiles along the peninsula are high after the inlet relocation in 1997 and are the highest until 2006 (latest results of the study) reaching at the most eastward 2 km an overall accumulation of  $2-3 \times 10^5 \text{ m}^3$ . However, such sand volumes, as the Lidar and AUV measurements reveal on the backshore (Figures 6.20, 6.21 & 6.22; Table 8), do not seem to reach from the berm to the backshore and the dunes. Simultaneously, progradation of the shoreline is marked, especially in the last examined period (2001-2014) (Figure 6.14). Presumably this is explained, as Costas et al. (2017) suggested, due to restricted retention capacity in the upper part of the beach. Sediment, and especially at the inlet vicinity is supplied to the beach, and accommodation space through shoreline progradation has formed. Nevertheless, the low intensity and frequency of wind events in conjunction with the coarse grain size at the beachface ( $466 \mu\text{m}$ ) do not facilitate high transfer rates of the sand to the backshore. The sediment supplied to the berm is then removed by wave action. Therefore, the foredune development is slow. In the western part, the narrow beach is very often exposed to wave processes and hence the sedimentation for embryo dunes development is unlikely to occur.

## 8. Conclusions

Aeolian sediment transport potentials were investigated in the present study to ascertain the wind influence on the dune system of Ancão Peninsula. Grain size analysis in distinct morphologies, beachface, backshore and dune, in five profiles along the peninsula took place. The average grain size of the beachface was used to determine the shear threshold wind velocity, considering that beachface sand is the supplier to the dunes. The mean grain size at the beachface was defined at 466  $\mu\text{m}$ , and by the existent wind field dataset of the last twenty years, it was determined that sediment transport can be achieved by wind of  $>8.9$  m/s. Those events, referred as windy events, accounting for the onshore winds and the direction of the peninsula, had very low occurrence, namely 1.7%. Thus, the sediment transport potentials, using two textural approaches, showed very low transport capacity for the twenty-year period. The first approach considered an average beachface grain size and the second used the percentages of the grain size distribution. Both approaches resulted in similar annual average rates, 1.00  $\text{m}^3/\text{m}$  and 1.16  $\text{m}^3/\text{m}$  correspondingly. Potential sediment transport was higher for 1998, 2009 and 2010 (annual average: 1.9  $\text{m}^3/\text{m}$ ). At the same time 2002, 2009 and 2010 were the windier years (monthly average: 10.2 m/s). Furthermore, dune morphology was evaluated using beach profiles for the years 2009, 2011 and 2016. This allowed, firstly the morphological characterisation, but also the differentiation of two sectors along Ancão Peninsula. The western sector of the peninsula is constituted by one main dune crest ridge without embryo dunes and rather high in elevation (in average 8 m to 10 m). The dune slope is steep,  $\sim 0.5$ , featured by an eroded dune toe and the beach is approximately 23 m. On the other hand, the eastern sector comprises one mature dune and one or two additional foredunes at sites. Hummocks and embryo dunes are colonizing on the most eastward part of the peninsula, in the vicinity of Ancão Inlet. The highest dune elevation does not exceed 8 m with an average slope  $\sim 0.1$ . The beach width is  $\sim 32$  m and widens near the inlet to  $\sim 45$  m. Actual volume measurements of 2009-2011 and 2011-2016, extracted from Lidar and UAV datasets on three distinct backshore polygons, revealed annual rates 1.20  $\text{m}^3/\text{m}$  in the eastern sector for 2009-2011 and 0.85  $\text{m}^3/\text{m}$  in the western, and 0.86  $\text{m}^3/\text{m}$  for 2011-2016 in the eastern sector. The results also showed an abrupt increase near the inlet, 7.32  $\text{m}^3/\text{m}$  and 6.32  $\text{m}^3/\text{m}$  in periods 2009-2011 and 2011-2016 respectively. The theoretical volume estimations seem to agree with the real measurements of the polygons in the western and eastern sector, but there is underestimation for



the eastern-most polygon. In addition, the examined period 2009-2011, which includes windy years, has higher mean annual rates as the 2011-2016 period.

An additional aspect investigated, was the vegetational species and their density in transects along the peninsula. In general, the western sector is dominated by species of fixed coastal dunes (*Artemisia crithmifolia*, *Helichrysum italicum*; 2130) and there is limited presence of incipient dune vegetation (*Elymus farctus*; 2110). Contrarily, in the eastern sector drift line vegetation exists (e.g. *Calystegia soldanella*; 1210) and the embryo dunes are in some degree colonised by the respective species (*Pancratium maritimum*, *Medicago marina*; 2110). The second foredune crest (present in Transects 4 and 3) hosts species of both shifting (2120) and fixed dunes (2130). On the most eastward transect an additional foredune has been developed and hummocks are formed, vegetated mainly by incipient dune vegetation (2110).

Incipient dune vegetation was used as a trustworthy shoreline evolution indicator, from which later safe conclusions in a medium time scale (Crowell et al., 1993) regarding shifts on the dune system and morphological features can be extracted. Shoreline evolution rates from 1952 to 2014 have shown non-linear trends along three sectors of the peninsula (western, central and eastern). The western sector was mainly eroding until 2001 ( $\sim -0.20$  m/yr) and has stabilised since then. The central sector, where data was available, was also affected by erosion ( $\sim -0.25$  m/yr). In the eastern sector, trends are mainly accretional, besides period 1972-1989 ( $\sim 0.79$  m/yr).

The dune development was assessed considering altogether mainly the wind field regime, the shoreline rates, the dune system morphology, the vegetational communities and the Lidar and UAV measurements. It can be inferred that at the periods of erosive shoreline (1972-1989), the dune system was either migrating landwards or the seaward foredune was scarped or embryo hummocks/ dunes were disappearing. On the contrary, during accumulation periods (2001-2014) the shoreline progradation in the eastern sector was signifying wider accommodation space that supported incipient dune vegetation growth and subsequent hummocks and embryo dunes formation. In the western sector, during that period (2001-2014), the shoreline was stabilised and erosion was impeded. Using vegetational communities (2017) as bioindicators, the western sector is consisted by a single mature dune ridge with lack of embryo dune vegetation (Transects 5-7), and hence dune development is not noted on this part of the peninsula. On the eastern sector two or three crests are found, however due to fixed dune vegetation species in incipient dunes of Transects 4 and 3 the dune system is in a non-dynamic state. Approaching to the inlet area, in

Transect 2, the colonisation of embryo dune vegetation communities at the seaward area and formation of a new embryo and foredune ridge, designate dune growth. Hence, also from a morphological aspect, it can be ascertained that the dune system in the western sector with steep dune bluffs and narrow beach has ceased developing, and at the eastern sector is active basically only at the eastern-most area.

Updrift nourishments that started in 1998 in Quarteira until recently in 2010 have facilitated shoreline stabilization in the western sector and progradation in the eastern sector, especially near the inlet, which consequently positively impacted the dune system along the entire peninsula. Although this could enhance dune system development, the low intensity of winds and limited frequency of windy events cannot promote prompt development. In conjunction with the coarse beachface grain size, aeolian transport capacity is restricted, even at areas, e.g. near the inlet, where sediment supply is enhanced. Therefore, slow dune growth is expected, but only in the inlet vicinity. It can be finally concluded that the coarse grain size, few and low intensity windy events, and shoreline evolution are the determining factors for dune evolution in Ancão Peninsula.

## Bibliography

- Aagard, T., Orford, J., & Murray, A. S. (2007). Environmental controls on coastal dune formation; Skallingen Spit, Denmark. *Geomorphology*, p. 29-47.
- Achab, M., Ferreira, O., & Dias, J. A. (2014). Evaluation of sedimentological and morphological changes induced by the rehabilitation of sandy beaches from the Ria Formosa barrier island system (South Portugal). *Thalassas*, p. 21-31.
- Almeida, L. P., Vousdukas, M. V., Ferreira, O., Rodrigues, B. A., & Matias, A. (2012). Thresholds for storm impacts on an exposed sandy coastal area in southern Portugal. *Geomorphology*, p. 3-12.
- Alves, M. V. (2007). *Detection of physical shoreline indicators in a object-based classification approach, Master Thesis*. Enschede, The Netherlands: International Institute for Geo-Information Science and Earth Observation.
- Andrade, C. F. (1990). *O ambiente de barreira da Ria Formosa, Algarve, Portugal. PhD Thesis*. University of Lisboa.
- Arens, S. M. (1996a). Rates of aeolian transport on a beach in a temperate humid climate. *Geomorphology*, p. 3-18
- Arens, S. M. (1996b). Patterns of sand transport on vegetated foredunes. *Geomorphology*, p. 339-350.
- Arens, S. M., Baas, A. C., Boxel, J. H., & Kalkman, C. (2001). Influence of Reed Stem density on Fore-dune Development. *Earth Surface Processes and Landforms*, p. 1161-1176.
- Arens, S. M., van Boxel, J. H., & Abuodha, J. O. (2002). Changes in grain size of sand in transport over a fore-dune. *Earth Surface Processes and Landforms*, p. 1163-1175.
- Arens, S. M., Kaam-Peters, V., & Van Boxel, J. (1995). Airflow over foredunes and implications for sand transport. *Earth surf. Process. Landf.*, p. 314-332.
- Asensi, A., & Diez-Garretas, B. (2017). Coastal Vegetation . In J. L. (Ed.), *The Vegetation of the Iberian Peninsula, Plant and Vegetation Vol. 2* (pp. p. 397-432). Springer International Publishing.
- Attore, F., Maggini, A., Di Tragglia, M., De Sanctis, M., & Vitale, M. (2012). A methodological approach for assessing the effects of disturbance factors on the conservation status of Mediterranean coastal dune systems. *Applied Vegetation Science*, p. 1-10.
- Bagnold, R. A. (1941). *The physics of blown sand and desert dunes*. London: Methuen.
- Bauer, B. O., Davidson-Arnott, R. G., Hesp, P. A., Namikas, S. L., Ollerhead, J., & Walker, I. J. (2009). Aeolian sediment transport on a beach: Surface moisture, wind fetch, and mean transport. *Geomorphology*, p. 106-116.
- Bauer, B. O., Davidson-Arnott, R. G., Nordstrom, K. F., Ollerhead, J., & Jackson, N. L. (1996). Indeterminacy in Aeolian Sediment Transport Across Beaches. *Journal of Coastal Research*, p. 641-653.

- Bauer, B. O., Yi, J., Namikas, S. L., & Sherman, D. J. (1998). Event detection and conditional averaging in unsteady aeolian systems. *Journal of Arid Environments*, p. 345-375.
- Bauer, B., & Davidson-Arnott, R. (2003). A general framework for modelling sediment supply to coastal dunes including wind angle, beach geometry and fetch effects. *Geomorphology*, p. 89-108.
- Beachapedia. (2013). *Vegetation*. Retrieved from [www.beachapedia.org](http://www.beachapedia.org)
- Bearden W. O., (1982). Sample size effects on chi square and other statistics used in evaluating causal models. *Journal of Marketing Research*, 425-430.
- Bettencourt, P. (1994). *Les Environnements Sedimentaires de la Cote Sotavento (Algarve, Sud Portugal) et leur Evolution Holocene et Actuelle. PhD Thesis, 2 Volumes (in French)*. University of Bordeaux.
- Bird, E. C. (1985). *Coastline changes: A global review*. London: Wiley & Sons.
- Bird, E. C. (2008). *Coastal Geomorphology*. West Sussex, England: John Wiley & Sons, Ltd .
- Bisal, F., & Hsieh, J. (1966). Influence of moisture on erodibility of soil by wind. *J. Soil Science*, p. 143-146.
- Bisal, F., & Nielsen, K. E. (1962). Movement of soil particles in saltation. *Can. J. Soil Sci.*, p. 81-86.
- Blott, S. J., & Pye, K. (2001). a grain size distribution and statistics package for the analysis of unconsolidated sediments. *Earth Surface Processes and Landforms*, 1237-1248.
- Boak, E. H., & Turner, I. L. (2005). Shoreline definition and detection: A review. *Journal of Coastal Research*, p. 688-703.
- Brinks , L., Gerber, K. E., Sin, J.-L., Swineford, J. T., & Zapata, A. K. (2013). *The Effects of Two Fall Storms on a Lake Michigan Foredune*. Department of Geology, Geography and Environmental Studies. Grand Rapids, Michigan: Calvin College.
- Burmingham, H., & French, J. (2017). Understanding coastal change using shoreline trend analysis supported by cluster-based segmentation. *Geomorphology*, p. 131-149.
- Bush, D. M., & Young, R. (2009). Coastal features and processes. *The Geological Society of America*, p. 47-67.
- Carter, R. W. (1991). Near-future sea level impacts on coastal dune landscapes. *Landscape ecology*, p.29-39.
- Ceia, F. R., Patricio, J., Marques, J. C., & Dias, J. A. (2010). Coastal vulnerability in barrier islands: The high risk areas of the Ria Formosa (Portugal) system. *Ocean & Coastal Management*, p. 478-486.
- CERC. (1977). *Shore Protection Manual*. Fort Belvoir: U.S. Army Coastal Engineering Research Centre.
- Chepil, W. S. (1956). Influence of moisture on erodibility of soil by wind. *Proc. Soil Sci. Soc. Am.*, (pp. p. 288-292).

- Chepil, W. S., & Siddoway, F. H. (1959). Strain-gauge anemometer for analyzing various characteristics of wind turbulence. *J. Meteorol.*, p. 411-418.
- Chiara Popesso, A. P. (2016). Evolution of a relocated inlet migrating naturally along an open coast. *Journal of Coastal Research Special Issue*, 233-237.
- Ciccarelli, D. (2014). Mediterranean Coastal Sand Dune Vegetation: Influence of Natural and Anthropogenic Factors. *Environmental Management*, p. 194-204.
- Costa, M., Silve, R., & Vitorino, J. (2001). Contribuicao para o estudo do clima de agitacao maritima na costa portuguesa. *Proceedings of 2as Jornadas Portuguesas de Engenharia Costeira e Portuaria*. Sines, Portugal: International Navigation Association, PIANC.
- Costas, S., Bon de Sousa, L., Plomaritis, T. A., Pliatsika, D. A., & Ferreira, O. (2017). Aeolian sediment transport enhanced by storms and human pressure at coarse sandy barrier islands. *IX Jornadas de Geomorfologia Litoral* (pp. p. 301-306). Menorca: Geo-Temas.
- Crowell, M., Honeycutt, M., & Hatheway, D. (1999b). Coastal Erosion Hazards Study: Phase One Mapping. *Journal of Coastal Research*, p.10-20.
- Crowell, M., Leatherman, S. P., & Buckley, M. K. (1991). Historical Shoreline Change: Error Analysis and Mapping Accuracy. *Journal of Coastal Research*, p. 839-852.
- Crowell, M., Leatherman, S. P., & Buckley, M. K. (1993). Shoreline Change Rate Analysis: Long term versus short term data. *Shore and Beach*, p. 13-30.
- Csahok, Z., Misbah, C., Rioual, F., & Valance, A. (2000). Dynamics of aeolian sand ripples. *Eur. Phys. J.*, p. 71-86.
- Davidson-Arnott, R. (2010). *An Introduction to Coastal Processes and Geomorphology*. New York: Cambridge University Press.
- Davidson-Arnott, R. G., Bauer, B. O., Walker, I. J., hesp, P. A., Ollerhead, J., & Chapman, C. (2012). High-frequency sediment transport responses on a vegetated foredune. *Earth and Surface Processes and Landforms*, p. 1227-1241.
- Davidson-Arnott, R. G., MacQuarrie, K., & Aagaard, T. (2005). The effect of wind gusts, moisture content and fetch length on sand transport on a beach. *Geomorphology*, p. 115-129.
- Davidson-Arnott, R., & Law, M. (1996). Measurement and prediction of long-term sediment supply to coastal foredunes. *J. Coast. Res.*, p. 654-663.
- de Vries, S., Southgate, H. N., Kanning, W., & Ranasinghe, R. (2012). Dune behavior and aeolian transport on decadal timescales. *Coastal engineering*, p. 41-53.
- Dias, A. J., & Neal, W. (1992). Sea Cliff Retreat in Southern Portugal: Profiles, Processes, and Problems. *Journal of Coastal Research*, p. 641-654.
- Dias, A. J. (1988). Aspectos geologicos do Litoral Algarvio. *Geonovas (Lisboa)*, p. 113-128.
- Dias, J. A., Ferreira, O., Matias, A., Vila-Concejo, A., & Sa-Pires, C. (2003). Evaluation of Soft Protection Techniques in Barrier Islands by Monitoring Programs: CAse Studies from Ria Formosa (Algarve-Portugal). *Journal of Coastal Research*, p. 117-131.

- Dias, J. M., & Gonzalez, R. (2000). The Ria Formosa and the Guadiana Delta (SW Iberia): Contrasting response of coastal environments to highstand conditions. *Coastal Interactions during sea-level highstands*, p. 29-32.
- Dissanayake, P., Brown, J., Wisse, P., & Karunaratna, H. (2015). Effects of storm clustering in beach/dune evolution. *Marine Geology*, p. 63-75.
- Dolan, R., Fenster, M. S., & Holme, S. J. (2012). Temporal analysis of shoreline recession and accretion. *Coastal Education & Research Foundation*, p. 723-744.
- Dry Tropics Wiki. (2015, January). *Coastal Zones*. Retrieved from NQ Dry Tropics: [http://wiki.bdnrm.org.au/index.php/Coastal\\_Zones](http://wiki.bdnrm.org.au/index.php/Coastal_Zones)
- Duran , O., & Moore, L. J. (2013). Vegetation controls on the maximum size of coastal dunes. *PNAS*, p. 17217–17222.
- Esaguy, E. (1986). Ria de Faro, Ilha do Ancao, Evolucao 1950-1985. *Direcao Geral de Portos. Internal Report*, p. 7.
- EUNIS, E. N. (2004). *EUNIS habitat classification*. Retrieved from EUNIS, the European Nature Information System: <https://www.eea.europa.eu/themes/biodiversity/eunis/eunis-habitat-classification#tab-derived-datasets>
- European Environmental Agency (EEA). (2017, August). *Habitat Annex I Directive hierarchical view, Coastal and Halophytic Habitats*. Retrieved from European Nature Information System, EUNIS: <https://eunis.eea.europa.eu/habitats>
- Everard, M., Jones, L., & Watts, B. (2010). Have we neglected the societal importance of sand dunes? An ecosystem services perspective. *Aquatic Conservation: Marine and Freshwater Ecosystems*, p. 476-487.
- Feagin , R. A., Wu, X. B., Smeins, F. E., Whisenant, S. G., & Grant, W. E. (2005). Individual versus community level processes and pattern formation in a model of sand dune plant succession. *Ecological Modelling*, p. 435-449.
- Feagin, R. A., Figlus, J., Zinnert, J. C., Sigren, J., Maritnez, M. L., Silva, R., . . . Carter, G. (2015). Going with the flow or against the grain? The promise of vegetation for protecting beaches, dunes and barrier islands from erosion. *Front. Ecol. Environ.*, p. 203-210.
- Feagin, R. A., Mukherjee, N., Shanker, K., Baird, A. H., Cinner, J., Kerr, A. M., . . . Dahdoud-Guebas, F. (2010). Shelter from the storm? Use and misuse of coastal vegetation bioshields for managing natural disasters. *Conservation Letters*, p. 1-11.
- Ferreira, O. (2011). Morphodynamic impact of inlet relocation to the updrift coast: Ancão Peninsula (Ria Formosa, Portugal)., (pp. p. 497-504).
- Ferreira, O., & Matias, A. (2013). Portugal. In E. Pranzini, & A. T. Williams, *Coastal Erosion and Proteccion in Europe* (pp. p. 275-293). London: Routledge.
- Ferreira, O., Garcia, T., Matias, A., Taborda R., & Dias , J. (2006). An integrated method for the determination of set-back lines for coastal erosion hazards on sandy shores. *Continental Shelf Research*, p. 1030-1044.

- Ferreira, O., Martins, J., & Dias, J. (1997). Morfodinamica e vulnerabilidade da Praia de Faro. *EUROCOAST* (pp. p. 67-76). Portugal: Livro de Comunicacoes do Seminario Sobre a Zona Costeira do Algarve.
- Ferreira, O., Matias, A., & Pacheco, A. (2016). The East Coast of Algarve: a Barrier Island Dominated Coast. *Thalassas*, p. 75-85.
- Field Studies Council. (2012). Sand Dunes Guide. *Smartphone Application*.
- Finnigan, J. J., & Belcher, S. E. (2004). Flow over a hill covered with a plant canopy. *Quarterly Journal of the Royal Meteorological Society*, p. 1-29.
- Folk, R. L., & Ward, W. C. (1957). Brazos River bar: a study in the significance of grain size parameters. *Journal of Sedimentary Petrology*, p. 3-26.
- Garcia, T., Ferreira, O., Matias, A., & Dias, J. (2010). Overwash vulnerability assessment based on long-term washover evolution. *Natural Hazards*, p. 225-244.
- Garcia, T., Ferreira, Ó., Matias, A., & Dias, J. A. (2002). Recent Evolution of Culatra Island (Algarve – Portugal). *Littoral*. Porto, Portugal.
- Goldsmith, V. (1978). Coastal Dunes. In R. A. Davis, *Coastal Sedimentary Environments* (pp. p. 171-230). New York: Springer Verlag.
- Greene, K. (2002). *Beach nourishment: a review of the biological and physical impacts*. Washington DC: Atlantic States Marine Fisheries Commission.
- Hansom, J. D., Switzer, A. D., & Pile, J. (2015). Extreme Waves: Causes, Characteristics and Impact on Coastal Environments and Society. In J. Ellis, & D. J. Sherman, *Coastal and Marine Hazards, Risks and Disasters* (pp. p. 307-334). Elsevier.
- Hesp, P. (1983). Morphodynamics of incipient foredunes in New South Wales, Australia. In M. E. Brookfield, & T. S. Ahlbrandt, *Eolian Sediments and Processes* (pp. 0. 325-342). Amsterdam: Elsevier.
- Hesp, P. (1988). Surfzone, beach and foredune interactions on the Australian South East Coast. *Journal of Coastal Research*, p. 15-25.
- Hesp, P. (1989). A review of biological and geomorphological processes involved in the initiation and development of incipient foredunes. In C. Gimingham, W. Ritchie, B. Willets, A. Willis, & (Eds.), *Coastal Sand Dunes* (pp. p. 181-202). Proceedings of the Royal Society of Edinburgh, Section B.
- Hesp, P. (2002). Foredunes and blowouts: initiation, geomorphology and dynamics. *Geomorphology*, p. 245-268.
- Hesp, P. A., Dillenburg, S. R., Barboza, E. G., Tomazelli, L. J., Ayup-Zouain, R. N., Esteves, L. S., Clerot, L. C. (2005). Beach ridges, foredunes or transgressive dunefields? Definitions and an examination of the Torres to Tramandai barrier system, Southern Brazil. *Anais da Academia Brasileira de Ciências*, p. 493-508.

- Hesp, P. A., Walker, I. J., Namikas, S. L., Davidson-Arnott, R., Bauer, B. O., & Ollerhead, J. (2009). Storm wind flow over a foredune, Prince Edward Island, Canada. *Journal of Coastal Research*, p. 312-316.
- Hijma, M., & Lodder, Q. J. (2001). *An evaluation of aeolian sand transport models using four different sand traps at the Hors, Texel*. Utrecht University .
- Hoeke, R. K., Zarillo, G. A., & Synder, M. (2001). *A GIS Based Tool for Extracting Shoreline Positions from Aerial Imagery (BeachTools) Revised*. Washington, DC: US Army Corps of Engineers.
- Hoonhout, B. M., & de Vries, S. (2016). A process- based model for aeolian sediment transport and spatiotemporal varying sediment availability. *Journal of Geophysical Research*, p. 1555-1575.
- Howe, M. A., Knight, G. T., & Clee, C. (2009). The importance of coastal sand dunes for terrestrial invertebrates in Wales and the UK, with particular reference to aculeate Hymenoptera (bees, wasps & ants). *Journal of Coastal Conservation*, p. 91-102.
- Hsu, Shih-Ang (1971). Measurement of shear stress and Roughness Length on a Beach. *Journal of Geophysical Research*, (p. 2880-2885).
- Hyndman, R. J. (2011). Retrieved from <http://robjhyndman.com>
- IPCC. (2007). *Contribution of Working Group I to the Fourth Assessment Report of the Intergovernmental Panel on Climate Change*. (S. Solomon, D. Qin, M. Manning, Z. Chen, M. Marquis, K. B. Averyt, H. L. Miller, (Eds.) Cambridge, UK: Cambridge University Press.
- Jackson, N. L., & Nordstrom, K. F. (1998). Aeolian transport of sediment on a beach during and after rainfall, Wildwood, NJ, USA. *Geomorphology*, p. 151-157.
- Jensen, J. L., & Sorensen, M. (1983). On the mathematical modelling of aeolian saltation. In B. M. Sumer, A. Müller, & (Eds.), *Mechanics of Sediment Transport* (pp. p. 65-72). Balkema, Rotterdam.
- Kark, S. (2013). Ecotones and Ecological Gradients. In R. L. (Ed.), *Ecological Systems* (p. 147-160). New York: Springer.
- Keijsers, J. G., De Groot, A. V., & Riksen, M. J. (2015). Vegetation and sedimentation on coastal foredunes. *Geomorphology*, p. 723-734.
- Kim, D., & Yu, K. B. (2009). A conceptual model of coastal dune ecology synthesizing spatial gradients of vegetation, soil, and geomorphology. *Plant Ecology*, p. 135-148.
- Kocurek, G., & Lancaster, N. (1999). Aeolian Sediment States: Theory and Mojave Desert Kelso Dunefield example. *Sedimentology*, p. 505-516.
- Kocurek, G., & Lancaster, N. (1999). Aeolian system sediment state: theory and Mojave Desert Kelso dune field example. *Sedimentology*, p. 505-515.
- Kuriyama, Y., Mochizuki, N., & Nakashima, T. (2005). Influence of vegetation on aeolian sand transport rate from a backshore to a foredune in Hasaki, Japan. *Sedimentology*, p. 1123-1132.



- Lancaster, N. (2009). Dune morphology and dynamics. In A. J. Parsons, & A. D. Abrahams, *Geomorphology of Desert Environments (2nd 2dition)* (pp. p. 557-596). Springer Science+Business Media.
- Leatherman, S. P. (1979). Beach and dune interactions during storm conditions. *Q. J. Eng. Geol.*, *12*, 281–290.
- Lettau, K., & Lettau, H. (1977). Experimental and micrometeorological field studies of dune migration. In K. Lettau, H. Lettau, & (Eds.), *Exploring the Wold's Driest Climate* (pp. p. 110-147). Madison: University of Winsconsin Press.
- Levin, N., Ben-Dor, E., Kidron, G. J., & Yaakov, Y. (2008). Estimation of surface roughness ( $z_0$ ) over a stabilizing coastal dune field based on vegetation and topography. *Earth Surface Processes and Landforms*, p. 1520-1541.
- Lira, C. P., Silva, A. N., Tabprda, R., & de Andrade, C. F. (2016). Coastline evolution of Portuguese low-lying sandy coast in the last 50 years: an integrated approach. *Earth System Science Data*, p. 265-278.
- Lomba, A., Alves, P., & Honrado, J. (2008). Endemic Sand Dune Vegetation of the Northwest Iberian Peninsula: Diversity, Dynamics , and Significance for Bioindication and Monitoring of Coastal Landscapes. *Journal of Coastal Research*, p. 131-121.
- Lomba, A., Granja, H., Honrado , J., Favennec, J., & Vidal-Romani, J. (19-23 September 2005). Conservation of dune systems: contributions from morphodynamics and vegetation ecology. In J.-L. Herrier, J. Mees, S. A., S. J., H. van Nieuwhnhuyse, D. I., & (Eds.), *Proceedings 'Dunes and Estuaries 2005' - International Conference on Nature Restoration Practices in European Coastal Habitats* (pp. p. 633-635). Proceedings 'Dunes and Estuaries 2005' - International Conference on Nature Restoration Practices in European Coastal Habitats,: VLIZ Special Publication 19.
- Lyles, L., & Krauss, R. K. (1971). Threshold velocities and initial particle motion as influenced by air turbulence. *Trans. Am. Soc. Agric. Eng. Abs*, p. 563-566.
- Malina, F. J. (1941). Recent developments in the dynamics of wind erosion . *Trans. Am. Geophys. Union*, p. 262-284.
- Martinez , M. L., Hesp, P. A., & Gallego-Fernandez, J. B. (2013). Coastal Dunes: Human Impact and Need for Restoration. In M. L. Martinez, & e. a. (Eds.), *Restoration of Coastal Dunes* (pp. p. 1-14). Berlin: Springer.
- Martínez, M., Psuty, N., & Lubke, a. R. (2004). A perspective on Coastal Dunes. In M. L. Martínez, & N. P. (Eds.), *Coastal Dunes: Ecology and Conservation*. Springer.
- Martins, J. T., Ferreira , O., & Dias, J. M. (1997). A susceptibilidade da Praia de Faro a erosao por tempestade. *Proc. 9o Congresso Do Algarve*, (pp. p. 206-213). Racal Clube.
- Martins, J., Ferreira, O., Ciavola, P., & Dias, J. (1996). Monitoring of profile changes at Praia de Faro, Algarve: A tool to predict and solve problems. In J. Taussik, & J. (. Mitchell, *Partnerhip in Coastal Zone Management* (pp. p. 615-622). Samara Publishing.

- Martins, M. C., Neto, C. S., & Costa, J. C. (2013 ). The meaning of mainland Portugal beaches and dunes' psammophilic plant communities: a contribution to tourism management and nature conservation. *Journal of Coastal Research*, p. 279-299.
- Martins, M., Neto, C., Gutierrez, F., & Costa, J. (2014). Bioindicators of erosive dynamics in beach and dune systems in the Portuguese mainland coast. *Documents phytosociologiques*, p. 324-337.
- Mathew, S., Davidson-Arnott, R. G., & Ollerhead , J. (2010). Evolution of a beach–dune system following a catastrophic storm overwash event: Greenwich Dunes, Prince Edward Island, 1936–2005. *Canadian Journal of Earth Sciences*, p. 273-290.
- Matias, A., Ferreira, O., Mendes, I., & Dias , J. (1998). Monitorizacao da alimentacao artificial da Peninsula de Cacela. *Seminario sobre Dragagens, Dragados e Ambientes Costeiros* (pp. p. 47-56). Lisbon: EUROCOAST.
- Maun, M. A. (2009). *The Biology of Coastal Sand Dunes*. New York: Oxford University Press.
- Melrose, D. C., Rebuck, N. D., Townsend, D. W., Thomas, M., & Taylor, C. (2016, May 23). *NOAA, National Centers for Environmental Information*. doi:doi:10.7289/V5HQ3WV3 [access date: 12 June 2016]
- Mendez, M. (2007). *Detection of physical shoreline indicators in an object-based classification approach, MSc Thesis*. Netherlands: ITC.
- Moore, L. J. (2000). Shoreline Mapping Techniques. *Journal of Coastal Research*, p. 111-124.
- Muzavor, S. (2010). *Roteiro Ecologico da Ria Formosa*. Faro: Algarve Em Foco.
- Nalpanis, P. (1985). Saltating and suspended particles over flat and sloping surfaces. II. Experiments and numerical simulations. In O. E. Barndorff-Nielsen, J. T. Moller, K. R. Rasmussen, B. B. Willets, & (Eds.), *Proceedings of the international Workshop on the Physics of Blown Sand* (pp. p. 37-66). Dept. Theoretical Statistics of Mathematics, Aarhus University.
- Navarro, M., Munoz-Perez, J. J., Roman-Sierra, J., Ruiz-Canavate, A., & Gomez-Pina, G. (2015). Characterization of wind-blown sediment transport with height in a highly mobile dune (SW Spain). *Geologica Acta*, p.155-166.
- Neuman, C. M., Li, B., & Nash, D. (2012). Micro-topographic analysis of shell pavements formed by aeolian transport in a wind tunnel simulation. *Journal of Geophysical Research*.
- NOAA, *National Ocean Service*. (2015, March 18). Retrieved June 11, 2016, from NOAA, National Oceanic and Atmospheric Administration: <http://oceanservice.noaa.gov/facts/>
- NOAA *National Oceanographic and Atmospheric Administration*. Retrieved from [http://www.star.nesdis.noaa.gov/sod/lisa/SeaLevelRise/LSA\\_SLR\\_timeseries\\_regional.php](http://www.star.nesdis.noaa.gov/sod/lisa/SeaLevelRise/LSA_SLR_timeseries_regional.php)
- Nordstrom, K. F. (1992). *Estuarine Beaches*. London: Elsevier.
- Nordstrom, K. F., & Jackson, N. L. (1994). Aeolian processes and dunefields in estuaries. *Physical Geography*, p. 358-371.

- Nordstrom, K. F., & McCluskey, J. M. (1985). The Effects of Houses and Sand Fences on the Eolian Sediment Budget at Fire Island, New York. *Journal of Coastal REsearch*, p. 39-46.
- NSW Department of Land and Water Conservation. (2001). *Coastal Dune Management: A Manual of Coastal Dune Management and Rehabilitation Techniques*. Newcastle: Coastal Unit.
- Ollerhead, J., Davidson-Arnott, R., Walker, I. J., & Mathew, S. (2013). Annual to decadal morphodynamics of the foredune system at Greenwich Dunes, Prince Edward Island, Canada. *Earth Surface Processes and Landforms*, p. 284-298.
- Pacheco, A., Vila-Concejo, A., Ferreira, Ó., & Dias, A. (2007). Present hydrodynamics of Ancão Inlet, 10 years after its relocation. *Coastal Sediments '07*.
- Pacheco, A., Williams, J. J., Ferreira, O., Garel, E., & Reynolds, S. (2011). Applicability of sediment transport models to evaluate medium term evolution of tidal inlet systems. *Estuarine, Coastal and Shelf Science*, p. 119-134.
- Petersen, P. S., Hilton, M. J., & Wakes, S. J. (2011). Evidence of aeolian sediment transport across an *Ammophila arenaria*-dominated foredune, Mason Bay, Stewart Island. *New Zealand Geographer*, p. 174-189.
- Pilkey, O., Neal, W., Monteiro, J., & Dias, J. (1989). Algarve Barrier Islands: A Noncoastal-Plain System in Portugal. *Journal of Coastal Research*, 239-261.
- Popesso, C., Pacheco, A., Ferreira, Ó., & Fontolan, a. G. (2016). Evolution of a relocated inlet migrating naturally along an open coast. *Journal of Coastal Research*, p. 233-237.
- Prandl, L. (1904). Über Flüssigkeiten bei sehr kleiner Reibung. *Verhandlungen des III. Internationalen Mathematiker Kongress*, p. 484-491.
- Prisco, I., Acosta, A. T., & Ercole, S. (2012). An Overview of the Italian Coastal Dune EU Habitats. *Annali di Botanica*, p.39-48.
- Pruszek, Z., Ostrowski, R., & Schönhofer, J. (2011). *Variability and correlations of shoreline and dunes on the southern Baltic coast (CRS Lubiatowo, Poland)*. p. 97-120: Oceanologia.
- Psuty, N. (1988). Dune/beach interaction. *Journal of Coastal Research Special Issue*.
- Psuty, N. P. (2004). The Coastal Foredune: A Morphological Basis for Regional Coastal Dune Development. In M. I. Martinez, & N. P. Psuty, *Coastal Dunes, Ecology and Conservation* (pp. p. 11-28). Berlin Heidelberg: Springer.
- Psuty, N. P., & Silveira, T. M. (2010). Global climate change: an opportunity for coastal dunes?? *Journal of Coastal Conservation*, p. 153-160.
- Pye, K. (1983). Coastal dunes. *Progress in Physical Geography*, p. 531-557.
- Pye, K., & Neal, A. (1994). Coastal dune erosion at Formby Point, north Merseyside,. *Marine Geology*, p. 39-56.
- Pye, K., & Tsoar, H. (2009). *Aeolian Sand and Sand Dunes*. Leipzig: Springer-Verlag Berlin Heidelberg.

- Ramos, L., & Dias, J. M. (2000). Atenuacao do vulnerabilidade a galgamentos oceanicos no sistema da Ria Formosa mediante intervencoes suaves. *Proceedings of the 3rd Symposium on the Iberian Margin*, (pp. p. 361-362).
- Rodriguez, B., Matias, A., & Ferreira, O. (2012). Overwash Hazard Assessment. *Geologica Acta*, p. 427-437.
- Ruz, M.-H., Anthony, E. J., & Laurent, F. (2005). Coastal dune evolution on a shoreline subject to strong human pressure: the Dunkirk area, northern France. *Proceedings 'Dunes and Estuaries 2005' - nternational Conference on Nature Restoration Practices in European Coastal Habitats* , (pp. p. 441-449). Koksijde, Belgium.
- Sallenger Jr., A. H. (2000). Strom impact scale for barrier islands. *Journal of Coastal Research*, p. 890-895.
- Sarre, R. (1989). The morphological significance of vegetation and relief on coastal foredune processes. *Z. Geomorphol.*, p.17-31.
- Schwämmle, V. (2002). *Modeling of Dune Morphology (Diplomarbeit)*. Universität Stuttgart .
- Sherman, D. J., & Bauer, B. O. (1993). Dynamics of beach-dune systems. *Progress in Physical Geography*, p. 413-447.
- Sherman, D. J., Jackson, D. W., Namikas, S. L., & Wang, J. (1998). Wind-blown sand on beaches: an evaluation of models. *Geomorphology*, p. 113-133.
- Short, A. (1999). *Handbook of Beach and Shoreface Morphodynamics*. Baffins Lane, Chichester, West Sussex: John Wiley & Sons, Ltd.
- Short, A. D., & Hesp, P. A. (1982). Wave, beach and dune interactions in southeastern Australia. *Marine Geology*, p. 259-284.
- Sociedade Portuguesa de Botânica. (2014). *Flora-On: Flora de Portugal Interativa*. Retrieved from [www.flora-on.pt](http://www.flora-on.pt)
- Sousa, C., Boski, T., Gomes, A., Pereira, L., Lampreia, J., & Oliveira, S. (2013). Holocene history of Ria Formosa Coastal Lagoon System (Southern Portugal): Borehole evidence and Thredimensional Paleotopography. *VIII Reunion de Cuaternario Iberico*, (pp. 254-258). Sevilla.
- Stafford, D. B., & Langefelder, J. (1972). Air photo survey of coastal erosion. *Photogrammetric Engineering*, p. 565–575.
- Stark, N., Hay, A. E., Cheel, R., & Lake, C. B. (2014). The impact of particle shape on the angle of internal friction and the implications for sediment dynamics at a steep, mixed sand-gravel beach. *Earth Surface Dynamics*, p. 469-480.
- Sutton-Grier, A. E., Wowk, K., & Bamford, H. (2015). Future of our coasts: the potential for natural and hybrid infrastructure to enhance the resilience of our coastal communities, economies and ecosystems. *Environmental Science & Policy*, p. 138-147.
- Svasek, J. N., & Terwindt, J. H. (1974). Measurements of sand transport vy wind on a natural beach. *Sedimentology*, p. 311-322.

- Taborda, R., Magalhaes, F., & Angelo, C. (2005). Evaluation of coastal defence strategies in Portugal. In C. Zimmermann, & e. al., *Environmentally Friendly Coastal Protection* (pp. p. 255-265). Netherlands: Springer.
- Thieler, R. E., Himmelstoss, E. A., Zichichi, J. L., & Ergul, A. (2009). *The Digital Shoreline Analysis System (DSAS) Version 4.0 - An ARcGIS extension for calculating shoreline change*. U.S. Geological Survey.
- Udden, J. A. (1914). Mechanical composition of clastic sediments. *Bulletin of the Geological Society of America*, p. 655-744.
- Universidade do Aveiro. (2017). *www.biorede.pt*. Retrieved from diversidade vegetal: <http://www.biorede.pt/index2.htm>
- van Dijk, P. M., Arens, S. M., & van Boxel, J. H. (1999). Aeolian processes across transverse dunes. II: modelling the sediment transport and profile development. *Earth Surface Processes and Landforms*, p. 319-333.
- van Rijn, L. C. (2010). *Coastal erosion control based on the concept of sediment cells*. CONSCIENCE Project.
- van Rijn, L. C. (2013). *Design of hard coastal structures against erosion*. Retrieved from <http://www.leovanrijn-sediment.com/>:<http://www.leovanrijn-sediment.com/papers/Coastalstructures2013.pdf>
- Vila, A., Dias, J. M., Ferreira, O., & Matias, A. (1999). Natural evolution of an artificial inlet. *Coastal Sediments*, p. 1478-1488.
- Vila-Concejo, A., Ferreira, O., Matias, A., & Dias, J. A. (2003). The first two years of an inlet: sedimentary dynamics. *Continental Shelf Research*, p. 1425-1445.
- Vila-Concejo, A., Ferreira, O., Matias, A., Morris, B. D., & Dias, J. A. (2004). Lessons from inlet relocation: examples from Southern Portugal. *Coastal Engineering*, p. 967-990.
- Vila-Concejo, A., Matias, A., Ferreira, O., Duarte, C., & Dias, J. M. (2002). Recent Evolution of the Natural Inlets of a Barrier Island System in Southern Portugal. *Journal of Coastal Research*, p. 741-752.
- Vousdoukas, M., Almeida, L., & Ferreira, O. (2012). Beach erosion and recovery during consecutive storms at a steep-sloping, mesotidal beach. *Earth Surface Processes and Landform*, p. 583-593.
- Wal, A., & McManus, J. (1993). Wind regime and sand transport on a coastal beach-dune complex, Tentsmuir, eastern Scotland. In K. (. Pye, *The Dynamics and Environmental Context of Aeolian Sedimentary Systems* (pp. p.159-171). London, UK: The Geological Society.
- Walker, I. J., & Nickling, W. (2003). Simulation and measurement of surface shear stress over isolated and closely spaced transverse dunes in a wind tunnel. *Earth. Surf. Proc. Land*, p. 1111-1124.

- Walker, I. J., Davidson-Arnott, R. G., Bauer, B. O., Hesp, P. A., Delgado-Fernandez, I., Ollerhead, J., & Smyth, T. A. (2017). Scale-dependent perspectives on the geomorphology and evolution of beach-dune systems. *Earth-Science Reviews*, p. 220-253.
- Walker, I. J., Hesp, P. A., Davidson-Arnott, R. G., Bauer, B. O., Namikas, S. L., & Ollerhead, J. (2009). Responses of three-dimensional flow to variations in the angle of incident wind and profile form of dunes: Greenwich Dunes, Prince Edward Island, Canada. *Geomorphology*, p. 127-138.
- Weaver, C. M., & Wiggs, G. F. (2011). Field measurements of mean and turbulent airflow over a barchan sand dune. *Geomorphology*, p. 32-41.
- Weinholtz, M. (1964; 1968). O Cordao Litoral da Ria de Faro e a sua Utilizacao para Fins turisticos e Balneares - Contribuicao para o Estudo da Evolucao des Flechas de Areia na Costa Sotavento do Algarve. (in Portuguese). *Separata Bol. Trimestral de Inf. Geral Serv. Hidr.*
- Wentworth, C. K. (1922). A scale of grade and class terms for clastic sediments. *Journal of Geology*, p. 377-392.
- Wolfe, S. A., & Nickling, W. G. (1993). The protective role of sparse vegetation in wind erosion. *Progress in Physical Geography: Earth and Environment*, p. 50-68.
- Wolman, M., & Gerson, R. (1978). Relative scales of time and effectiveness of climate in watershed geomorphology. *Earth Surf. Process. Landf.*, p.189-208.
- Zenkovich, V. P. (1967). *Processes of Coastal Development*. London: Oliver and Boyd.

## Annex 1

Vegetation species and coverage density in the eastern sector of Ancaão Peninsula. Site 4 represents the most westward and Site 2 respectively the most eastward

	Trans_humm.	Trans4_Dune2To	Trans4Crest2	Trans4Crest3	Trans4_Lee	Trans3_humm.	Trans3_Dune2Toe	Trans3Crest2	Trans3_Crest3	Trans_Lee	Trans2_Embryo	Trans2_Crest1	Trans2_Crest2	Trans2_Dune3Toe	Trans2_Crest3	Trans2_Lee
<i>Panicratium maritimum</i>	0.08	<b>0.6</b>	0.46	0.99	0.91	0	0.07	1.28	0.59	2.08	0	0.04	0.12	0.91	0.38	0.1
<i>Medicago marina</i>	0	<b>0.8</b>	0.72	1.06	0	0	<b>1.24</b>	<b>2.36</b>	0.44	0.28	0	0	<b>10.71</b>	<b>16.12</b>	9.6	0.2
<i>Elymus farctus</i>	0.01	0	0.01	0.01	0.01	0.01	0.01	0	0.01	0.01	0.01	0.01	0.01	0.01	0	0
<i>Eryngium maritimum</i>	0	0.04	0.06	0.04	0.05	0.06	0.15	0.07	0	0	<b>1.19</b>	0.7	0	0	0	0
<i>Othanthus maritimus</i>	0	0	0.01	0	0	0.01	0.01	0.01	0	0	0	0.04	0.01	0	0	0
<i>Ammophila arenaria</i>	0	0	0	1.16	0	0	0	0.24	0	0	0	<b>6.48</b>	0.06	0	0	0
<i>Crucianella maritima</i>	0	0.08	1.52	<b>3.34</b>	0.24	0.04	<b>0.96</b>	1.12	0	0.23	0	0.83	5.88	0	0.04	5.68
<i>Artemisia crithmifolia</i>	0	0.03	<b>6.84</b>	<b>3.28</b>	<b>6.72</b>	0	0	0.72	<b>29.92</b>	<b>6.92</b>	0	0	1.92	<b>18.96</b>	<b>42.28</b>	<b>38.8</b>
<i>Lotus creticus</i>	0	0	0.24	0.8	2.08	0	0	0	0.36	2.32	0	0	0	1.29	4.84	7
<i>Cakile maritima</i>	0	0	0	0.01	0	0	0	0	0	0	0	0	0	0	0	0
<i>Leontodon taraxacoides</i>	0	0	0	0	0	0	0	0	0	0.1	0	0	0	0	0.06	0.04
<i>Silene nicaeensis</i>	0	0.34	0.01	1.1	0.08	<b>0.24</b>	<b>2.21</b>	0.64	0.01	2	0	0.2	0.05	0.57	0.17	0.43
<i>Malcolmia littorea</i>	0	0	0.08	0	0.82	0	0	0	0.39	0.09	0	0	0.02	0.96	1.88	0.36
<i>Polygonum maritimum</i>	0.01	0	0	0	0	0	0.03	0	0	0	0	0	0.01	0	0	0
<i>Senecio gallicus</i>	0	0	0	0	0	0	0	0	0.04	0.07	0	0	0	0	0.05	0.19
<i>Calystegia soldanella</i>	<b>0.43</b>	<b>0.23</b>	0.14	0.3	0	0.21	0.06	0.06	0	0	0.76	0.12	0.12	0	0	0
<i>Paronychia argentea</i>	0	0	0	0	0	0	0	0	0	0.68	0	0	0	0.28	2.4	0
<i>Reichardia gaditana</i>	0	0	0	0	1.1	0	0	0	0.02	0.15	0	0	0	0	0.2	0
<i>Cyperus capitatus</i>	0.01	0.02	0	0	0	0	0	0	0	0	0	0	0	0	0	0
<i>Linaria polygalifolia</i>	0.01	0	0.08	0	0	0.01	0.01	0	0	0	0	0.01	0.01	0	0	0
<i>Euphorbia paralias</i>	0	0.01	0.01	0	0	0	0	0	0	0	0	0	0	0	0	0
<i>Oxalis pes-caprae</i>	0	0	0	0	0.04	0	0	0	0	0	0	0	0	3.2	1.56	0.15
<b>total</b>	<b>0.55</b>	<b>2.15</b>	<b>10.18</b>	<b>12.09</b>	<b>12.05</b>	<b>0.58</b>	<b>4.75</b>	<b>6.5</b>	<b>31.78</b>	<b>14.93</b>	<b>1.96</b>	<b>8.43</b>	<b>18.92</b>	<b>42.3</b>	<b>63.46</b>	<b>52.95</b>

## Annex 2

Vegetation species and coverage density in the western sector of Anção Peninsula. Site 8 represents the most westward and Site 5 respectively the most eastward site.

	Trans5_ DuncToe	Trans5_Cr est	Trans5_Lee	Trans6_ DuncToe	Trans6_ Crest_Lee	Trans6_Lee	Trans7_ DuncToe	Trans7_Cr est	Trans7_Lee	Trans8_ Embryo	Trans8_ DuncToe	Trans8_ Crest_Lee	Trans8_Lee
<i>Panicratium maritimum</i>	0	0	0	0.02	0	0	0	0.03	0	0	0	0	0
<i>Medicago marina</i>	<b>1.04</b>	0.64	0.32	0.52	1.88	0	0	0	0	0	0	0	0
<i>Elymus farctus</i>	0.01	0.01	0	0.01	0	0.01	0.01	0.01	0	<b>1.82</b>	2.73	0	0
<i>Eryngium maritimum</i>	0.04	0	0	0	0	0	0	0	0	0.05	0	0	0
<i>Othanthus maritimus</i>	0.01	0	0	0.22	0	0	0.01	0.01	0	0.01	0	0	0
<i>Ammophila arenaria</i>	0	0	0	<b>3</b>	0	0	0.6	0	0	0	0	0	0
<i>Crucianella maritima</i>	0.02	1.02	1.48	0.01	2.89	0.8	0	1.8	0.36	0	0	0.04	0.4
<i>Artemisia campestris</i>	0.16	<b>4.76</b>	<b>33.88</b>	<b>0.68</b>	4.36	<b>7.22</b>	0	0.04	<b>16.68</b>	0	5.12	34	0.96
<i>Lotus creticus</i>	0	<b>3.52</b>	0.8	<b>5.6</b>	2.16	1.6	0	<b>4.78</b>	0	0	<b>5.85</b>	0.2	0.8
<i>Leontodon taraxacoides</i>	0	0	0.08	0	0	0.45	0	0	0.57	0	0	0.44	0
<i>Paronychia argentea</i>	0	0	0	0	0	4.24	0	0	0	0	0	0	0.16
<i>Silene nicacensis</i>	0.37	1.32	0.16	0.04	1.66	1.38	0.01	0	0.01	0.01	0.66	0	0.01
<i>Malcolmia littorea</i>	0	0.76	0	0	0.12	0.57	0	0	0.01	0	0	0.02	0.01
<i>Helichrysum italicum</i>	0	0	0	0	0	1	0	0	0	0	0	0	3.25
<i>Polygonum maritimum</i>	0	0	0	0.01	0	0	0	0	0	0	0	0	0
<i>Armeria pungens</i>	0	<b>2.84</b>	<b>8.08</b>	0	<b>6.44</b>	<b>8.84</b>	0	1.08	1.8	0	2.88	<b>5.75</b>	<b>6.12</b>
<i>Calystegia soldanella</i>	0	0	0	0	0	0	0.04	0	0	0	0	0	0
<i>Paronychia argentea</i>	0	1.92	<b>10.08</b>	0	0.44	0	0	0	0.2	0	0	0.12	0
<i>Reichardia gaditana</i>	0	1.08	0.09	0	0.13	0.15	0	0	0	0	0	0	0
<i>Cyperus capitatus</i>	0	0	0	0	0	0	0.01	0	0	0	0	0	0
<i>Linaria polygalifolia</i>	0	0	0	0.01	0	0	0.01	0	0	0	0	0	0
<i>Honkenya peploides</i>	0	0	0	0	0	0	0.01	0	0	0	0	0	0
<i>Carpobrotus edulis</i>	0	0	0	0	0	0	0	0	4.8	0	0	0.08	0
total	<b>1.65</b>	<b>17.87</b>	<b>54.97</b>	<b>10.12</b>	<b>20.08</b>	<b>26.26</b>	<b>0.7</b>	<b>7.75</b>	<b>24.43</b>	<b>1.89</b>	<b>17.24</b>	<b>40.65</b>	<b>11.71</b>